ornl

ORNL/TM-11989

OAK RIDGE NATIONAL LABORATORY

MARTIN MARIETTA

Measurements for the Jasper Program In-Vessel Fuel Storage Experiment

F. J. Muckenthaler
R. R. Spencer
H. T. Hunter
J. L. Hull
A. Shono

MANAGED BY
MARTIN MARIETTA ENERGY SYSTEMS, INC.
FOR THE UNITED STATES
DEPARTMENT OF ENERGY

ORNL/TM-11989
Distribution Category
UC 534

Engineering Physics and Mathematics Division

MEASUREMENTS FOR THE JASPER PROGRAM IN-VESSEL FUEL STORAGE EXPERIMENT

F. J. Muckenthaler
R. R. Spencer
H. T. Hunter
J. L. Hull*
A. Shono**

Date Published: January 1992

Oak Ridge National Laboratory
Oak Ridge, Tennessee 37831-6363

Prepared for the
U.S. DOE Office of
Liquid Metal Converter Reactor

*Research Reactors Division
**Japan Power Reactor and Nuclear Fuel Development Corporation

DISCLAIMER

Prepared by the
OAK RIDGE NATIONAL LABORATORY
Oak Ridge, Tennessee 37831
managed by
MARTIN MARIETTA ENERGY SYSTEMS, INC.
for the
U.S. Department of Energy
under contract DE-AC05-84OR21400

TABLE OF CONTENTS

LIST OF TABLES

LIST OF FIGURES

ABSTRACT

The In-Vessel-Fuel-Storage (IVFS) experiment was conducted at the Oak Ridge National Laboratory's (ORNL) Tower Shielding Facility (TSF) during the first nine months of 1991 as part of the continuing series of eight experiments planned for the Japanese-American Shielding Program for Experimental Research (JASPER) that was started in 1986. This is the fourth in a series of eight experiments that were planned, all of which are intended to provide support in the development of current reactor shield designs proposed for liquid metal reactor (LMR) systems both in Japan and the United States. The program is a cooperative effort between the United States Department of Energy (U.S. DOE) and the Japanese Power Reactor and Nuclear Development Corporation (PNC).

The experimental configurations consisted of a neutron spectrum modifier followed by various shield mockups. The same spectrum modifier that was used in the three previous JASPER experiments was used to alter the Tower Shielding Reactor (TSR) source spectrum to one representing the calculated LMR neutron spectrum incident on the removable radial shield. For the U.S. portion of this program the modifier included sodium to provide the advanced liquid metal reactor (ALMR) neutron spectrum calculated for the above-core position of the fuel.

The spectrum modifiers were followed by one of three pin storage vessels fabricated for this experiment that either: (1) contained a maximum number of fuel pins available to give the maximum neutron multiplication; (2) provided an example of a heterogeneous slab containing three separated regions of fuel pins to simulate individual fuel pin assemblies; or (3) represented a homogeneous slab that contained approximately the same amount of aluminum (sodium substitute) and fuel pins as in the heterogeneous slab but with the aluminum and fuel pins more evenly distributed. In both the Japanese

and U.S. phases of the experiment one of the radial blanket slabs that had been used in numerous earlier experiments was substituted for the IVFS vessels to help promote a better understanding of the neutron flux at that location. Also included in the data plan were two mockups that contained arrangements of material designed for use beyond the fuel pin arrays in the Japanese tank-type LMR.

1. INTRODUCTION

This experiment is the fourth in a series of eight experiments to be performed at the Tower Shielding Facility (TSF) that were jointly planned by the Oak Ridge National Laboratory (ORNL), participant for the U.S. DOE, and the Japan Power Reactor and Nuclear Fuel Development Corporation (PNC). This phase of the program, called the In-Vessel Fuel Storage (IVFS) experiment, was preceded by the Radial Shield Attenuation and Fission Gas Plenum experiments completed in 1986-1987 and the Axial Shield experiment completed in 1990.

The IVFS experiment was designed to study source multiplication and three-dimensional effects relating to in-vessel storage of spent fuel elements in the Liquid Metal Reactor (LMR) designed systems. The presence of the fuel within the reactor vessel has created significant shielding and flux monitoring problems during the design studies, yet the concept could provide certain advantages by storing the fuel internally. Two previous experiments performed much earlier at the TSF, but not as part of this program, demonstrated the difficulty in determining the neutron multiplication in a fuel pin array, leading to large uncertainties in earlier Fast Flux Test Facility (FFTF) design analyses. The present measurements were made in an attempt to resolve this difficulty.

Fuel pins obtained from the University of Florida containing 4.81 wt% of enriched ^{235}U were used to mock up the fissile material planned to be stored within the LMR vessel. These pins were used in three different IVFS mockups studied: (1) a thick slab designed to provide an array of the maximum number of pins available for optimum neutron output; (2) a heterogeneous arrangement in which three bundles of the pins were separated by aluminum (sodium) to represent individual reactor fuel assemblies; and (3) a so-called homogeneous slab which contained nearly the same number of fuel pins as in the heterogeneous slab, but provided a more uniform distribution of pins and aluminum.

In this experiment two different spectrum modifiers were used. The modifier for the Japanese LMR design studies included iron, aluminum, boral, and two slabs of "radial blanket," the same arrangement as was used in the three previous experiments. The modifier was followed by mockups that included graphite and/or boron carbide (B_4C) plus stainless steel (SS), aluminum, and the fuel pins. The shield mockups in the U.S. LMR study were preceded by the iron, aluminum, and boral in the previous modifier plus slabs of sodium.

Measurements were made behind each of the mockups as the slabs of material were placed in the horizontal neutron beam emanating from the Tower Shielding Reactor-II (TSR-II) as described in the program plan in Appendix A.

2. INSTRUMENTATION

The TSF Bonner ball detection system consists of a series of detectors (polyethylene balls), each of which measures an integral of the neutron flux weighted by the energy-dependent response function for that ball. The detection device of a Bonner ball consists of a 5.1-cm-diameter spherical proportional counter filled with BF_3 gas ($^{10}B/B$ concentration = 0.96) to a pressure of 0.5 atmospheres. In order to cover a range of neutron energies, the counter is used bare, covered with cadmium, or enclosed in various thicknesses of polyethylene shells surrounded by cadmium, each detector being identified by the diameter of its shell. Bonner ball experimental results are predicted analytically by folding a calculated neutron spectrum with the Bonner ball response functions determined by R. E. Maerker et al.[1] and C. E. Burgart et al.[2]

A NE-213 liquid scintillator spectrometer covered the neutron spectral region from about 800 keV to 15 MeV. This device makes use of pulse-shape discrimination (PSD) to distinguish neutrons from gamma-ray pulses. Pulse-height data obtained with the spectrometer were unfolded with the FERD code[3] to yield absolute neutron energy spectra.

Spherical proton-recoil counters, filled with hydrogen to pressures of 1, 3, and 10 atmospheres, covered the neutron energy range from about 50 keV to 1 MeV. Pulse-height data from the counters were unfolded with the SPEC-4 code,[4] which makes use of the unfolded NE-213 neutron spectrum to correct for effects of higher-energy neutrons.

The measurements for each detector were referenced to the reactor power (watts) using the data from two fission chambers positioned along the reactor centerline as a basis. The response of these chambers as a function of reactor power level was established previously through several calorimetric measurements of the heat generated in the reactor during a temperature equilibrium condition (heat power run).

A fission chamber was added to the list of instruments available at the TSF for measurement of the neutron transmission through shield mockups. The sensitive area consists of 29 mg of Uranium enriched to 93.15% ^{235}U (27 mg) plated on a .0254-cm-thick nickel plate, covering a circular area of 31 cm^2. The detector is identical in physical features to that of the fission chambers used to monitor the reactor power on a daily basis and serves as a replacement. The fission chamber was used in this experiment to provide a direct measure of the thermal neutron fission rate. Its response to thermal neutrons was

compared to that of gold (Au) foils when exposed to a reactor flux. This calibration gave a thermal neutron sensitivity of 6.37×10^{-1} neutrons/cm^2/sec per count/minute difference between the bare and Cd-covered fission chamber readings.

3. EXPERIMENTAL CONFIGURATION

The experimental program plan was divided essentially into three parts, listing the mockups and measurements for the spectrum modifiers, the Japanese LMR, and the U.S. Advanced Liquid Metal Reactor (ALMR) studies. In the Japanese study the effort was centered on mockups that contained a removable radial shield design since in their LMR concept the fuel storage is to be located radially beyond the reactor shield. This effort included a comparative study of the neutron attenuation properties of graphite and B_4C at different locations within the shield. The U.S. ALMR design locates the fuel storage radially above the core in the sodium coolant region, hence the necessity to include sodium in the spectrum modifier. The program plan calls for neutron measurements to be made behind a series of these mockups as different slab arrangements are added to the configuration.

The neutron sources were modified TSR-II collimated beams, altered to represent the neutron spectrum predicted to exist at each of the pin locations in the actual reactor designs. For the Japanese mockups this consisted of slabs of iron, aluminum, boral, and "radial blankets" as used in the three previous experiments. For the U.S. design the radial blankets were replaced by sodium.

It should be noted that throughout the program plan the material thicknesses mentioned are nominal values, the actual thicknesses for each slab are given in the various figures displayed throughout the report. The dimensions noted in the configuration schematic for the B_4C slabs include the SS thicknesses of the faces of the containers. Thicknesses for each of the containers are shown in Figure 1 in Appendix C of the report. All dimensions quoted for distances from the reactor centerline to the back of the slabs in the mockup schematics are the distances as measured along the centerline of the collimated reactor beam.

3.1 SPECTRUM MODIFIERS

Two different spectrum modifiers, noted in the program plan as SM-1 and SM-2, were necessary to provide the proper neutron energy distribution incident on the mockups for the PNC and U.S. DOE phases of this experiment. The SM-1 modifier was an extension of the first modifier listed in the program plan, SM-0, whose schematic is shown in Figure 2. In the SM-1 modifier used in the Japanese mockups, calculations indicated

that 10 cm of iron followed by 10 cm of aluminum, 2.5 cm of boral, all in SM-0, and 20.3 cm of "radial blanket" would provide the desired incident neutron spectrum. In the actual mockup of the modifier, see Figure 3, the iron component consisted of two slabs 5.16 and 5.11 cm thick, both being 152.4 cm on an edge. The aluminum thickness consisted of three slabs totalling 9.17 cm. The boral consisted of two slabs for a total thickness of 2.54 cm. Throughout the experiment, except for the fuel pin vessels, the slabs used were nominally 152.4 cm on an edge. Compositions of the iron, aluminum, and boral are given in Tables 1, 2, and 3 respectively. (Note: All tables are included in Appendix B.)

The UO_2 slabs described as "radial blankets" had been fabricated for use in earlier experiments performed as part of the Liquid Metal Fast Breeder Reactor (LMFBR) program at the TSF. The slabs contain natural uranium (UO_2) pellets, 1.397 cm OD, enclosed in aluminum cylinders having an OD of 1.524 cm. The space between the aluminum cylinder and the UO_2 pellets, 0.00508-0.01016 cm, is filled with argon. The cylinders are stacked side by side vertically in a triangular pitch of 1.608 cm. The space between the aluminum cylinders is filled with sodium. This arrangement of UO_2 pellets is enclosed in an iron vessel having an overall thickness of 11.05 cm and a length of 152.4 cm on each edge as seen in the schematic in Figure 4.

Each of the two radial blankets used in the modifier, along with a third one used as part of the shield mockups in the experiment, contain 522 rods amounting to 64.6% of the volume of the slab. The rods are placed vertically in alternate rows of 74 and 75 pins each. The UO_2 density is 10.28 g/cc (94% of theoretical). The volume fraction of the aluminum cladding is 11.2 % and that for the sodium is 23.3%, leaving a void (argon) volume fraction between the pellet and aluminum cylinder of 1%. The stacked length of the pellets in each of the rods is approximately 121.9 cm. These rods were built by the Numes Corporation in 1962 to conform, in general, to the then AEC/RDT design standards for the FFTF. Analyses of the UO_2 and aluminum are given in Tables 4 and 5 respectively.

The sides of the spectrum modifier and all the succeeding slabs were surrounded with lithiated paraffin whose thickness was not constant. On the vertical sides the thickness was limited to 10.16 cm because of the limited number of bricks available. The mockup slabs were supported by a 30.5-cm-thick slab having a 20.3 cm layer of lithiated

paraffin and a 10.2 cm layer of concrete with the lithiated paraffin layer adjacent to the mockup slabs. Due to the tie-off pieces at the top of the configuration slabs, the thickness of lithiated paraffin in that area varied from 20 cm to 30.5 cm to provide sufficient shielding. In all cases the paraffin was usually surrounded by a minimum of 61 cm of concrete. Additional concrete was placed around the sides of the mockup to reduce the background reaching the detector. The composition of the lithiated paraffin and the ensuing concrete blocks adjacent on the sides of the mockup are presented in Tables 6 and 7 respectively.

The second spectrum modifier, designated SM-2 in the program plan, contained the same iron, aluminum, and boral slabs as in SM-1, with the radial blanket being replaced by 180 cm of sodium, as seen in Figure 5. The sodium slabs were obtained from Atomics International during the 1960s and have been used in various TSF experiments since then. The walls of the sodium tanks are made of 6061 aluminum having the same edge length as the other slabs, 152.4 cm. The thickness is nominally 30.5 cm plus 0.635 cm for each of the aluminum faces. During the years, the sodium in some of the tanks has settled, causing some bulging in the middle of the tanks. The dimensions of the tanks quoted in the configuration schematics were measured along the centerline, see Figure 6, and include the aluminum thickness. The composition of the sodium and aluminum are given in Tables 8 and 2 respectively. As with the previous modifier, the sides of the sodium tanks were covered with a minimum of 10.16 cm lithiated paraffin followed by the previously discussed concrete. When placed in the mockup the center of the slabs coincided with the center of the reactor beam.

3.2 FUEL PIN ASSEMBLIES

A total of 1200 fuel pins were secured from the University of Florida for this experiment. The pins were originally fabricated for use at the United States Atomic Energy Commission's National Reactor Testing Station near Idaho Falls, Idaho, for Special Power Excursion Reactor tests, hence the notation SPERT fuel. Each of the rods consists of slightly enriched (4.81%), sintered UO_2 pellets encased in a 304 stainless steel tube and capped at both ends with SS. In each rod there exists an aluminum oxide (Al_2O_3) insulator between the UO_2 pellets and the SS caps at each end. Gas gaps for fuel expansion are provided at the upper end of the rod and around the pellets. A spring is located atop the fuel pellets to keep the pellets in place. The characteristics of a typical

SPERT fuel rod may be seen, along with the schematic, in Figure 7. As is noted in the figure, the active fuel length is 91.44 cm, with an overall length of the fuel rod, ends included, of 106.05 cm. The pellets are 1.067 cm in diameter and are clad in 1.184-cm-OD SS tubing with walls 0.051 cm thick. The UO_2 fuel pellet density is 10.08 g/cc and the ^{235}U in each rod amounts to 35.2 grams. Each of the pins is numbered to enhance record keeping. What was not noted in the schematic is that each of the pins has a weld bead at the top and bottom of the rod where the end caps join the tubing containing the fuel. This weld is slightly larger in diameter (1.20 cm) than the SS tubing (1.184 cm), and this larger diameter required some last minute changes in the fabrication of the vessels.

The fuel pins were contained in one of three vessels during the IVFS experiment. These vessels have been described in the program plan as: (1) the "thick" one in which 1148 pins are closely packed to provide a maximum neutron multiplication; (2) the heterogeneous one in which 564 pins are divided into three groups separated by rectangular pieces of aluminum that simulates individual reactor fuel assemblies; and (3) the closest arrangement to homogeneity in which 536 pins are split into groups of 230 and 306 pins by a thickness of aluminum that extends the full width of the vessel. This vessel contains essentially the same aluminum and pin volume fractions as the heterogeneous vessel but is considered more homogeneous in makeup.

The "thick" vessel was 94.96 cm wide, 18.31 cm thick, 111.3 cm high, and fabricated of SS as shown in the schematic in Figure 8. The pins were stacked vertically in the vessel, resulting in eight rows of 77 pins each alternating with seven rows of 76 pins each spaced on a triangular pitch of 1.20 cm based on the diameter of the welds. Because the diameter of the welds was slightly greater than the diameter of the rods there existed a small void between the pins.

The heterogeneous vessel was made of aluminum to mock up the presence of sodium coolant surrounding the fuel pins. This vessel is slightly smaller in stature than the "thick" vessel, having the same height but a smaller width (92.18 cm) and less thickness (only 16.89 cm). As seen in the schematic of the vessel, Figure 9, the coolant widths (aluminum spacers) separating the pins were 15.75 cm while the pin assemblies themselves were 15.56 cm wide. Each of the fuel groups contained 188 pins.

The pin arrangement in the third vessel provided a somewhat more homogeneous approach to the pin-aluminum distribution while maintaining the same fuel pin to

aluminum volume fraction ratio as in the heterogeneous slab. In this homogeneous arrangement (see Figure 10), the pins, 536 total, were split into two groups by a 3.46-cm-thick aluminum divider that ran the full width of the vessel. On one side of the divider were two rows of 77 and 76 pins each, while on the other side were two rows of 77 pins and one row of 76 pins. The same triangular pitch was maintained for the pins in all three slabs.

When the IVFS vessels were placed in the mockup it was necessary to place additional support beneath them to center the vessel on the reactor beam centerline. This was accomplished with 20.3 cm of lithiated paraffin. Likewise, since the width of the vessels were much smaller than the typical configuration slabs (97 cm and under compared to 152.4 cm), the additional space between the vessels and concrete on each side was filled with additional lithiated paraffin bricks.

Measurements behind a configuration using one of the "radial blankets" as a fuel pin mockup were added to the program plan to provide reference-type data since the characteristics of the slab were well understood from measurements and calculations in earlier experiments in the LMFBR program. The slab contents were described earlier in the discussion of spectrum modifiers.

3.3 B_4C SLABS

The five B_4C slabs used in this experiment consisted of stainless steel cans filled with 120 grit boron carbide powder. Three different thicknesses were filled, nominally 5.08 cm (2 inches), 10.16 cm (4 inches), and 15.24 cm (6 inches) denoted 4W and 5W, 2W and 3W, and 1W respectively in Figure 1. The actual thicknesses of the slab (SS included) were measured along the centerline as indicated in the figure. Spacer pins were used in both the nominally 5 cm and 15-cm-thick slabs to maintain constant thickness with the thinner walls. All slabs were 152.4 cm (60 in) on an edge. The densities are 1.42 g/cc for container 1W, 1.39 g/cc for 2W, 1.37 g/cc for 3W, 1.41 g/cc for 4W, and 1.44 g/cc for container 5W. An analysis of the B_4C powder is given in Table 9. The amount of boron nitride (BN) as a component in these slabs was not established. However, previous analysis (see ORNL/TM-11839) indicated there were several percent present in similar B_4C samples.

3.4 GRAPHITE

A combination of graphite pieces, 30.48 cm (12 in) and 121.9 cm long and 10.16 cm on a side, were stacked to form a slab 152.4 cm on an edge and 10.16 cm thick. The pieces were precisely machined to provide good surface-to-surface contact and eliminate possible voids for neutron streaming. An analysis and density are given in Table 10.

3.5 ALUMINUM SLABS

Thin aluminum slabs, 1.27 cm and 2.54 cm, were used as part of the configuration to mock up spaces that would be occupied by the sodium coolant in a typical LMR reactor design. Those slabs are of the same aluminum (6061) used in the spectrum modifiers described earlier.

3.6 STAINLESS STEEL SLABS

The stainless steel slabs used in this experiment were nominally either 2.54 cm or 5.08 cm thick and 152.4 cm on an edge. These slabs are typical type 304 SS, whose elemental composition can be found in Table 11.

3.7 BACKGROUND SHIELDS

It has been the custom in past measurements to obtain background measurements along with foreground measurements when the detectors were located at sufficient distances behind the mockups where neutron contributions to the detector from areas other than the mockup itself might not be negligible. For these measurements a container of lithiated paraffin bricks, 91.4 cm x 91.4 cm x 40.6 cm thick, was usually placed between the detector and mockup in such a manner that contributions directly to the detector from just the mockup would be greatly reduced. Background measurements were made behind each mockup at 150 cm with the Bonner balls but similar measurements with the fission chamber were limited to Items IA, IB, and IIA only (configurations are described later in section 4.0). The bare fission chamber measurements behind these three mockups showed very little difference between foreground and background count rates, a difference so small that its reliability would be subject to question. After completing measurements for Item IIA, the background measurements behind the next mockup with the bare detector were replaced by a bare detector measurement with a cadmium sheet covering the face of the mockup. The cadmium sheet absorbed the thermal neutron flux leaving the mockup

while not interfering with the thermal neutron contribution from any other source. This measurement, when subtracted from the thermal detector measurement without Cd over the mockup face, gives the value of the thermal flux leaving the mockup. Without the lithiated paraffin background measurement for the bare detector there was no need to continue a similar measurement for the Cd-covered detector, so it was also eliminated.

In Item IIP it was necessary to expand the concrete background shield into the shape of an enclosed structure around the detector at 150 cm to reduce the air scattered contribution sufficiently to obtain a reasonable difference in the foreground-background Bonner ball measurement. The nearby presence of the walls, however, added an additional background component from scattering, a component that could not be adequately evaluated by the usual background procedure. This wall scattered component was essentially eliminated by placing a 30.5-cm-thick lithium hydride (LiH) slab directly behind the last slab in the mockup. The presence of the LiH permitted a measurement of the background contribution from outside the enclosed structure.

The Cd hut used in this experiment to make bare fission chamber measurements at 0.7 and 30 cm behind the mockup may be best described as a small structure, 152.4 cm on an edge matching the dimensions of the mockup slabs, and 45.7 cm deep, covered with 30-40 mils cadmium except for one face which was left exposed. The open face was always placed against the face of the last slab in the mockup, thus allowing thermal neutron entry from the mockup slab while at the same time denying entry from any other direction. Thus it was possible to place the bare detector within the hut, make a measurement, and through a subtraction of the detector Cd-covered value at that location, obtain a measure of the thermal flux leaving the mockup.

4. MEASUREMENTS

The typical mockup consists of a series of slabs, 152.4 cm on a side, that are stacked in proper sequence in front of the reactor shield collimator as requested for a particular measurement in the data plan. The usual procedure is to surround the slabs with lithiated paraffin and concrete to provide both a reasonable medium for calculating the albedo for neutrons reflected back into the slabs and a satisfactory arrangement of concrete for minimizing the effect of background contribution to the measurements. Normally 20.3 cm of lithiated paraffin surrounds each mockup, but for these measurements the lithiated paraffin on the lateral edges was limited to 10.16 cm because of the limited number of bricks available to cover the larger mockups. There was, however, 20.3 cm of lithiated paraffin beneath the mockup as that amount is inherently part of the concrete slab that supports the mockup. The amount of lithiated paraffin between the top of the slabs in the mockup and the concrete slabs placed overhead for background suppression varied but was usually never less than 20-30 cm.

Beyond the lithiated paraffin wall on the sides of the mockup the concrete pieces varied from small blocks 15.24 cm on an edge x 30.5 cm long to large 61-cm-square x 30.5-cm-thick blocks whose concrete mixtures were not the same. The analyses for the various blocks are given in Tables 7 and 12. Larger concrete blocks (91 x 91 cm) were used to extend the background coverage but their presence did not affect the neutron flux reflected back into the mockup.

Once into the experimental program, it was recognized that some of the measurements listed for the fission chamber should be changed to provide data that would be more beneficial to the calculations. Since the thermal neutron flux emerging from the back of the IVFS vessels was usually less than contributions reaching the detector from the shielding around the mockup and air scattering, the program plan was altered to include measurements with a more positive approach to measuring the thermal flux. After completing measurements for Item IIA the backround data requested at 150 cm using the lithiated paraffin shadow shield was replaced with several definitive measurements using cadmium instead as discussed earlier in section 3.7.

Measurements were included at 0.7 cm behind the mockup with the fission chamber bare, Cd covered, and bare-faced with a Cd sleeve around the cylindrical housing of the detector. The latter arrangement limited the thermal-flux contribution entering the

sensitive area of the detector to that from the mockup only. Instead of the usual background measurements at 150 cm with the lithiated paraffin the shadow shield was replaced by a sheet of Cd over the face of the mockup; for this setup, measurements were made with the bare detector at both 30 and 150 cm. To limit the thermal contribution to the bare detector count rate to that just from the mockup, measurements were also made at 0.7 and 30 cm inside a Cd hut. The thermal-flux count rate can then be obtained through a series of subtractions involving measurements with and without the Cd sheet over the face of the mockup or in the Cd hut and the Cd-covered detector measurements at the same locations. Since these measurements permit determinations of the thermal flux by two different techniques, the difference in the two results gives an indication of the error in the measurements.

For background measurements with the Bonner balls at 150 cm on centerline, a 40.6-cm-thick lithiated-paraffin-brick-filled slab, 91 cm on a side, was placed approximately halfway between the detector and mockup so that neutrons leaving the face of the last slab would have to penetrate the lithiated paraffin to reach the detector. For the mockups where the last slab was the IVFS vessel surrounded by lithiated paraffin, the width of the mockup area shadow-shielded was equivalent to the previous widths (i.e. that of a 152.4-cm-square slab), which meant that some of the lithiated paraffin around the fuel pins was also shadow shielded.

Except for measurements behind two mockups the need for background measurements using the NE-213 and hydrogen counters were eliminated for the spectral measurements by moving the detector close to the last slab. This was made possible where there existed a gamma-ray to neutron count-rate ratio greater than 10 to 1, by placing a slab or two of lead (see Table 13 for chemical analysis) between the detector and mockup, reducing the count-rate ratio to an acceptable number and allowing the detector to be positioned closely behind the lead; hence no background measurement was required. For the two exceptions it was possible to make the measurements without the lead.

The number of calendar days allotted for this particular experiment also dictated the need for changes in the program as the experiment evolved. In part III of the program plan, which pertained to the U.S.-requested measurements for data pertaining to the above core ALMR simulated mockup, the requested data was reduced to centerline

measurements with the fission chamber and Bonner balls except for Items IIIA and IIIF which remained unchanged. The program plan in Appendix A reflects only the measurements that were made, not the data requests as originally planned.

The order in which the measurements were performed did not follow the order as listed in the program plan. It was decided to minimize the number of times the fuel pins were moved from one vessel to the other to limit personnel exposure to their radiation. Thus, all of the mockups using a particular vessel were completed before swapping vessels with one exception, Item IIIA, a mockup that did not fit into the rotation selected for performing the program plan. The reporting of the data in this report, however, will follow the order in which the program plan is written. Throughout this report the words configuration, item, and mockup are used interchangeably when referring to the contents of the program plan.

4.1 SPECTRUM MODIFIER (ITEMS IA, IB, IC)

The program plan called for measurements behind three spectrum modifiers, the first of which (SM-0) combines with two "radial blankets" to form SM-1. This modifier transformed the TSR-II neutron spectrum to one reasonably representative of the spectrum incident upon the removable shield design for the Japanese part of the program. The third modifier (SM-3) serves to provide a spectrum incident upon the above core area where the fuel pins will be stored in the ALMR design for the U.S. The presence of the lead slab for the NE-213 measurements as shown in the schematics of the mockup for Items IA and IC was necessary to lower the gamma-ray to neutron count-rate ratio to a reasonable value, less than 10 to 1, that allowed good count-rate statistics within a reasonable period.

Measurements of the neutron spectra behind the spectrum modifier SM-0, shown in Figure 2, were made with both the NE-213 and hydrogen-filled detectors on centerline at 25 cm behind a lead slab inserted between detector and mockup to obtain an acceptable gamma-ray to neutron count rate. The resulting spectra are listed in Tables 14 and 15, and plotted in Figures 11 and 12 respectively. Integral flux measurements with the 3-, 5-, and 10-in Bonner balls at this same location are listed in Table 16.

Measurements were made with the 3-, 4-, 5-, 8-, 10-, and 12-in Bonner balls on centerline at 30 cm (foreground) and 150 cm (foreground and background) behind the mockup with the lead slab removed, and these results are given in Tables 17 and 18. The

measurements were repeated at these same locations with the fission chamber bare and Cd covered, and the results are listed in Tables 19 and 20 respectively.

Spectral measurements were made at 179.1 cm behind the next modifier, SM-1, obtained by adding two "radial blankets" to SM-0 (see Figure 3). Locating the detector at that distance eliminated the need for a lead slab to attenuate the gamma flux but made it necessary to include a background run. The results from the NE-213 measurement are listed in Table 21 and plotted in Figure 13. The low-energy part of the neutron measurement obtained with the hydrogen-filled detectors is given in Table 22 and plotted in Figure 14. Data from the 3-, 5-, and 10-in Bonner ball measurements at this same location are given in Table 16.

Results from the 3-, 4-, 5-, 8-, 10-, and 12-in Bonner ball measurements on centerline at 30 and 150 cm behind the radial blankets are given in Tables 17 and 18. Similar measurements with the fission chamber bare and Cd covered gave results that are listed in Tables 19 and 20.

The "radial blankets" were removed from SM-1 and replaced with six slabs of sodium to create the third spectrum modifier, SM-2, that would be used in the ALMR experiments in Items IIIA-IIIF. NE-213 and hydrogen-filled detectors were used to measure the neutron spectrum behind SM-2, but not until a slab of lead had been added to the configuration to reduce the gamma ray flux incident on the spectrometer (see Figure 5). Results from spectral measurements at 25 cm behind the lead are listed in Tables 23 and 24 and plotted in Figures 15 and 16. The 3-, 5-, and 10-in Bonner ball data obtained at that same location are given in Table 16.

Bonner ball data on centerline at 30 and 150 cm with the lead slab removed are given in Tables 17 and 18. Changes were made in the approach to the requested fission chamber measurements during the progress of the experimental program and these changes should be noted both in the program plan and in the data reported here for Item IC. Data were obtained with the bare and Cd-covered fission chamber at 0.7, 30, and 150 cm and those results are in Tables 25, 19, and 20 respectively. Bare detector measurements were made on centerline at 30 and 150 cm with a Cd sheet covering the face of the mockup. This data is given in Tables 19 and 20. Bare detector measurements were made at 0.7 and 30 cm inside a Cd hut arrangement that limited the thermal flux to that leaving the face of the mockup. The results are listed in Tables 25 and 19.

4.2 REMOVABLE RADIAL SHIELD ITEMS IIA-IIQ

The purpose of this particular phase of the experiment was to study three different designs of fuel pin storage arrangements when located along the axis of the radial shield in the Japanese LMR design. Measurements were made behind different designs of the radial shield mockups followed by the addition of the three IVFS vessels. In two cases the study included results from *in-situ* measurements beyond the fuel pins.

The initial mockup, Item IIA, consisted of the spectrum modifier SM-1 followed by, in sequence, slabs of aluminum, SS, aluminum, graphite, and SS, see Figure 17. Measurements made with the 3-, 4-, 5-, 8-, 10-, and 12-in Bonner balls on centerline at 30 cm (foreground only) and 150 cm (foreground and background) behind the mockup are given in Tables 26 and 27. Measurements with the fission chamber bare and Cd covered at 30 cm (foreground only) and at 150 cm (foreground and background) are listed in Tables 28 and 29. Bare detector data at the 150 cm point with a Cd sheet over the face of the mockup are given in Table 29.

The configuration was changed to Item IIB by adding some more aluminum, graphite, SS, Al, and SS in that order as seen in Figure 18. This series of measurements included spectral data using the NE-213 and hydrogen-filled proton recoil detectors following the addition of a lead slab. These spectra are listed in Tables 30 and 31 respectively, and plotted in Figures 19 and 20. Bonner ball measurements made at this same location are given in Table 16. Centerline measurements with the six Bonner balls at 30 and 150 cm without the lead slab in the mockup are given in Tables 26 and 27. Fission chamber data at these same locations are given in Tables 28 and 29 for bare and Cd-covered detectors. Bare detector results at the two locations with Cd over the face of the mockup are also in Tables 28 and 29. Traverses through the horizontal midplane were made at 30 cm behind the mockup using the 3- and 10-in Bonner balls and the bare and Cd-covered fission chambers. Results with the Bonner balls are listed in Tables 32 and 33. The bare and Cd-covered fission chamber results are listed in Tables 34 and 35, and the bare fission chamber traverse was repeated with Cd covering the face of the mockup and these results are given in Table 36.

In Item IIC, the "thick" IVFS vessel was placed in the configuration as shown in Figure 21. NE-213 and hydrogen recoil spectral data were obtained at 178 cm behind the mockup without the use of a lead slab. The results for the NE-213 are listed in Table 37

and plotted in Figure 22. The low-energy spectrum obtained with the three hydrogen recoil detectors is listed in Table 38 and plotted in Figure 23. The Bonner ball measurements at this same location are given in Table 16.

Results from centerline measurements with the six Bonner balls reside in Tables 26 and 27. Data obtained at these same locations with the fission chamber bare, Cd covered, and bare with Cd over the face of the mockup are recorded in Tables 28 and 29.

Radial traverses at 30 cm behind the mockup were made with the 3- and 10-in Bonner balls and these results reside in Tables 32 and 33. Traverse results at 30 cm with the bare and Cd-covered fission chamber are shown in Tables 34 and 35 while the bare fission chamber traverse data with Cd over the mockup face is located in Table 36.

In the next mockup, Item IID, the IVFS thick vessel was replaced with the heterogeneous vessel of fuel pins as shown in Figure 24. Radial traverse results with the 3- and 10-in Bonner balls at 30 cm behind the mockup are listed in Tables 32 and 33. The bare and Cd-covered fission chamber data for the same traverse are located in Tables 34 and 35. Cd was placed over the face of the mockup and the bare fission chamber traverse repeated, and these results are given in Table 36. Bonner ball measurements on centerline at 30 and 150 cm are given in Tables 26 and 27. Bare and Cd-covered fission chamber measurements were made on centerline at 0.7, 30, and 150 cm behind the mockup. These results are given in Tables 39, 28, and 29 respectively. Bare detector data at 30 and 150 cm with a Cd sheet over the face of the mockup are in Tables 28 and 29. Bare detector measurements inside the Cd hut at 0.7 and 30 cm are given in Tables 39 and 28. Data obtained with the fission chamber's housing cylinder wrapped in Cd and the bare face placed against the fuel pin vessel (0.7-cm point) are given in Table 39.

The heterogeneous vessel was replaced with the homogeneous vessel to give Item IIE (see Figure 25) and the measurements with the Bonner balls and fission chamber in Item IID were repeated again. Radial traverse results with the Bonner balls are given in Tables 32 and 33. Traverses radially with the bare fission chamber were made at 30 cm with and without the Cd sheet over the face of the mockup and these results are in Tables 34 and 36. Results from a radial traverse with the Cd-covered detector at 30 cm are given in Table 35.

Bonner ball results on centerline at 30 and 150 cm are given in Tables 26 and 27. Fission chamber data for bare and Cd-covered detectors at 0.7, 30, and 150 cm are

recorded in Tables 39, 28, and 29. Bare detector measurements at 30 and 150 cm with Cd over the face of the shield are presented in Tables 28 and 29. Bare detector data inside the Cd hut at 0.7 and 30 cm are listed in Tables 39 and 28.

The fuel pin vessel was removed and 5 cm of B_4C placed in the mockup just prior to the last slab of SS to give Item IIF as shown in Figure 26. Spectral measurements were made at 25 cm behind the slab of lead added to reduce the gamma-ray flux. The results for the NE-213 spectrometer are given in Table 40 and plotted in Figure 27. The hydrogen recoil spectral data are listed in Table 41 and plotted in Figure 28. Bonner ball results at the same location are given in Table 16. Bonner ball centerline data at 30 and 150 cm are recorded in Tables 26 and 27. Fission chamber measurements were made on centerline at 30 and 150 cm with the detector bare, Cd-covered, and bare with Cd over the mockup face and these data are given in Tables 28 and 29. There were no radial traverses behind this mockup.

The thick fuel pin vessel was placed back in the configuration to give Item IIG in the program plan as seen in Figure 29. Once again spectral measurements were made with the NE-213 and hydrogen-filled detectors at 25 cm behind an added lead slab. Data with the NE-213 scintillator are listed in Table 42 and plotted in Figure 30. The low-energy spectrum using the hydrogen-filled detectors is located in Table 43 and plotted in Figure 31. Bonner ball data at this same location are given in Table 16. Bonner ball results from measurements on centerline at 30 and 150 cm are given in Tables 26 and 27. Fission chamber data on centerline at the Bonner ball locations are given in Tables 28 and 29 for the bare and Cd-covered detectors. Bare detector count rates at 30 and 150 cm with Cd over the mockup face are also included in Tables 28 and 29.

The fuel pins were removed from the configuration and the thickness of B_4C located prior to the last SS slab was increased from 5 cm to 15 cm nominally, giving the mockup of Item IIH as seen in Figure 32. Radial traverses at 30 cm behind the mockup were made with the 3- and 10-in Bonner balls, and these results are in Tables 32 and 33. Bare fission chamber count rates for the same traverse are in Table 34, and those using the Cd-covered detector are in Table 35. Results from putting Cd over the mockup face and making a bare detector traverse are part of Table 36.

Bonner ball count rates at 30 and 150 cm on centerline are given in Tables 26 and 27. Bare and Cd-covered fission chamber data on centerline at 0.7, 30, and 150 cm

are part of Tables 39, 28, and 29. Bare detector data at 30 and 150 cm with Cd over the mockup are also in Tables 28 and 29. Count rates at 0.7 and 30 cm with Cd wrapped around the cylinder walls of the fission chamber and the face of the detector bare reside in Tables 39 and 28.

The thick fuel vessel with 1148 pins was returned to the configuration to advance the mockup to Item II I (see Figure 33). Results from a radial traverse with the Bonner balls are given in Tables 32 and 33. Similar traverses with the bare and Cd-covered fission chamber gave results that are located in Tables 34 and 35. The bare detector traverse data with Cd over the face of the mockup are in Table 36. Bonner ball measurements on centerline at 30 and 150 cm are shown in Tables 26 and 27. Bare and Cd-covered fission chamber data at 0.7, 30, and 150 cm on centerline are in Tables 39, 28, and 29. Bare detector measurements at 30 and 150 cm were repeated with Cd over the mockup face, and the data are in Tables 28 and 29. Cd was wrapped around the cylinder wall of the detector housing and the face of the detector placed against the fuel pins (0.7 cm). This count rate is in Table 39. The bare detector was placed inside the Cd hut at 0.7 and 30 cm and these results are in Tables 39 and 28.

The lithiated paraffin around the fuel pin vessel in Item II I was removed to give Item II IA and the centerline measurements done in Item II I were repeated here with both detectors to provide information on what effect lithiated paraffin had on the neutron count rates. The results of these measurements are recorded in the same tables for similar measurements with the lithiated paraffin present.

The thick IVFS vessel was replaced by the heterogeneous vessel to advance the mockup to Item IIJ, as shown in Figure 34, and the same measurements repeated. Data from the traverses at 30 cm with the Bonner balls can be seen in Tables 32 and 33. Data from the bare fission chamber traverse are in Table 34, those from the Cd-covered detector traverse are in Table 35, and the bare detector traverse results with Cd over the mockup face are in Table 34. Bonner ball results from measurements on centerline are in Tables 26 and 27. Bare fission chamber data inside the CD hut at 0.7 and 30 cm are in Tables 39 and 28. The bare and Cd-covered detector data at 0.7, 30, and 150 cm are listed in Tables 39, 28, and 29. The bare detector results with Cd over the mockup face are also in Tables 28 and 29.

For Item IIK, Figure 35, the heterogeneous slab was replaced by the homogeneous

slab and the measurements made for the previous mockup were repeated. Radial traverse measurements with Bonner balls at 30 cm are listed in Tables 32 and 33. Bare fission chamber traverse data at that location with and without the Cd sheet over the mockup are reported in Tables 34 and 36. Results from the radial traverse with the Cd-covered detector are listed in Table 35. Bonner ball measurements on centerline at 30 and 150 cm are given in Tables 26 and 27. Data from the measurements with the bare and Cd-covered fission chamber at 0.7, 30, and 150 cm on centerline are given in Tables 39, 28, and 29. Bare detector data at 30 and 150 cm with Cd over the mockup face are contained in Tables 28 and 29. Results from bare detector measurements at 0.7 and 30 cm inside the Cd hut are listed in Tables 39 and 28.

The homogeneous slab in the previous mockup was replaced by one slab of the radial blanket (see section 3.2 for description) to complete the mockup for Item IIL, shown in Figure 36. The Bonner ball data obtained on centerline at 30 and 150 cm are listed in Tables 26 and 27. The fission chamber measurements on centerline at 0.7, 30, and 150 cm are given in Tables 39, 28, and 29 for the bare and Cd-covered detectors. The bare detector results at 30 and 150 cm with Cd over the mockup face are listed in Tables 28 and 29. A measurement was made with the detector on centerline at 0.7 cm with the cylindrical housing wrapped in a Cd sleeve. This count rate is listed in Table 39. Data at 0.7 and 30 cm inside the Cd hut with the bare fission chamber are in Tables 39 and 28.

A major change in the content of the mockup and its arrangement was necessary to obtain Item IIM, seen in Figure 37 The graphite was removed and in its place was put 15 cm (nominally) of B_4C. Some of the SS slabs were removed along with the radial blanket that served as the fuel pin mockup in the previous configuration. The same series of measurements was repeated. Fission chamber radial traverses, bare and Cd-covered, were made at 30 cm behind the mockup and these results are in Tables 34 and 35. A bare detector traverse was repeated with Cd over the mockup face, and the data are in Table 36. Data obtained with the Bonner balls at 30 and 150 cm on centerline are listed in Tables 26 and 27. Fission chamber measurements at 0.7, 30, and 150 cm behind the mockup for the detector bare and Cd-covered are given in Tables 39, 28, and 29. Repeats with bare detector at 30 and 150 cm with Cd over the mockup are recorded in Tables 28 and 29. The datum from the run with the bare detector wrapped in the Cd sleeve is in

Table 39. Results with the bare detector inside the Cd hut at 0.7 and 30 cm are given in Tables 39 and 28.

The thick IVFS vessel was added to complete the mockup for Item IIN (see Figure 38). Results from the NE-213 spectral measurements obtained at 25 cm behind the mockup followed by a lead slab are recorded in Table 44 and plotted in Figure 39, while the hydrogen-filled detector spectrum is listed in Table 45 and plotted in Figure 40. Bonner ball measurements at this same location are given in Table 16. Bonner ball radial traverse results at 30 cm behind the mockup with the lead removed are listed in Tables 32 and 33. Results from the same traverses with the bare and Cd-covered fission chamber are recorded in Tables 34 and 35, and those with the bare detector when Cd covers the mockup are in Table 36. Bonner ball measurements on centerline at 30 and 150 cm are given in Tables 26 and 27. Fission chamber measurements on centerline at 0.7, 30, and 150 cm were made with the detector bare and Cd covered and those results are in Tables 39, 28, and 29. With Cd over the face of the mockup, measurements were made at 30 and 150 cm with the bare detector and these data are in Tables 28 and 29. Measurements were repeated at 0.7 cm with the bare detector when its cylindrical housing was wrapped with Cd. The resulting datum point is in Table 39. Bare detector data obtained inside the Cd hut at 0.7 and 30 cm are listed in Tables 39 and 28.

The thick IVFS slab was replaced with the heterogeneous slab, changing the mockup to Item IIO (see Figure 41). Spectra were again obtained with the NE-213 and hydrogen-filled detectors behind a slab of lead added to reduce the gamma-ray flux behind the mockup. The NE-213 spectrum is listed in Table 46 and plotted in Figure 42. The data obtained with the hydrogen-filled detector are printed in Table 47 and plotted in Figure 43. The Bonner ball measurements at that location are in Table 16. Horizontal traverses were made behind the mockup with the Bonner balls and fission chamber. The Bonner ball data are listed in Tables 32 and 33, while the bare and Cd-covered fission chamber data are in Tables 34 and 35 respectively. The bare detector was traversed again with Cd over the mockup face and these values are in Table 36. Bonner ball measurements at 30 and 150 cm on centerline are recorded in Tables 26 and 27. The fission chamber results at 0.7, 30, and 150 cm for the bare and Cd-covered detector are placed in Tables 39, 28, and 29. The repeats at 30 and 150 cm with the bare detector when Cd covered the mockup are in Tables 28 and 29. Data inside the Cd hut with the

bare detector at 0.7 and 30 cm are given in Tables 39 and 28. The result at 0.7 cm with the bare detector inside the Cd sleeve is in Table 39.

The first two 15-cm B_4C slabs were replaced with 10 cm of graphite for this next mockup, Item IIP, and the thick IVFS vessel was substituted for the heterogeneous vessel (see Figure 44A and 44B). The vessel was followed by a void in the mockup that was backed by Al, SS, and B_4C to simulate additional shielding that would follow the stored fuel in the LMR. Measurements were made inside the void with the fission chamber bare, Cd-covered, and with the cylindrical housing enclosed in a Cd sleeve to deny thermal-neutron access to the fissile material in the detector except from the fuel-pin vessel itself. These data points are located in Table 48.

The very thick mockup attenuated the neutron flux through it with such magnitude that the measurements behind the mockup indicated that essentially all of the neutrons reaching the detector were being air scattered into it from leakage flux (background) around the concrete enclosing the mockup. To minimize this contribution the measurements with the Bonner balls beyond the 30-cm point were made inside an enclosed-room-type arrangement in which the walls were several feet of concrete and the upper half of the entry from the rear was always covered with 20.3 cm (8 inches) of borated polyethylene as seen in the schematic in Figure 44B. This arrangement was quite effective, the count rate was greatly reduced, but its presence possibly introduced a new contributor to the count rate from wall scattering. For the data points at 30 cm and closer the contribution from wall scattering was negligible. To somewhat understand what the contribution from wall scattering might be, a second background measurement was performed in which the flux leaving the mockup was absorbed by 30.5 cm of lithium hydride (LiH). Measurements behind the LiH at the 150-cm point should essentially give count rates that result from neutrons penetrating the concrete blocks from outside the enclosure.

Measurements were limited to behind the last slab in the mockup (13.06 cm B_4C) along the axis of the reactor beam centerline. Bonner ball measurements were obtained at 30 and 150 cm without the LiH present and results are in Table 26 and 27. Data with the LiH present were obtained at the same 150-cm point as when the LiH was not present. These data obtained behind the LiH are indicated in Table 27 as LiH background.

Fission chamber measurements were made bare and Cd-covered at 0.7, 30, and 150 cm, and these results are in Tables 39, 28, and 29. Bare detector results at 30 and 150 cm with Cd over the mockup are listed in Tables 28 and 29. Data from bare detector measurements in the Cd hut at 0.7 and 30 cm are part of Tables 39 and 28. The measurement at 0.7 cm with the detector in the Cd sleeve is part of Table 39.

The 20 cm of B_4C in Item IIP was removed and the mockup extended by the addition of slabs of Al, graphite, and SS to become Item IIQ as seen in the schematic in Figures 45A and 45B. The same concrete block house was used to surround the detectors during the measurement as was used in Item IIP.

Bonner ball data was obtained beyond the mockup at 30 and 150 cm along the centerline and these results are part of Tables 26 and 27. The fission chamber measurements along the axis were repeated behind this mockup and the results at 0.7, 30, and 150 cm with detectors bare and Cd-covered are in Tables 39, 28, and 29. The results at 30 and 150 cm with the bare detector when the mockup was Cd-covered are in Tables 28 and 29. The data at 0.7 cm with the detector in a Cd sleeve is in Table 39, and the measurements inside the Cd hut at 0.7 and 30 cm are in Tables 39 and 28.

Three measurements were made in the void adjacent to (0.7 cm) the face of the IVFS vessel. The results from the bare, Cd-covered, and bare detector inside a Cd sleeve measurements are in Table 48.

4.3 ABOVE-CORE SHIELD (ALMR) ITEMS IIIA-IIIF

The mockups used during this part of the study pertain to the location of the stored fuel above the core area in the vicinity of the Intermediate Heat Exchanger (IHX). Hence, the spectrum modifier contained 180 cm of sodium behind which sodium and other shielding materials were interspersed to mock up present-day U.S. concepts of shield designs for that area. This spectrum modifier was discussed earlier in section 4.1.

For the first mockup, Item IIIA, the heterogeneous slab of fuel pins was placed behind SM-2 as seen in Figure 46. Bonner ball measurements were made on centerline at 30 and 150 cm and these results are given in Tables 49 and 50. Radial traverses were made at 30 cm behind the mockup with the 3- and 10-in Bonner balls and these data are in Tables 51 and 52. Repeats of these traverses were made with the bare and Cd-covered fission chambers and with the bare detector when Cd covered the face of the mockup.

Data from these traverses are recorded in Tables 53, 54, and 55. Bare and Cd-covered detector measurements were made at 0.7, 30, and 150 cm behind the mockup and the data are reported in Tables 25, 56, and 57. Data with the bare detector at 30 and 150 cm with Cd placed over the mockup are given in Tables 56 and 57. Count rates obtained with the bare detector inside the Cd hut at 0.7 and 30 cm are part of Tables 25 and 56.

The homogeneous slab was substituted for the heterogeneous slab behind the spectrum modifier to give the mockup in Item IIIB (see Figure 47). Foreground measurements were made on centerline at 30 and 150 cm and background measurements were made at 150 cm with the Bonner balls. These data are located in Tables 49 and 50. Bare and Cd-covered fission chamber measurements were made at 0.7, 30, and 150 cm on centerline, and the data are placed in Tables 25, 56, and 57. With Cd over the face of the mockup, data was obtained at 30 and 150 cm with a bare detector, and these results are in Tables 56 and 57. Data from runs with the bare detector in the Cd hut at 0.7 and 30 cm are given in Tables 25 and 56.

Radial traverses were made at 30 cm behind the mockup with the 3- and 10-in Bonner balls and these count rates are listed in Tables 51 and 52. Similar traverses were made with the bare fission chamber with and without Cd over the face of the mockup. These results are in Tables 53 and 54. The same traverse was made with the detector Cd covered and the data are in Table 55.

The radial blanket used earlier in the experiment replaced the homogeneous fuel pin vessel in Item IIB to give Item IIIC, as seen in Figure 48. Results from Bonner ball measurements at 30 and 150 cm are given in Tables 49 and 50. Fission chamber count rates with the detector bare and Cd covered at 0.7, 30, and 150 cm are part of Tables 25, 56, and 57. Bare detector data at 30 and 150 cm with Cd over the mockup are located in Tables 56 and 57. Data from the bare detector in the Cd hut are located in Table 25 for the 0.7-cm location and Table 56 for the 30-cm location.

The homogeneous IVFS vessel was returned to the mockup in place of the radial blanket and 5 cm of B_4C placed after it to give the mockup in Item IIID as shown in Figure 49. The measurements made in IIIC were repeated here, with the Bonner ball data in Tables 49 and 50, and the bare and Cd-covered fission chamber data at 0.7, 30, and 150 cm in Tables 25, 56, and 57. The data with the bare detector at 30 and 150 cm and Cd over the mockup are listed in Tables 56 and 57. Data from measurements inside

the Cd hut at 0.7 and 30 cm are in Tables 25 and 56.

The locations of the IVFS vessel and the B_4C slab were reversed in Item IIIE (see Figure 50). Measurements with the Bonner balls and fission chamber were repeated again. Bonner ball data are given in Tables 49 and 50. Bare and Cd-covered fission chamber measurements at 0.7, 30, and 150 cm are given in Tables 25, 56, and 57. Results from measurements at 30 and 150 cm with Cd over the mockup are in Tables 56 and 57. Data at 0.7 and 30 cm inside the Cd hut are listed in Tables 25 and 56.

In the final mockup listed for this experiment, Item IIIF, the IVFS homogeneous slab was followed by a void, 2.5 cm SS, 5 cm B_4C, and 2.5 cm Al as seen in Figure 51. Bare and Cd-covered measurements were made at 0.7 cm inside the void and these results are listed in Table 48. Behind the mockup, measurements were made with the Bonner balls at 30 and 150 cm and these data are located in Tables 49 and 50. Bare and Cd-covered fission chamber data at 0.7, 30, and 150 cm are given in Tables 56, 57, and 53. Bare detector data at 30 and 150 cm with Cd over the mockup are in Tables 56 and 57. Data in the Cd hut are listed in Tables 25 and 56.

5. ANALYSIS OF EXPERIMENTAL ERRORS

The errors associated with the measurements are due to a number of uncertainties: (1) the sizes of the gaps between slabs, unavoidably introduced in the configurations, (2) in the positions of the detectors, (3) the detector count rate statistics and calibrations, (4) the reactor power determinations, and (5) the effects of the exposure of the configurations to the weather. Of these, the uncertainty due to the weather is the least understood and probably beyond simple estimation. The uncertainty lies in the amount of moisture between the slabs and in the lithiated paraffin surrounding them. During this experiment the mockups were covered with a plastic tarpaulin that would limit the amount of moisture reaching the slabs. Thus, for this experiment, the effect of the weather was assumed to be negligible.

The TSR-II power level for each measurement was determined from the output of two fission chambers located in the reactor shield along the midplane of the reactor. The response of these chambers to the reactor source was monitored prior to the experiment through the use of gold foils and this ratio, detector response to gold foil results, agreed within about 5% with a history of earlier such comparisons. These detectors were calibrated on a daily basis using a ^{252}Cf source, with the calibration values lying within about a 6% spread (±3% of an average value). During any one detector traverse in a given day, the variation in the reactor power indicated by the monitor outputs was at most only 3%; however, during the several months the experiment was being performed, the monitors indicated a spread in any one power level of about ±5%. Thus, the uncertainty in the reactor power determination was assumed to be ±5%.

Count-rate statistics are expressed in a manner specific to each detector. For the NE-213 measurements, counting statistics and unfolding errors are included in the unfolding of the pulse-height spectra using the FERD code, with the resulting flux expressed in terms of lower and upper limits that represent a 68% confidence interval. Similar errors are expressed in the tabular data for the hydrogen measurements unfolded using SPEC4. Neither of the spectra, NE-213 or hydrogen counter, reflects the error in determining the reactor power since this error is not included in the unfolding program. This, as seen above, could be as much as ±5%.

The Bonner balls were calibrated on a daily basis using ^{252}Cf as a source, with the resulting count rates falling within about ±3% of an average value obtained throughout

the years. Movement of the Bonner balls along a traversing mechanism can vary the detector location with respect to the configuration several millimeters on either side of a straight line. For the measurements perpendicular to the configuration centerline at 30 cm behind the configuration, such variations in the detector position could amount to a change in the count rate of about 2%. For the measurements on centerline beyond the 30 cm point, the error in positioning several millimeters either side of the selected location would lie within the statistics of the measurement. Rather than calculate probable errors for each measurement in a series of measurements during a traverse, we prefer, in general, to quote a value for the error in the measurements for a given experiment. Thus, assuming the estimated upper limit for all the errors, the errors assigned to the Bonner ball measurements should be less than ±10%.

The fission chamber used throughout this experiment as a companion detector to the Bonner balls was calibrated on a daily basis using the thermal neutron flux generated by placement of the ^{252}Cf in a jug of lucite. The resulting count rates fell within about ±5% of an average value obtained throughout the experiment. Movement of the fission chamber was similar to that of the Bonner ball described earlier and the procedure in determining the possible errors with this detector follow that described for the Bonner balls.

REFERENCES

1. R.E. Maerker et al., *Calibration of the Bonner Ball Neutron Detectors Used at the Tower Shielding Facility*, ORNL/TM-3465 (June 1971).

2. C. E. Burgart and M. B. Emmett, *Monte Carlo Calculations of the Response Functions of Bonner Ball Neutron Detectors*, ORNL/TM-3739 (April 1972).

3. B. W. Rust, D. T. Ingersoll, and W. R. Burrus, *A User's Manual for the FERDO and FERD Unfolding Codes*, ORNL/TM-8720 (September 1983).

4. J. O. Johnson and D. T. Ingersoll, *User's Guide for the Revised SPEC-4 Neutron Spectrum Unfolding Code*, ORNL/TM-7384 (August 1980).

ACKNOWLEDGEMENTS

The author is deeply indebted to D. T. Ingersoll and J. V. Pace, III, of ORNL's Engineering Physics and Mathematics Division, to P. B. Hemmig of DOE/Washington, and to the JASPER working group from Japan for their participation and assistance in formulating the Experimental Program Plan. A deep gratitude is expressed to the TSR-II operating crew of the Research Reactors Division and TSF assigned members of the Instrumentation and Controls Division for not only maintaining a viable source but for experimental help when needed. Appreciation is expressed to E. R. Specht, Rockwell International, W. H. Harless, General Electric Company, R. K. Disney, Westinghouse-ARD, W. L. Bunch, Westinghouse-Hanford for timely suggestions. Special thanks go to G. A. Marvin and S. A. Raby for their efforts in editing and preparing this report.

APPENDIX A

EXPERIMENTAL PROGRAM PLAN FOR THE JASPER IN-VESSEL FUEL STORAGE (IVFS) EXPERIMENT

I. Spectrum Modifier (SM-0)
- A. SM-0 (10 cm Fe + 9 cm Al + 2.54 cm boral).
  1. NE 213 and hydrogen counter spectral measurements on centerline as close as feasible behind shield mockup
  2. 3-, 5-, and 10-in Bonner ball measurements on centerline at location of NE 213 measurements
  3. 3-, 4-, 5-, 8-, 10-, and 12-in Bonner ball measurements on centerline:
     a. 30 cm behind shield mockup
     b. 150 cm behind shield mockup (foreground and background)
  4. ^{235}U fission chamber (bare and Cd-covered) on centerline:
     a. 30 cm behind shield mockup
     b. 150 cm behind shield mockup (foreground and background)
- B. SM-1 (10 cm Fe + 9 cm Al + 2.54 cm boral + 20 cm radial blanket slabs)
  1. NE 213 and hydrogen counter spectral measurements on centerline as close as feasible behind shield mockup
  2. 3-, 5-, and 10-in Bonner ball measurements on centerline at location of NE 213 measurements
  3. 3-, 4-, 5-, 8-, 10-, and 12-in Bonner ball measurements on centerline:
     a. 30 cm behind shield mockup
     b. 150 cm behind shield mockup (foreground and background)
  4. ^{235}U fission chamber (bare and Cd-covered) on centerline:
     a. 30 cm behind shield mockup
     b. 150 cm behind shield mockup (foreground and background)
- C. SM-2 (10 cm Fe + 9 cm Al + 2.54 cm boral + 180 cm Na)
  1. NE 213 and hydrogen counter spectral measurements on centerline as close as feasible behind shield mockup
  2. 3-, 5-, and 10-in Bonner ball measurements on centerline at location of NE 213 measurements
  3. 3-, 4-, 5-, 8-, 10-, and 12-in Bonner ball measurements on centerline:
     a. 30 cm behind shield mockup
     b. 150 cm behind shield mockup (foreground and background)
  4. ^{235}U fission chamber on centerline:
     a. 0.7, 30, and 150 cm behind shield mockup (bare and Cd-covered detector)
     b. bare detector at 30 and 150 cm, cadmium over face of shield mockup
     c. bare detector with cadmium hut, 0.7 and 30 cm

II. Removable Radial Shield
- A. SM-1 + 1.3 cm Al + 15 cm SS + 1.3 cm Al + 10 cm C + 5 cm SS
  1. 3-, 4-, 5-, 8-, 10-, and 12-in Bonner ball measurements on centerline:
     a. 30 cm behind shield mockup

b. 150 cm behind shield mockup (foreground and background)

2. ^{235}U fission chamber on centerline:
   a. 30 cm behind shield mockup (bare and Cd-covered detector)
   b. 150 cm behind shield mockup (foreground and background), (bare and Cd-covered detector)
   c. bare detector at 150 cm, cadmium over face of shield mockup

B. SM-1 + 1.3 cm Al + 15 cm SS + 1.3 cm Al + 10 cm C + 5 cm SS + 1.3 cm Al + 10 cm C + 5 cm SS + 1.3 cm Al + 2.5 cm SS
   1. NE 213 and hydrogen counter spectrum measurements on centerline as close as feasible behind shield mockup (also background if necessary)
   2. 3-, 5-, and 10-in Bonner ball measurements on centerline at location of NE 213 measurements
   3. 3- and 10-in Bonner ball horizontal traverses at 30 cm behind shield mockup
   4. ^{235}U fission chamber horizontal traverses at 30 cm behind shield mockup
      a. bare detector
      b. Cd-covered detector
      c. bare detector, cadmium over face of shield mockup
   5. 3-, 4-, 5-, 8-, 10-, and 12-in Bonner ball measurements on centerline:
      a. 30 cm behind shield mockup
      b. 150 cm behind shield mockup (foreground and background)
   6. ^{235}U fission chamber measurements on centerline:
      a. 30 and 150 cm behind shield mockup (bare and Cd-covered detector)
      b. bare detector at 30 and 150 cm, cadmium over face of shield mockup

C. SM-1 + 1.3 cm Al + 15 cm SS + 1.3 cm Al + 10 cm C + 5 cm SS + 1.3 cm Al + 10 cm C + 5 cm SS + 1.3 cm Al + 2.5 cm SS + 18.3 cm thick IVFS vessel
   1. NE 213 and hydrogen counter spectrum measurements on centerline as close as feasible behind shield mockup (also background if necessary)
   2. 3-, 5-, and 10-in Bonner ball measurements on centerline at location of NE 213 measurements (also background if necessary)
   3. 3- and 10-in Bonner ball horizontal traverses at 30 cm behind shield mockup
   4. ^{235}U fission chamber horizontal traverses at 30 cm behind shield mockup
      a. bare detector
      b. Cd-covered detector
      c. bare detector, cadmium over face of shield mockup
   5. 3-, 4-, 5-, 8-, 10-, and 12-in Bonner ball measurements on centerline:
      a. 30 cm behind shield mockup
      b. 150 cm behind shield mockup (foreground and background)
   6. ^{235}U fission chamber measurements on centerline:
      a. 30 and 150 cm behind shield mockup (bare and Cd-covered

detector)
b. bare detector at 30 and 150 cm, cadmium over face of shield mockup

D. SM-1 + 1.3 cm Al + 15 cm SS + 1.3 cm Al + 10 cm C + 5 cm SS + 1.3 cm Al + 10 cm C + 5 cm SS + 1.3 cm Al + 2.5 cm SS + 16.8 cm heterogeneous IVFS slab
1. 3- and 10-in Bonner ball horizontal traverses at 30 cm behind shield mockup
2. ^{235}U fission chamber horizontal traverses at 30 cm behind shield mockup
   a. bare detector
   b. Cd-covered detector
   c. bare detector, cadmium over face of shield mockup
3. 3-, 4-, 5-, 8-, 10-, and 12-in Bonner ball measurements on centerline:
   a. 30 cm behind shield mockup
   b. 150 cm behind shield mockup (foreground and background)
4. ^{235}U fission chamber measurements on centerline:
   a. 0.7, 30, and 150 cm behind shield mockup (bare and Cd-covered detector)
   b. bare detector at 30 and 150 cm, cadmium over face of shield mockup
   c. bare detector inside cadmium hut, 0.7 and 30 cm
   d. 0.7 cm, bare detector with cadmium wrapped around cylinder housing the detector

E. SM-1 + 1.3 cm Al + 15 cm SS + 1.3 cm Al + 10 cm C + 5 cm SS + 1.3 cm Al + 10 cm C + 5 cm SS + 1.3 cm Al + 2.5 cm SS + 16.15 cm homogeneous IVFS slab
1. 3- and 10-in Bonner ball horizontal traverses at 30 cm behind shield mockup
2. ^{235}U fission chamber horizontal traverses at 30 cm behind shield mockup
   a. bare detector
   b. Cd-covered detector
   c. bare detector, cadmium over face of shield mockup
3. 3-, 4-, 5-, 8-, 10-, and 12-in Bonner ball measurements on centerline:
   a. 30 cm behind shield mockup
   b. 150 cm behind shield mockup (foreground and background)
4. ^{235}U fission chamber measurements on centerline:
   a. 0.7, 30, and 150 cm behind shield mockup (bare and Cd-covered detector)
   b. bare detector at 30 and 150 cm, cadmium over face of shield mockup
   c. bare detector inside cadmium hut, 0.7 and 30 cm

F. SM-1 + 1.3 cm Al + 15 cm SS + 1.3 cm Al + 10 cm C + 5 cm SS + 1.3 cm Al + 10 cm C + 5 cm SS + 1.3 cm Al + 5 cm B_4C + 2.5 cm SS
1. NE 213 and hydrogen counter spectrum measurements on centerline as close as feasible behind shield mockup
2. 3-, 5-, and 10-in Bonner ball measurements on centerline at location

of NE 213 measurements

3. 3-, 4-, 5-, 8-, 10-, and 12-in Bonner ball measurements on centerline:
   a. 30 cm behind shield mockup
   b. 150 cm behind shield mockup (foreground and background)
4. ^{235}U fission chamber measurements on centerline:
   a. 30 and 150 cm behind shield mockup (bare and Cd-covered detector)
   b. bare detector at 30 and 150 cm, cadmium over face of shield mockup

G. SM-1 + 1.3 cm Al + 15 cm SS + 1.3 cm Al + 10 cm C + 5 cm SS + 1.3 cm Al + 10 cm C + 5 cm SS + 1.3 cm Al + 5 cm B_4C + 2.5 cm SS + 18.3 cm thick IVFS slab

1. NE 213 and hydrogen counter spectrum measurements on centerline as close as feasible behind shield mockup
2. 3-, 5-, and 10-in Bonner ball measurements on centerline at location of NE 213 measurements
3. 3-, 4-, 5-, 8-, 10-, and 12-in Bonner ball measurements on centerline:
   a. 30 cm behind shield mockup
   b. 150 cm behind shield mockup (foreground and background)]
4. ^{235}U fission chamber measurements on centerline:
   a. 30 and 150 cm behind shield mockup (bare and Cd-covered detector)
   b. bare detector at 30 and 150 cm, cadmium over face of shield mockup

H. SM-1 + 1.3 cm Al + 15 cm SS + 1.3 cm Al + 10 cm C + 5 cm SS + 1.3 cm Al + 10 cm C + 5 cm SS + 1.3 cm Al + 15 cm B_4C + 2.5 cm SS

1. 3- and 10-in Bonner ball horizontal traverses at 30 cm behind shield mockup
2. ^{235}U fission chamber horizontal traverses at 30 cm behind shield mockup
   a. bare detector
   b. Cd-covered detector
   c. bare detector, cadmium over face of shield mockup
3. 3-, 4-, 5-, 8-, 10-, and 12-in Bonner ball measurements on centerline:
   a. 30 cm behind shield mockup
   b. 150 cm behind shield mockup (foreground and background)
4. ^{235}U fission chamber measurements on centerline:
   a. 0.7, 30, and 150 cm behind shield mockup (bare and Cd-covered detector)
   b. bare detector at 30 and 150 cm, cadmium over face of shield mockup
   c. 0.7 and 30 cm, bare detector with cadmium wrapped around cylinder housing the detector

I. SM-1 + 1.3 cm Al + 15 cm SS + 1.3 cm Al + 10 cm C + 5 cm SS + 1.3 cm Al + 10 cm C + 5 cm SS + 1.3 cm Al + 15 cm B_4C + 2.5 cm SS + 18.3 cm thick IVFS slab

1. 3- and 10-in Bonner ball horizontal traverses at 30 cm behind shield mockup

2. ^{235}U fission chamber horizontal traverses at 30 cm behind shield mockup
   a. bare detector
   b. Cd-covered detector
   c. bare detector, cadmium over face of shield mockup
3. 3-, 4-, 5-, 8-, 10-, and 12-in Bonner ball measurements on centerline:
   a. 30 cm behind shield mockup
   b. 150 cm behind shield mockup (foreground and background)
4. ^{235}U fission chamber measurements on centerline:
   a. 0.7, 30, and 150 cm behind shield mockup (bare and Cd-covered detector)
   b. bare detector at 30 and 150 cm, cadmium over face of shield mockup
   c. 0.7 cm, bare detector with cadmium wrapped around cylinder housing the detector
   d. 0.7 and 30 cm, bare detector inside cadmium hut
5. Remove lithiated paraffin blocks from around fuel pins
   a. Repeat 3 and 4 above

J. SM-1 + 1.3 cm Al + 15 cm SS + 1.3 cm Al + 10 cm C + 5 cm SS + 1.3 cm Al + 10 cm C + 5 cm SS + 1.3 cm Al + 15 cm B_4C + 2.5 cm SS + 16.8 cm heterogeneous IVFS slab
   1. 3- and 10-in Bonner ball horizontal traverses at 30 cm behind shield mockup
   2. ^{235}U fission chamber horizontal traverses at 30 cm behind shield mockup
      a. bare detector
      b. Cd-covered detector
      c. bare detector, cadmium over face of shield mockup
   3. 3-, 4-, 5-, 8-, 10-, and 12-in Bonner ball measurements on centerline:
      a. 30 cm behind shield mockup
      b. 150 cm behind shield mockup (foreground and background)
   4. ^{235}U fission chamber measurements on centerline:
      a. 0.7, 30, and 150 cm behind shield mockup (bare and Cd-covered detector)
      b. bare detector at 30 and 150 cm, cadmium over face of shield mockup
      c. 0.7 and 30 cm, bare detector inside cadmium hut

K. SM-1 + 1.3 cm Al + 15 cm SS + 1.3 cm Al + 10 cm C + 5 cm SS + 1.3 cm Al + 10 cm C + 5 cm SS + 1.3 cm Al + 15 cm B_4C + 2.5 cm SS + 16.15 cm homogeneous IVFS slab
   1. 3- and 10-in Bonner ball horizontal traverses at 30 cm behind shield mockup
   2. ^{235}U fission chamber horizontal traverses at 30 cm behind shield mockup
      a. bare detector
      b. Cd-covered detector
      c. bare detector, cadmium over face of shield mockup
   3. 3-, 4-, 5-, 8-, 10-, and 12-in Bonner ball measurements on centerline:

a. 30 cm behind shield mockup
b. 150 cm behind shield mockup (foreground and background)

4. ^{235}U fission chamber measurements on centerline:
   a. 0.7, 30, and 150 cm behind shield mockup (bare and Cd-covered detector)
   b. bare detector at 30 and 150 cm, cadmium over face of shield mockup
   c. 0.7 and 30 cm, bare detector inside cadmium hut

L. SM-1 + 1.3 cm Al + 15 cm SS + 1.3 cm Al + 10 cm C + 5 cm SS + 1.3 cm Al + 10 cm C + 5 cm SS + 1.3 cm Al + 15 cm B_4C + 2.5 cm SS + 10 cm radial blanket

1. 3- and 10-in Bonner ball horizontal traverses at 30 cm behind shield mockup
2. ^{235}U fission chamber horizontal traverses at 30 cm behind shield mockup
   a. bare detector
   b. Cd-covered detector
   c. bare detector, cadmium over face of shield mockup
3. 3-, 4-, 5-, 8-, 10-, and 12-in Bonner ball measurements on centerline:
   a. 30 cm behind shield mockup
   b. 150 cm behind shield mockup (foreground and background)
4. ^{235}U fission chamber measurements on centerline:
   a. 0.7, 30, and 150 cm behind shield mockup (bare and Cd-covered detector)
   b. bare detector at 30 and 150 cm, cadmium over face of shield mockup
   c. 0.7 cm, bare detector with cadmium wrapped around cylinder housing the detector
   d. 0.7 and 30 cm, bare detector inside cadmium hut

M. SM-1 + 1.3 cm Al + 15 cm SS + 1.3 cm Al + 15 cm B_4C + 2.5 cm SS + 1.3 cm Al + 15 cm B_4C + 1.3 cm Al + 15 cm B_4C (Loop-type mockup)

1. ^{235}U fission chamber horizontal traverses at 30 cm behind shield mockup
   a. bare detector
   b. Cd-covered detector
   c. bare detector, cadmium over face of shield mockup
2. 3-, 4-, 5-, 8-, 10-, and 12-in Bonner ball measurements on centerline:
   a. 30 cm behind shield mockup
   b. 150 cm behind shield mockup (foreground and background)
3. ^{235}U fission chamber measurements on centerline:
   a. 0.7, 30, and 150 cm behind shield mockup (bare and Cd-covered detector)
   b. bare detector at 30 and 150 cm, cadmium over face of shield mockup
   c. 0.7 cm, bare detector with cadmium wrapped around cylinder housing the detector
   d. 0.7 and 30 cm, bare detector inside cadmium hut

N. SM-1 + 1.3 cm Al + 15 cm SS + 1.3 cm Al + 15 cm B_4C + 2.54 cm SS +

1.3 cm Al + 15 cm B_4C + 1.3 cm Al + 15 cm B_4C + 18.3-cm-thick IVFS slab (Loop-type mockup)

1. NE 213 and hydrogen counter spectrum measurements on centerline as close as feasible behind shield mockup (also background if necessary)
2. 3-, 5-, and 10-in Bonner ball measurements on centerline at location of NE 213 measurements.
3. 3- and 10-in Bonner ball horizontal traverses at 30 cm behind shield mockup.
4. ^{235}U fission chamber horizontal traverses at 30 cm behind shield mockup
   a. bare detector
   b. Cd-covered detector
   c. bare detector, cadmium over face of shield mockup
5. 3-, 4-, 5-, 8-, 10-, and 12-in Bonner ball measurements on centerline:
   a. 30 cm behind shield mockup
   b. 150 cm behind shield mockup (foreground and background)
6. ^{235}U fission chamber measurements on centerline:
   a. 0.7, 30, and 150 cm behind shield mockup (bare and Cd-covered detector)
   b. bare detector at 30 and 150 cm, cadmium over face of shield mockup
   c. 0.7 cm, bare detector with cadmium wrapped around cylinder housing the detector
   d. 0.7 and 30 cm, bare detector inside cadmium hut

O. SM-1 + 1.3 cm Al + 15 cm SS + 1.3 cm Al + 15 cm B_4C + 2.54 cm SS + 1.3 cm Al + 15 cm B_4C + 1.3 cm Al + 15 cm B_4C + 16.8 cm heterogeneous IVFS slab (Loop-type mockup)

1. NE 213 and hydrogen counter spectrum measurements on centerline as close as feasible behind shield mockup (also background if necessary)
2. 3-, 5-, and 10-in Bonner ball measurements on centerline at location of NE 213 measurements.
3. 3- and 10-in Bonner ball horizontal traverses at 30 cm behind shield mockup.
4. ^{235}U fission chamber horizontal traverses at 30 cm behind shield mockup
   a. bare detector
   b. Cd-covered detector
   c. bare detector, cadmium over face of shield mockup
5. 3-, 4-, 5-, 8-, 10-, and 12-in Bonner ball measurements on centerline:
   a. 30 cm behind shield mockup
   b. 150 cm behind shield mockup (foreground and background)
6. ^{235}U fission chamber measurements on centerline:
   a. 0.7, 30, and 150 cm behind shield mockup (bare and Cd-covered detector)
   b. bare detector at 30 and 150 cm, cadmium over face of shield mockup

c. 0.7 cm, bare detector with cadmium wrapped around cylinder housing the detector
d. 0.7 and 30 cm, bare detector inside cadmium hut

P. SM-1 + 1.3 cm Al + 15 cm SS + 1.3 cm Al + 10 cm C + 5 cm SS + 1.3 cm Al + 10 cm C + 5 cm SS + 1.3 cm Al + 15 cm B_4C + 2.5 cm SS + 18.3-cm-thick IVFS slab + void + 2.5 cm Al + 5 cm SS + 20 cm B_4C
1. 3-, 4-, 5-, 8-, 10-, and 12-in Bonner ball measurements on centerline:
   a. 30 cm behind shield mockup
   b. 150 cm behind shield mockup (foreground and background)
2. ^{235}U fission chamber measurements on centerline:
   a. 0.7, 30, and 150 cm behind shield mockup (bare and Cd-covered detector)
   b. bare detector at 30 and 150 cm, cadmium over face of shield mockup
   c. 0.7 cm, bare detector with cadmium wrapped around cylinder housing the detector
   d. 0.7 and 30 cm, bare detector inside cadmium hut
3. ^{235}U fission chamber measurements on centerline in the void:
   a. bare detector
   b. Cd-covered detector
   c. bare detector with cadmium wrapped around the detector's cylindrical housing

Q. SM-1 + 1.3 cm Al + 15 cm SS + 1.3 cm Al + 10 cm C + 5 cm SS + 1.3 cm Al + 10 cm C + 5 cm SS + 1.3 cm Al + 15 cm B_4C + 2.5 cm SS + 18.3-cm-thick IVFS slab + void + 2.5 cm Al + 5 cm SS + 1.3 cm Al + 10 cm C + 5 cm SS + 1.3 cm Al + 10 cm C + 5 cm SS + 1.3 cm Al + 10 cm C + 5 cm SS
1. 3-, 4-, 5-, 8-, 10-, and 12-in Bonner ball measurements on centerline:
   a. 30 cm behind shield mockup
   b. 150 cm behind shield mockup (foreground and background)
2. ^{235}U fission chamber measurements on centerline:
   a. 0.7, 30, and 150 cm behind shield mockup (bare and Cd-covered detector)
   b. bare detector at 30 and 150 cm, cadmium over face of shield mockup
   c. 0.7 cm, bare detector with cadmium wrapped around cylinder housing the detector
   d. 0.7 and 30 cm, bare detector inside cadmium hut
3. ^{235}U fission chamber measurements on centerline in the void:
   a. bare detector
   b. Cd-covered detector
   c. bare detector, with cadmium wrapped around the detector's cylindrical housing

III. Above-Core (ALMR)

A. SM-2 + 16.8 cm heterogeneous IVFS slab
1. 3-, 4-, 5-, 8-, 10-, and 12-in Bonner ball measurements on centerline:
   a. 30 cm behind shield mockup

b. 150 cm behind shield mockup (foreground and background)

2. 3- and 10-in Bonner ball horizontal traverses at 30 cm behind shield mockup

3. ^{235}U fission chamber measurements on centerline:
   a. 0.7, 30, and 150 cm behind shield mockup (bare and Cd-covered detector)
   b. bare detector at 30 and 150 cm, cadmium over face of shield mockup
   c. 0.7 and 30 cm, bare detector inside Cd hut

4. ^{235}U fission chamber horizontal traverses at 30 cm behind shield mockup:
   a. bare detector
   b. Cd-covered detector
   c. bare detector, cadmium over face of shield mockup

B. SM-2 + 16.15 cm homogeneous IVFS slab

1. 3-, 4-, 5-, 8-, 10-, and 12-in Bonner ball measurements on centerline:
   a. 30 cm behind shield mockup
   b. 150 cm behind shield mockup (foreground and background)

2. 3- and 10-in Bonner ball horizontal traverses at 30 cm behind shield mockups

3. ^{235}U fission chamber measurements on centerline:
   a. 0.7, 30, and 150 cm behind shield mockup (bare and Cd-covered detector)
   b. bare detector at 30 and 150 cm, cadmium over face of shield mockup
   c. 0.7 and 30 cm, bare detector inside Cd hut

4. ^{235}U fission chamber horizontal traverses at 30 cm behind shield mockup:
   a. bare detector
   b. Cd-covered detector
   c. bare detector, cadmium over face of shield mockup

C. SM-2 + 10 cm radial blanket

1. 3-, 4-, 5-, 8-, 10, and 12-in Bonner ball measurements on centerline:
   a. 30 cm behind shield mockup
   b. 150 cm behind shield mockup (foreground and background)

2. ^{235}U fission chamber measurements on centerline:
   a. 0.7, 30, and 150 cm behind shield mockup (bare and Cd-covered detector)
   b. bare detector at 30 and 150 cm, cadmium over face of shield mockup
   c. 0.7 and 30 cm, bare detector inside Cd hut

D. SM-2 + 16.15 cm homogeneous IVFS slab + 5 cm B_4C

1. 3-, 4-, 5-, 8-, 10, and 12-in Bonner ball measurements on centerline:
   a. 30 cm behind shield mockup
   b. 150 cm behind shield mockup (foreground and background)

2. ^{235}U fission chamber measurements on centerline:
   a. 0.7, 30, and 150 cm behind shield mockup (bare and Cd-covered detector)

b. bare detector at 30 and 150 cm, cadmium over face of shield mockup
c. 0.7 and 30 cm, bare detector inside Cd hut

E. SM-2 + 5 cm B_4C + 16.15 cm homogeneous IVFS slab
1. 3-, 4-, 5-, 8-, 10, and 12-in Bonner ball measurements on centerline:
a. 30 cm behind shield mockup
b. 150 cm behind shield mockup (foreground and background)
2. ^{235}U fission chamber measurements on centerline:
a. 0.7, 30, and 150 cm behind shield mockup (bare and Cd-covered detector)
b. bare detector at 30 and 150 cm, cadmium over face of shield mockup
c. 0.7 and 30 cm, bare detector inside Cd hut

F. SM-2 + 16.15 cm homogeneous IVFS slab + void + 2.5 cm SS + 5.15 cm B_4C + 2.5 cm Al
1. 3-, 4-, 5-, 8-, 10-, and 12-in Bonner ball measurements on centerline:
a. 30 cm behind shield mockup
b. 150 cm behind shield mockup (foreground and background)
2. ^{235}U fission chamber measurements on centerline:
a. 0.7, 30, and 150 cm behind shield mockup (bare and Cd-covered detector)
b. bare detector at 30 and 150 cm, cadmium over face of shield mockup
c. 0.7 and 30 cm, bare detector inside Cd hut
3. ^{235}U fission chamber measurements on centerline in the void:
a. bare detector
b. Cd-covered detector

APPENDIX B

TABLES OF DATA

Table 1. Analysis of iron slabs (ρ = 7.86 g/cc) used in spectrum modifier

Element	wt %
Fe	98.4
C	.25
Cr	.15
Cu	.03
Mn	1.0
Mo	.02
Ni	.05
Si	.25

Table 2. Analysis of 6061 aluminum (ρ = 2.70 g/cc)

Element	wt %	ppm
Al	97.5	
Cr	.22	
Cu	.23	
Fe	.47	
Mg	.86	
Mn	.01	
Si	.63	
Ti	.042	
Zn	.07	
Li		3
Ni		50
Sn		<10
V		150

Table 3. Composition of boral slabs used in spectrum modifier

	(B_4C - 40-43 vol % in B_4C-Al mixture)		
Component	Density (g/cc)	Elemental Composition (wt %)	With Al Cladding (wt %)
B_4C	2.3		
Al	2.70	65	~75
B		27.5	~19.6
C		7.5	~5.4

Table 4. Composition of UO_2 radial blanket

Component	vol %	Density (g/cc)
UO_2 (pellets)	64.6	10.28
Al (8001)	11.2	2.8
Na	23.2	0.92
Void	1.0	----

UO_2 content 88.18 wt %

Isotope %

^{234}U	.0053	^{236}U	---
^{235}U	.713	^{238}U	99.28

Metallic Impurities in UO_2 (ppm)*

Al	<20	Cu	1	Na	<20
B	<1	F	<2	Ni	<10
Be	<2	Fe	<20	Pb	<4
Bi	<2	H_2O	2.1	Si	<20
C	<10	Li	<1	Sn	<2
Ca	<20	Mg	<10	Ta	<25
Cd	<0.5	Mn	<4	Tu	<4
Cl	<3.3	Mo	<10	W	<25
Co	<2	N	54	Zr	<25
Cr	<10				

*ppm = parts per million

Table 5. Analysis of aluminum used in UO_2 radial blanket cladding (ρ = 2.7 g/cc)

Element	wt %	ppm
Al	Major	
Fe	.59	
Ni	1.13	
B		<6
Be		<20
Cd		<20
Co		<20
Cr		<6
Cu		52.9
Li		6
Mg		3.04
Mn		11.2
Mo		<6
Pb		<20
Si		27.5
Sn		<60
T		<2000
Ti		65.5
V		44.2
W		<60
Zr		<20

Table 6. Composition of lithiated-paraffin bricks (ρ = 1.15 g/cc)

Component	wt %
C_nH_{2n+2}	60
Li_2CO_3	40

Table 7. Composition of the small concrete blocks on each side of the spectrum modifier (ρ = 2.39 g/cc)

Element	wt %
C	10.36
O	49.03
Ca	38.05
Fe	0.37
Si	0.78
Mg	0.23
S	0.17
P	0.04
Na	0.03
K	0.04
H	0.42
R*	0.47
	99.99

*R is an unspecified mix of Al, Ti, Cr, and possibly other trace metals.

Table 8. Composition of sodium slabs (ρ = 0.945 g/cc)

Element	wt %
Na	99.7
Ca, Zn	0.3

Table 9. Analysis of boron carbide used in shield mockups

Element	wt%	ppm
B	76.7	
C	19.52	
Al		50
Ca		800
Cl		10
Co		<1
Cr		2
Cu		<1
Fe		600
Mg		25
Mn		10
Na		1
P		2
S		5
Si		50
Ti		225

Table 10. Analysis of graphite used in shield mockup (ρ = 1.62 g/cc)

Metallic Impurities in Carbon (ppm)					
Ag	<0.5	Ge	<5	Sb	<10
Al	12.5	Hg	<10	Si	100
B	1.5	In	<10	Sn	<10
Ba	<5	K	<100	Sr	<10
Be	<0.5	Li	<2	Ta	<10
Bi	<10	Mg	7.5	Te	<25
Ca	150	Mn	<1	Ti	30
Cd	<25	Mo	<5	V	100
Co	<10	Na	<5	W	<5
Cr	<10	Nb	<5	Zn	10
Cu	7.5	Ni	<10	Zr	<5
Fe	50	Pb	<5		
Ga	<10	Rb	<5		

Table 11. Analysis of type 304 stainless steel (ρ = 7.92 g/cc)

Element	wt% Lower	Upper
Fe	68.1	- 71.2
Cr	18.0	- 19.1
Ni	8.8	- 9.8
Mn	1.04	- 1.65
Si	0.33	- 0.65
C	0.024	- 0.085
O_2	0.013	- 0.021
P		0.028
S		0.022
Mo		0.30
Cu		0.26
Co		0.10

Table 12. Analysis of 61-cm x 61-cm x 30.5-cm (ρ = 2.40 g/cc) concrete blocks used to surround configuration

Component	wt%	Component	wt%
CO_3	41.9	Al_2O_3	2.2
Ca	27.4	Fe_2O_3	.60
SiO_2	18.1	SO_3	.32
H_2O	4.0	P_2O_5	.035
Mg	3.66	K	.30
O_2	1.4		

Table 13. Analysis of lead slabs (ρ = 11.35 g/cc)

Element	wt%	PPM
Pb	99.9	
Al		<3
Ag		30
B		<1
Ca		1
Cr		10
Cu		800
Fe		1
Li		20
Mg		<3
Mn		5
Na		1
Ni		30
P		5
Si		<3
Sn		30

Table 14. Fast neutron fluxes (> 0.8 MeV) on centerline at 25 cm behind the lead slab (Item IA) Run 7900.A

Neutron Energy (MeV)	Flux (neutrons $cm^{-2}MeV^{-1}kW^{-1}s^{-1}$) Lower Limit	Upper Limit	Neutron Energy (MeV)	Flux (neutrons $cm^{-2}MeV^{-1}kW^{-1}s^{-1}$) Lower Limit	Upper Limit
8.11E -01	1.86E +06	1.88E +06	5.94E +00	1.39E +04	1.45E +04
9.07E -01	2.05E +06	2.06E +06	6.25E +00	1.11E +04	1.18E +04
1.01E +00	1.87E +06	1.88E +06	6.55E +00	9.20E +03	9.79E +03
1.11E +00	1.57E +06	1.57E +06	6.84E +00	7.89E +03	8.29E +03
1.20E +00	1.29E +06	1.29E +06	7.24E +00	6.36E +03	6.67E +03
1.31E +00	1.06E +06	1.07E +06	7.74E +00	4.56E +03	4.94E +03
1.41E +00	9.08E +05	9.13E +05	8.24E +00	3.39E +03	3.77E +03
1.51E +00	7.96E +05	8.01E +05	8.76E +00	2.56E +03	2.75E +03
1.61E +00	7.03E +05	7.07E +05	9.26E +00	1.77E +03	1.94E +03
1.71E +00	6.20E +05	6.24E +05	9.74E +00	1.26E +03	1.40E +03
1.81E +00	5.46E +05	5.49E +05	1.03E +01	9.27E +02	1.05E +03
1.93E +00	4.68E +05	4.71E +05	1.08E +01	7.29E +02	8.36E +02
2.10E +00	3.72E +05	3.74E +05	1.12E +01	5.58E +02	6.46E +02
2.30E +00	2.79E +05	2.81E +05	1.18E +01	3.61E +02	4.31E +02
2.50E +00	2.11E +05	2.13E +05	1.24E +01	2.09E +02	2.75E +02
2.70E +00	1.64E +05	1.66E +05	1.32E +01	1.32E +02	1.79E +02
2.90E +00	1.32E +05	1.34E +05	1.40E +01	8.59E +01	1.26E +02
3.10E +00	1.06E +05	1.08E +05	1.48E +01	6.55E +01	9.90E +01
3.30E +00	8.63E +04	8.78E +04	1.56E +01	3.55E +01	5.99E +01
3.50E +00	7.16E +04	7.33E +04	1.65E +01	1.10E +01	2.97E +01
3.71E +00	6.04E +04	6.17E +04	1.75E +01	-8.66E +00	5.89E +00
3.91E +00	5.20E +04	5.31E +04	1.85E +01	-6.41E +00	5.43E +00
4.15E +00	4.44E +04	4.54E +04	1.95E +01	-1.90E +00	8.80E +00
4.45E +00	3.68E +04	3.76E +04	2.05E +01	-5.26E +00	1.13E +01
4.75E +00	3.01E +04	3.09E +04	2.16E +01	-7.24E +00	1.01E +01
5.04E +00	2.48E +04	2.54E +04	2.26E +01	-6.41E +00	5.10E +00
5.34E +00	2.07E +04	2.13E +04	2.35E +01	-6.27E +00	3.79E +00
5.64E +00	1.72E +04	1.79E +04			

E1 (MeV)	E2 (MeV)	Integral neutrons $cm^{-2}kW^{-1}s^{-1}$	Error neutrons $cm^{-2}kW^{-1}s^{-1}$
0.811	1.000	3.77E +05	9.64E +02
1.000	1.200	3.19E +05	6.16E +02
1.200	1.600	3.81E +05	9.37E +02
1.600	2.000	2.24E +05	6.61E +02
2.000	3.000	2.33E +05	1.07E +03
3.000	4.000	7.62E +04	7.32E +02
4.000	6.000	5.59E +04	7.27E +02
6.000	8.000	1.57E +04	4.58E +02
8.000	10.000	4.73E +03	2.16E +02
10.000	12.000	1.40E +03	9.69E +01
12.000	16.000	5.16E +02	8.44E +01
16.000	20.000	2.34E +01	2.84E +01
3.000	10.000	1.52E +05	2.14E +03
1.500	15.000	6.87E +05	4.26E +03
3.000	12.000	1.54E +05	2.23E +03

Table 15. Neutron fluxes (50 keV to 1.4 MeV) on centerline at 25 cm behind the lead slab (Item IA) Runs 1573.D, 1573.B, 1573.A

N	Energy Boundary (MeV)		Flux (neutrons $cm^{-2}MeV^{-1}kW^{-1}s^{-1}$)	Error (%)
		RUN 1573.D		
1	0.0384	0.0447	1.28E +07	4.18
2	0.0447	0.0525	1.58E +07	3.07
3	0.0525	0.0619	1.96E +07	2.30
4	0.0619	0.0729	2.12E +07	2.00
5	0.0729	0.0870	1.41E +07	2.51
6	0.0870	0.1011	8.20E +06	4.99
7	0.1011	0.1199	1.09E +07	3.03
8	0.1199	0.1403	1.16E +07	2.98
9	0.1403	0.1654	7.81E +06	3.88
10	0.1654	0.1952	7.26E +06	3.87
		RUN 1573.B		
1	0.1411	0.1712	7.54E +06	1.34
2	0.1712	0.1952	7.19E +06	2.05
3	0.1952	0.2312	7.31E +06	1.49
4	0.2312	0.2733	8.53E +06	1.23
5	0.2733	0.3213	7.41E +06	1.37
6	0.3213	0.3814	6.02E +06	1.47
7	0.3814	0.4474	5.07E +06	1.76
8	0.4474	0.5255	4.58E +06	1.78
9	0.5255	0.6156	4.26E +06	1.76
10	0.6156	0.7297	3.18E +06	1.87
		RUN 1573.A		
1	0.5243	0.6216	3.92E +06	1.01
2	0.6216	0.7297	2.98E +06	1.28
3	0.7297	0.8595	2.28E +06	1.45
4	0.8595	1.0108	1.88E +06	1.58
5	1.0108	1.1838	1.47E +06	1.81
6	1.1838	1.4000	1.05E +06	1.99

Table 16. Bonner ball measurements on centerline at NE 213 location

Configuration[a]	Detector Location	Bonner ball count rates ($s^{-1}W^{-1}$)					
		3-inch Diam Ball		5-inch Diam Ball		10-inch Diam Ball	
		Foreground[c]	Background[d]	Foreground	Background	Foreground	Background
IA	25 cm behind lead[b]	1.66 (3)[e]		9.72 (3)		4.99 (3)	
IB	179.1 cm behind mockup	9.18 (1)	1.62 (1)	4.11 (2)	4.09 (1)	1.47 (2)	9.53 (0)
IC	25 cm behind lead[b]	2.10 (1)		3.32 (1)		4.82 (0)	
IIB	25 cm behind lead[b]	1.08 (1)		2.05 (1)		3.77 (0)	
IIC	178 cm behind mockup	1.39 (-1)	2.27 (-2)	6.92 (-1)	5.16 (-2)	3.61 (-1)	1.57 (-2)
IIF	25 cm behind lead[b]	4.11 (-1)		1.92 (0)		6.26 (-1)	
IIG	25 cm behind lead[b]	7.95 (-2)		4.38 (-1)		1.98 (-1)	
IIN	25 cm behind lead[b]	3.02 (-3)		1.63 (-2)		7.70 (-3)	
IIO	25 cm behind lead[b]	4.25 (-3)		2.22 (-2)		9.45 (-3)	

[a]See experimental program plan in Appendix A for description of configurations.
[b]Lead slab between configuration and detector (see schematics).
[c]Count rate without shadow shield between detector and configuration.
[d]Count rate with shadow shield between detector and configuration.
[e]Read: 1.66×10^3.

Table 17. Bonner ball measurements on centerline at 30 cm behind the spectrum modifiers

Configuration[a]	Bonner ball count rates ($s^{-1}W^{-1}$)					
	3-inch Diam Ball	4-inch Diam Ball	5-inch Diam Ball	8-inch Diam Ball	10-inch Diam Ball	12-inch Diam Ball
IA	2.65 (3)[b]	9.98 (3)	1.59 (4)	1.41 (4)	7.79 (3)	4.19 (3)
IB	6.78 (2)	2.40 (3)	3.44 (3)	2.36 (3)	1.25 (3)	5.70 (2)
IC	3.31 (1)	5.65 (1)	5.46 (1)	2.04 (1)	8.07 (0)	3.23 (0)

[a]See experimental program plan in Appendix A for description of configurations.
[b]Read: 2.65×10^3.

Table 18. Bonner ball measurements on centerline at 150 cm behind the spectrum modifiers

	Bonner ball count rates ($s^{-1}W^{-1}$)											
	3-inch Diam ball		4-inch Diam ball		5-inch Diam ball		8-inch Diam ball		10-inch Diam ball		12-inch Diam ball	
Configuration[a]	Foreground[b]	Background[c]	Foreground	Background	Foreground	Background	Foreground	Background	Foreground	Background	Foreground	Background
IA	4.90 (2)[d]	7.88 (1)	1.71 (3)	1.81 (2)	2.58 (3)	2.18 (2)	2.15 (3)	1.25 (2)	1.22 (3)	6.47 (1)	6.79 (2)	3.00 (1)
IB	1.22 (2)	1.91 (1)	3.99 (2)	4.13 (1)	5.64 (2)	4.64 (1)	3.81 (2)	2.13 (1)	1.98 (2)	1.01 (1)	9.39 (1)	4.50 (0)
IC	7.18 (0)	7.16 (-1)	1.20 (1)	1.09 (0)	1.14 (1)	1.02 (0)	4.34 (0)	3.52 (-1)	1.70 (0)	1.42 (-1)	6.55 (-1)	5.66 (-2)

[a]See experimental program plan in Appendix A for description of configurations.
[b]Count rate without shadow shield between detector and configuration.
[c]Count rate with shadow shield between detector and configuration.
[d]Read: 4.90×10^2.

Table 19. Fission chamber measurements on centerline at 30 cm behind the spectrum modifiers

	count rates ($s^{-1}W^{-1}$)		
Detector	Item IA[a]	Item IB	Item IC
bare	3.35 (0)[b]	7.39 (-1)	1.42 (-1)
Cd covered	2.37 (0)	5.43 (-1)	7.43 (-2)
bare Cd over face of mockup			9.05 (-2)
bare inside Cd hut			1.17 (-1)

[a]See experimental program plan in Appendix A for description of experiments.
[b]Read: 3.35×10^{0}.

Table 20. Fission chamber measurements on centerline at 150 cm behind the spectrum modifier

	Bonner ball count rates ($s^{-1}W^{-1}$)					
	Item IA [a]		Item IB		Item IC	
Detector	Foreground[b]	Background[c]	Foreground	Background	Foreground	Background
bare	1.36 (0)[d]	1.00 (0)	2.79 (-1)	1.98 (-1)	3.95 (-2)	
Cd covered	5.13 (-1)	1.59 (-1)	1.14 (-1)	3.17 (-2)	1.69 (-2)	
bare Cd over face of mockup					2.51 (-2)	

[a]See experimental program plan in Appendix A for description of experiments.
[b]Count rate without shadow shield between detector and configuration.
[c]Count rate with shadow shield between detector and configuration.
[d]Read: 1.36×10^{0}.

Table 21. Fast neutron fluxes (>0.8 MeV) on centerline at 179.1 cm behind the shield mockup (Item IB) Run 7903

Neutron Energy (MeV)	Flux (neutrons $cm^{-2}MeV^{-1}kW^{-1}s^{-1}$) Lower Limit	Upper Limit	Neutron Energy (MeV)	Flux (neutrons $cm^{-2}MeV^{-1}kW^{-1}s^{-1}$) Lower Limit	Upper Limit
8.11E -01	2.18E +04	2.23E +04	5.94E +00	5.13E +02	5.39E +02
9.07E -01	2.04E +04	2.06E +04	6.25E +00	4.16E +02	4.49E +02
1.01E +00	1.71E +04	1.73E +04	6.55E +00	3.47E +02	3.75E +02
1.11E +00	1.51E +04	1.53E +04	6.84E +00	2.93E +02	3.12E +02
1.20E +00	1.40E +04	1.41E +04	7.24E +00	2.24E +02	2.39E +02
1.31E +00	1.29E +04	1.31E +04	7.74E +00	1.58E +02	1.75E +02
1.41E +00	1.19E +04	1.20E +04	8.24E +00	1.19E +02	1.35E +02
1.51E +00	1.08E +04	1.10E +04	8.76E +00	8.64E +01	9.52E +01
1.61E +00	9.82E +03	9.96E +03	9.26E +00	6.15E +01	6.91E +01
1.71E +00	8.93E +03	9.05E +03	9.74E +00	4.70E +01	5.31E +01
1.81E +00	8.25E +03	8.37E +03	1.03E +01	3.34E +01	3.88E +01
1.93E +00	7.80E +03	7.92E +03	1.08E +01	2.14E +01	2.60E +01
2.10E +00	7.32E +03	7.43E +03	1.12E +01	1.43E +01	1.80E +01
2.30E +00	6.35E +03	6.45E +03	1.18E +01	9.63E +00	1.28E +01
2.50E +00	5.31E +03	5.39E +03	1.24E +01	5.61E +00	8.46E +00
2.70E +00	4.32E +03	4.40E +03	1.32E +01	3.93E +00	5.89E +00
2.90E +00	3.35E +03	3.43E +03	1.40E +01	1.91E +00	3.88E +00
3.10E +00	2.51E +03	2.59E +03	1.48E +01	9.22E -01	2.16E +00
3.30E +00	1.98E +03	2.05E +03	1.56E +01	9.53E -01	2.18E +00
3.50E +00	1.67E +03	1.75E +03	1.65E +01	2.78E -01	1.24E +00
3.71E +00	1.51E +03	1.57E +03	1.75E +01	-1.62E -01	5.39E -01
3.91E +00	1.42E +03	1.47E +03	1.85E +01	-3.55E -01	1.94E -01
4.15E +00	1.33E +03	1.38E +03	1.95E +01	-4.45E -01	7.95E -02
4.45E +00	1.19E +03	1.23E +03	2.05E +01	-5.02E -01	2.97E -01
4.75E +00	1.00E +03	1.04E +03	2.16E +01	-4.41E -01	3.97E -01
5.04E +00	8.41E +02	8.73E +02	2.26E +01	-2.68E -01	3.03E -01
5.34E +00	7.22E +02	7.51E +02	2.35E +01	-2.33E -01	2.59E -01
5.64E +00	6.15E +02	6.45E +02			

E1 (MeV)	E2 (MeV)	Integral neutrons $cm^{-2}kW^{-1}s^{-1}$	Error neutrons $cm^{-2}kW^{-1}s^{-1}$
0.811	1.000	3.82E +03	2.68E +01
1.000	1.200	3.09E +03	1.83E +01
1.200	1.600	4.82E +03	3.08E +01
1.600	2.000	3.41E +03	2.45E +01
2.000	3.000	5.36E +03	4.56E +01
3.000	4.000	1.86E +03	3.25E +01
4.000	6.000	1.85E +03	3.46E +01
6.000	8.000	5.77E +02	2.12E +01
8.000	10.000	1.67E +02	9.46E +00
10.000	12.000	4.38E +01	4.22E +00
12.000	16.000	1.46E +01	3.65E +00
16.000	20.000	7.65E -01	1.39E +00
3.000	10.000	4.45E +03	9.79E +01
1.500	15.000	1.43E +04	1.83E +02
3.000	12.000	4.49E +03	1.02E +02

Table 22. Neutron fluxes (50 keV to 1.4 MeV) on centerline at 179.1 cm behind the shield mockup (Item IB) Runs 1575.D, 1575.A, 1574.D

N	Energy Boundary (MeV)		Flux (neutrons $cm^{-2}MeV^{-1}kW^{-1}s^{-1}$)	Error (%)
		RUN 1575.D		
1	0.0385	0.0463	8.33E +05	3.39
2	0.0463	0.0542	8.87E +05	3.60
3	0.0542	0.0636	8.44E +05	3.44
4	0.0636	0.0746	8.67E +05	3.09
5	0.0746	0.0872	7.33E +05	3.42
6	0.0872	0.1029	4.87E +05	4.34
7	0.1029	0.1217	5.13E +05	3.69
8	0.1217	0.1437	5.04E +05	3.42
9	0.1437	0.1688	3.60E +05	4.43
10	0.1688	0.1987	3.13E +05	4.49
		RUN 1575.A		
1	0.1430	0.1690	3.76E +05	1.40
2	0.1690	0.1987	3.14E +05	1.57
3	0.1987	0.2321	2.51E +05	1.87
4	0.2321	0.2730	2.13E +05	1.74
5	0.2730	0.3212	1.91E +05	1.85
6	0.3212	0.3806	1.31E +05	2.26
7	0.3806	0.4475	7.83E +04	3.67
8	0.4475	0.5255	7.54E +04	3.53
9	0.5255	0.6183	8.98E +04	2.56
10	0.6183	0.7297	6.52E +04	2.87
		RUN 1574.D		
1	0.5243	0.6216	8.63E +04	1.02
2	0.6216	0.7297	6.42E +04	1.27
3	0.7297	0.8595	4.32E +04	1.57
4	0.8595	1.0108	2.25E +04	2.67
5	1.0108	1.1838	1.47E +04	3.83
6	1.1838	1.4000	1.32E +04	3.53

Table 23. Fast neutron fluxes (>0.8 MeV) on centerline at 25 cm behind the lead slab (Item IC) Run 7922.A

Neutron Energy (MeV)	Flux (neutrons $cm^{-2}MeV^{-1}kW^{-1}s^{-1}$) Lower Limit	Upper Limit	Neutron Energy (MeV)	Flux (neutrons $cm^{-2}MeV^{-1}kW^{-1}s^{-1}$) Lower Limit	Upper Limit
8.11E -01	9.04E +01	9.44E +01	5.94E +00	1.53E +00	1.73E +00
9.07E -01	1.06E +02	1.08E +02	6.25E +00	1.25E +00	1.49E +00
1.01E +00	1.07E +02	1.08E +02	6.55E +00	1.16E +00	1.37E +00
1.11E +00	1.00E +02	1.02E +02	6.84E +00	1.09E +00	1.24E +00
1.20E +00	9.25E +01	9.39E +01	7.24E +00	9.26E -01	1.06E +00
1.31E +00	8.70E +01	8.82E +01	7.74E +00	7.65E -01	9.11E -01
1.41E +00	8.10E +01	8.22E +01	8.24E +00	7.14E -01	8.54E -01
1.51E +00	7.29E +01	7.39E +01	8.76E +00	5.57E -01	6.42E -01
1.61E +00	6.35E +01	6.45E +01	9.26E +00	3.91E -01	4.64E -01
1.71E +00	5.46E +01	5.55E +01	9.74E +00	3.14E -01	3.76E -01
1.81E +00	4.65E +01	4.74E +01	1.03E +01	2.40E -01	2.94E -01
1.93E +00	3.87E +01	3.95E +01	1.08E +01	1.78E -01	2.24E -01
2.10E +00	2.99E +01	3.07E +01	1.12E +01	1.26E -01	1.67E -01
2.30E +00	2.23E +01	2.30E +01	1.18E +01	8.39E -02	1.17E -01
2.50E +00	1.78E +01	1.84E +01	1.24E +01	6.40E -02	9.50E -02
2.70E +00	1.49E +01	1.55E +01	1.32E +01	3.31E -02	5.76E -02
2.90E +00	1.26E +01	1.32E +01	1.40E +01	-1.50E -02	7.18E -03
3.10E +00	1.08E +01	1.13E +01	1.48E +01	-1.56E -02	5.67E -03
3.30E +00	9.20E +00	9.65E +00	1.56E +01	2.66E -02	4.27E -02
3.50E +00	7.72E +00	8.22E +00	1.65E +01	3.58E -02	5.42E -02
3.71E +00	6.62E +00	7.00E +00	1.75E +01	3.12E -03	1.38E -02
3.91E +00	5.68E +00	6.02E +00	1.85E +01	-4.07E -03	3.92E -03
4.15E +00	4.72E +00	5.03E +00	1.95E +01	-1.37E -04	8.05E -03
4.45E +00	4.10E +00	4.36E +00	2.05E +01	-7.59E -03	4.12E -03
4.75E +00	3.60E +00	3.84E +00	2.16E +01	-1.06E -02	1.78E -03
5.04E +00	3.02E +00	3.23E +00	2.26E +01	-5.61E -03	3.26E -03
5.34E +00	2.48E +00	2.68E +00	2.35E +01	-2.54E -03	4.78E -03
5.64E +00	1.96E +00	2.18E +00			

E1 (MeV)	E2 (MeV)	Integral neutrons $cm^{-2}kW^{-1}s^{-1}$	Error neutrons $cm^{-2}kW^{-1}s^{-1}$
0.811	1.000	1.98E +01	2.16E -01
1.000	1.200	2.02E +01	1.51E -01
1.200	1.600	3.24E +01	2.33E -01
1.600	2.000	1.94E +01	1.74E -01
2.000	3.000	1.99E +01	3.13E -01
3.000	4.000	8.23E +00	2.21E -01
4.000	6.000	6.53E +00	2.41E -01
6.000	8.000	2.21E +00	1.69E -01
8.000	10.000	1.07E +00	8.87E -02
10.000	12.000	3.60E -01	4.37E -02
12.000	16.000	1.19E -01	4.61E -02
16.000	20.000	5.38E -02	2.24E -02
3.000	10.000	1.80E +01	7.20E -01
1.500	15.000	6.48E +01	1.34E +00
3.000	12.000	1.84E +01	7.64E -01

Table 24. Neutron fluxes (50 keV to 1.4 MeV) on centerline at 25 cm behind the lead slab (Item IC) Runs 1591.A, 1590.A, 1589.A

N	Energy Boundary (MeV)		Flux (neutrons $cm^{-2}MeV^{-1}kW^{-1}s^{-1}$)	Error (%)
		RUN 1591.A		
1	0.0390	0.0456	1.26E +04	1.64
2	0.0456	0.0539	9.38E +03	1.90
3	0.0539	0.0639	8.84E +03	1.79
4	0.0639	0.0738	8.61E +03	1.97
5	0.0738	0.0871	6.41E +03	2.00
6	0.0871	0.1037	4.47E +03	2.36
7	0.1037	0.1219	4.19E +03	2.44
8	0.1219	0.1418	3.23E +03	3.05
9	0.1418	0.1684	2.40E +03	3.06
10	0.1684	0.1983	1.79E +03	3.85
		RUN 1590.A		
1	0.1434	0.1678	2.47E +03	1.19
2	0.1678	0.1983	1.82E +03	1.40
3	0.1983	0.2288	1.40E +03	1.98
4	0.2288	0.2715	1.43E +03	1.45
5	0.2715	0.3203	1.30E +03	1.46
6	0.3203	0.3752	7.51E +02	2.32
7	0.3752	0.4423	5.33E +02	2.79
8	0.4423	0.5216	4.59E +02	2.83
		RUN 1589.A		
1	0.3788	0.4447	4.87E +02	2.15
2	0.4447	0.5216	4.77E +02	1.95
3	0.5216	0.6204	3.03E +02	2.39
4	0.6204	0.7302	1.31E +02	5.36
5	0.7302	0.8510	1.22E +02	5.88
6	0.8510	1.0047	1.10E +02	5.42
7	1.0047	1.1804	1.01E +02	5.57
8	1.1804	1.4000	9.57E +01	4.69

Table 25. Fission chamber measurements on centerline at 0.7 cm behind SM-2 and ALMR shield mockups

	count rates ($s^{-1}W^{-1}$)						
Detector	Item IC[a]	Item IIIA	Item IIIB	Item IIIC	Item IIID	Item IIIE	Item IIIF
bare	2.06 (-1)[b]	1.50 (-2)	1.71 (-2)	3.24 (-2)	1.23 (-3)	2.45 (-4)	7.44 (-4)
Cd covered	1.23 (-1)	1.10 (-2)	1.42 (-2)	2.21 (-2)	1.08 (-3)	1.63 (-4)	4.34 (-4)
bare inside Cd hut	1.76 (-1)	1.38 (-2)	1.69 (-2)	3.01 (-2)	1.15 (-3)	1.83 (-4)	4.75 (-4)

[a]See experimental program plan in Appendix A for description of configurations.
[b]Read: 2.06×10^{-1}.

Table 26. Bonner ball measurements on centerline at 30 cm behind the removable radial shield mockups

Configuration[a]	Bonner ball count rates ($s^{-1}W^{-1}$)					
	3-inch Diam Ball	4-inch Diam Ball	5-inch Diam Ball	8-inch Diam Ball	10-inch Diam Ball	12-inch Diam Ball
IIA	1.26 (2)[b]	2.62 (2)	2.92 (2)	1.39 (2)	6.18 (1)	2.49 (1)
IIB	1.59 (1)	2.88 (1)	2.98 (1)	1.30 (1)	5.44 (0)	2.14 (0)
IIC	1.20 (0)	4.50 (0)	7.01 (0)	6.28 (0)	3.77 (0)	2.09 (0)
IID	4.32 (0)	9.91 (0)	1.22 (1)	8.17 (0)	4.49 (0)	2.40 (0)
IIE	3.19 (0)	8.48 (0)	1.14 (1)	8.64 (0)	5.13 (0)	2.77 (0)
IIF	5.27 (-1)	1.79 (0)	2.52 (0)	1.70 (0)	8.46 (-1)	3.86 (-1)
IIG	9.67 (-2)	3.51 (-1)	5.26 (-1)	4.20 (-1)	2.35 (-1)	1.22 (-1)
IIH	5.45 (-2)	2.07 (-1)	3.13 (-1)	2.45 (-1)	1.33 (-1)	6.50 (-2)
II I	1.37 (-2)	5.07 (-2)	7.60 (-2)	6.03 (-2)	3.40 (-2)	1.78 (-2)
II IA[c]	1.59 (-2)	5.62 (-2)	8.35 (-2)	6.42 (-2)	3.58 (-2)	1.81 (-2)
IIJ	2.39 (-2)	8.05 (-2)	1.14 (-1)	8.04 (-2)	4.35 (-2)	2.05 (-2)
IIK	2.31 (-2)	7.65 (-2)	1.09 (-1)	8.00 (-2)	4.27 (-2)	2.11 (-2)
IIL	2.40 (-2)	8.53 (-2)	1.22 (-1)	8.86 (-2)	4.63 (-2)	2.23 (-2)
IIM	1.13 (-2)	4.92 (-2)	7.70 (-2)	7.16 (-2)	4.11 (-2)	2.11 (-2)
IIN	3.29 (-3)	1.27 (-2)	1.95 (-2)	1.60 (-2)	9.52 (-3)	4.85 (-3)
IIO	5.45 (-3)	2.34 (-2)	2.85 (-2)	2.23 (-2)	1.20 (-2)	5.84 (-3)
IIP	1.35 (-4)	4.54 (-4)	6.81 (-4)	5.66 (-4)	3.26 (-4)	1.71 (-4)
IIQ	6.77 (-4)	1.20 (-3)	1.19 (-3)	5.27 (-4)	2.29 (-4)	9.53 (-5)

[a]See experimental program plan in Appendix A for description of configurations.
[b]Read: 1.26×10^2.
[c]Same configuration as Item II I except lithiated paraffin bricks removed from around IVFS vessel.

Table 27. Bonner ball measurements on centerline at 150 cm behind the removable radial shield mockups

	Bonner ball count rates ($s^{-1}W^{-1}$)								
	3-inch Diam Ball			4-inch Diam Ball			5-inch Diam ball		
Configuration[a]	Foreground[b]	Background[c]	LiH Background	Foreground	Background	LiH Background	Foreground	Background	LiH Background
IIA	2.13 (1)[d]	2.13 (0)		4.35 (1)	3.65 (0)		4.84 (1)	3.73 (0)	
IIB	2.70 (0)	1.73 (-1)		4.76 (0)	2.85 (-1)		4.89 (0)	2.79 (-1)	
IIC	1.83 (-1)	2.49 (-2)		6.20 (-1)	4.85 (-2)		9.27 (-1)	5.73 (-2)	
IID	6.83 (-1)	6.21 (-2)		1.48 (0)	1.18 (-1)		1.76 (0)	1.32 (-1)	
IIE	5.36 (-1)	4.98 (-2)		1.27 (0)	1.01 (-1)		1.64 (0)	1.14 (-1)	
IIF	9.85 (-2)	1.31 (-2)		3.21 (-1)	2.86 (-2)		4.39 (-1)	3.28 (-2)	
IIG	1.62 (-2)	3.28 (-3)		5.21 (-2)	6.45 (-3)		7.44 (-2)	7.19 (-3)	
IIH	1.20 (-2)	3.13 (-3)		4.11 (-2)	6.51 (-3)		5.98 (-2)	7.37 (-3)	
II I	2.89 (-3)	1.13 (-3)		8.74 (-3)	2.06 (-3)		1.22 (-2)	2.21 (-3)	

Table 27. (continued)

	Bonner ball count rates ($s^{-1}W^{-1}$)								
	8-inch Diam Ball			10-inch Diam Ball			12-inch Diam ball		
Configuration	Foreground	Background	LiH Background	Foreground	Background	LiH Background	Foreground	Background	LiH Background
IIA	2.31 (1)	1.48 (0)		1.02 (1)	6.34 (-1)		4.11 (0)	2.49 (-1)	
IIB	2.18 (0)	1.07 (-1)		8.91 (-1)	4.47 (-2)		3.49 (-1)	1.88 (-2)	
IIC	8.01 (-1)	3.36 (-2)		4.75 (-1)	1.77 (-2)		2.60 (-1)	8.32 (-3)	
IID	1.12 (0)	6.28 (-2)		5.92 (-1)	3.34 (-2)		3.04 (-1)	1.59 (-2)	
IIE	1.20 (0)	6.29 (-2)		6.63 (-1)	3.21 (-2)		3.56 (-1)	1.52 (-2)	
IIF	3.00 (-1)	1.62 (-2)		1.47 (-1)	7.72 (-3)		6.76 (-2)	3.69 (-3)	
IIG	5.75 (-2)	3.66 (-3)		3.14 (-2)	1.79 (-3)		1.63 (-2)	8.24 (-4)	
IIH	4.66 (-2)	3.82 (-3)		2.52 (-2)	1.84 (-3)		1.22 (-2)	8.16 (-3)	
II I	9.17 (-3)	1.09 (-3)		5.08 (-3)	5.09 (-4)		2.56 (-3)	2.31 (-4)	

Table 27. (continued)

	Bonner ball count rates ($s^{-1}W^{-1}$)								
	3-inch Diam Ball			4-inch Diam Ball			5-inch Diam ball		
Configuration	Foreground	Background	LiH Background	Foreground	Background	LiH Background	Foreground	Background	LiH Background
II IA	5.29 (-3)	2.05 (-3)		1.59 (-2)	4.27 (-3)		2.22 (-2)	4.39 (-3)	
IIJ	4.20 (-3)	9.59 (-4)		1.28 (-2)	1.85 (-3)		1.71 (-2)	2.01 (-3)	
IIK	4.15 (-3)	9.56 (-4)		1.23 (-2)	1.82 (-3)		1.69 (-2)	2.06 (-3)	
IIL	5.12 (-3)	1.38 (-3)		1.68 (-2)	2.80 (-3)		2.29 (-2)	3.11 (-3)	
IIM	2.89 (-3)	1.01 (-3)		1.06 (-2)	2.11 (-3)		1.61 (-2)	2.47 (-3)	
IIN	9.65 (-4)	5.85 (-4)		2.60 (-3)	1.05 (-3)		3.59 (-3)	1.10 (-3)	
IIO	1.32 (-3)	5.98 (-4)		3.68 (-3)	1.13 (-3)		4.97 (-3)	1.21 (-3)	
IIP	7.35 (-5)	4.35 (-5)	2.29 (-5)	1.80 (-4)	7.96 (-5)	3.70 (-5)	2.28 (-4)	8.74 (-5)	3.67 (-5)
IIQ	7.32 (-5)	3.19 (-5)		1.23 (-4)	5.27 (-5)		1.12 (-4)	5.16 (-5)	

Table 27. (continued)

	Bonner ball count rates ($s^{-1}W^{-1}$)								
	8-inch Diam Ball			10-inch Diam Ball			12-inch Diam ball		
Configuration	Foreground	Background	LiH Background	Foreground	Background	LiH Background	Foreground	Background	LiH Background
II IA	1.63 (-2)	2.30 (-3)		8.40 (-3)	1.12 (-3)		4.12 (-3)	5.08 (-4)	
IIJ	1.18 (-2)	9.76 (-4)		6.27 (-3)	4.82 (-4)		3.00 (-3)	2.04 (-4)	
IIK	1.19 (-2)	1.02 (-3)		6.32 (-3)	4.85 (-4)		3.05 (-3)	2.12 (-4)	
IIL	1.66 (-2)	1.49 (-3)		8.63 (-3)	6.97 (-4)		4.05 (-3)	3.10 (-4)	
IIM	1.46 (-2)	1.22 (-3)		8.30 (-3)	6.02 (-4)		4.26 (-3)	2.94 (-4)	
IIN	2.64 (-3)	5.39 (-4)		1.55 (-3)	2.53 (-4)		7.64 (-4)	1.13 (-4)	
IIO	3.63 (-3)	5.70 (-4)		1.95 (-3)	2.60 (-4)		9.37 (-4)	1.18 (-4)	
IIP	1.60 (-4)	4.38 (-5)	1.44 (-5)	8.73 (-5)	2.14 (-5)	6.81 (-6)	4.42 (-5)	9.55 (-6)	2.98 (-6)
IIQ	5.07 (-5)	1.98 (-5)		2.19 (-5)	8.73 (-6)		8.47 (-6)	4.25 (-6)	

[a]See experimental program plan in Appendix A for description of configurations.
[b]Count rates without shadow shield between detector and configuration.
[c]Count rates with shadow shield between detector and configuration.
[d]Read: 2.13×10^{1}.

Table 28. Fission chamber measurements on centerline at 30 cm behind the removable radial shield mockups

	count rates ($s^{-1}W^{-1}$)								
Detector	Item IIA[a]	Item IIB	Item IIC	Item IID	Item IIE	Item IIF	Item IIG	Item IIH	Item II I
bare	3.24 (-1)[b]	4.47 (-2)	1.67 (-3)	1.13 (-2)	7.05 (-3)	6.08 (-4)	1.78 (-4)	1.04 (-4)	3.62 (-5)
Cd covered	2.11 (-1)	3.23 (-2)	1.18 (-3)	7.42 (-3)	4.47 (-3)	4.02 (-4)	7.98 (-5)	4.14 (-5)	1.09 (-5)
bare detector Cd over face of mockup		3.44 (-2)	1.40 (-3)	8.24 (-3)	5.25 (-3)	5.45 (-4)	1.53 (-4)	8.63 (-5)	3.11 (-5)
detector bare inside Cd hut				1.01 (-2)	6.02 (-3)				1.32 (-5)
detector face bare, Cd wrapped around cylinder of detector								5.67 (-5)	1.75 (-5)

Table 28. (continued)

Detector	count rates ($s^{-1}W^{-1}$)								
	Item II IA*	Item IIJ	Item IIK	Item IIL	Item IIM	Item IIN	Item IIO	Item IIP	Item IIQ
bare	6.30 (-5)	5.08 (-5)	4.72 (-5)	4.88 (-5)	3.00 (-5)	1.85 (-5)	2.30 (-5)	1.48 (-5)	1.67 (-5)
Cd covered	1.45 (-5)	2.14 (-5)	1.90 (-5)	1.93 (-5)	8.72 (-6)	2.93 (-6)	4.74 (-6)	9.12 (-7)	1.29 (-6)
bare detector Cd over face of mockup	4.52 (-5)	3.69 (-5)	3.59 (-5)	3.77 (-5)	2.57 (-5)	1.56 (-5)	1.71 (-5)	1.26 (-5)	1.35 (-5)
detector bare, inside Cd hut		3.18 (-5)	2.80 (-5)	2.08 (-5)	9.82 (-6)	3.74 (-6)	7.57 (-6)	9.62 (-7)	1.57 (-6)
detector face bare, Cd wrapped around cylinder of detector									
detector bare, inside Cd hut	1.70 (-5)								

[a]See experimental program plan in Appendix A for description of configurations.
[b]Read: 3.24×10^{-1}.
*Item II IA is the same as II I except the lithiated paraffin bricks have been removed from around the IVFS vessel.

Table 29. Fission chamber measurements on centerline at 150 cm behind the removable radial shield mockups

	Bonner ball count rates ($s^{-1}W^{-1}$)									
	Item IIA[a]		Item IIB	Item IIC	Item IID	Item IIE	Item IIF	Item IIG	Item IIH	Item II I
Detector	Fgd[b]	Bkgd[c]								
bare	7.50 (-2)[d]	2.94 (-2)	1.01 (-2)	6.21 (-4)	2.72 (-3)	2.00 (-3)	3.40 (-4)	1.40 (-4)	7.42 (-5)	3.92 (-5)
Cd covered	3.85 (-2)	4.22 (-3)	5.47 (-3)	2.12 (-4)	1.29 (-3)	8.09 (-4)	9.51 (-5)	1.72 (-5)	1.20 (-5)	3.50 (-6)
bare Cd over face of mockup	5.89 (-2)		8.09 (-3)	5.32 (-4)	2.03 (-3)	1.56 (-3)	3.22 (-4)	1.31 (-4)	6.98 (-5)	3.82 (-5)

Table 29. (continued)

	Bonner ball count rates ($s^{-1}W^{-1}$)								
Detector	Item II IA*	Item IIJ	Item IIK	Item IIL	Item IIM	Item IIN	Item IIO	Item IIP	Item IIQ
bare	5.25 (-5)	3.47 (-5)	3.52 (-5)	3.84 (-5)	3.03 (-5)	2.28 (-5)	2.44 (-5)	3.92 (-6)	4.07 (-6)
Cd covered	6.28 (-6)	4.86 (-6)	4.83 (-6)	5.53 (-6)	3.29 (-6)	1.32 (-6)	1.74 (-6)	1.18 (-7)	1.52 (-7)
bare Cd over face of mockup	5.27 (-5)	3.12 (-5)	3.20 (-5)	3.57 (-5)	2.92 (-5)	2.27 (-5)	2.35 (-5)	3.86 (-6)	3.85 (-6)

*Item II IA is the same as II I except the lithiated paraffin bricks have been removed from around the IVFS vessel.
[a]See experimental program plan in Appendix A for description of configurations.
[b]Count rates without shadow shield between detector and configuration.
[c]Count rate with shadow shield between detector and configuration.
[d]Read: 7.50×10^{-2}.

Table 30. Fast neutron fluxes (>0.8 MeV) on centerline at 25 cm behind the lead slab (Item IIB) Run 7912

Neutron Energy (MeV)	Flux (neutrons $cm^{-2}MeV^{-1}kW^{-1}s^{-1}$) Lower Limit	Upper Limit	Neutron Energy (MeV)	Flux (neutrons $cm^{-2}MeV^{-1}kW^{-1}s^{-1}$) Lower Limit	Upper Limit
8.11E -01	2.80E +02	2.85E +02	5.94E +00	8.30E -01	9.42E -01
9.07E -01	2.88E +02	2.90E +02	6.25E +00	7.35E -01	8.72E -01
1.01E +00	2.44E +02	2.46E +02	6.55E +00	6.97E -01	8.13E -01
1.11E +00	1.92E +02	1.93E +02	6.84E +00	6.39E -01	7.21E -01
1.20E +00	1.49E +02	1.50E +02	7.24E +00	4.85E -01	5.54E -01
1.31E +00	1.13E +02	1.14E +02	7.74E +00	3.19E -01	3.97E -01
1.41E +00	8.93E +01	9.03E +01	8.24E +00	2.10E -01	2.85E -01
1.51E +00	7.31E +01	7.38E +01	8.76E +00	1.90E -01	2.36E -01
1.61E +00	6.04E +01	6.10E +01	9.26E +00	1.93E -01	2.35E -01
1.71E +00	4.97E +01	5.03E +01	9.74E +00	1.55E -01	1.91E -01
1.81E +00	4.06E +01	4.12E +01	1.03E +01	1.04E -01	1.34E -01
1.93E +00	3.19E +01	3.24E +01	1.08E +01	7.23E -02	9.84E -02
2.10E +00	2.24E +01	2.29E +01	1.12E +01	5.81E -02	8.08E -02
2.30E +00	1.49E +01	1.52E +01	1.18E +01	4.95E -02	6.60E -02
2.50E +00	9.94E +00	1.02E +01	1.24E +01	3.79E -02	5.29E -02
2.70E +00	6.99E +00	7.26E +00	1.32E +01	1.63E -02	2.66E -02
2.90E +00	5.07E +00	5.34E +00	1.40E +01	-9.99E -03	-7.19E -04
3.10E +00	3.67E +00	3.95E +00	1.48E +01	-1.57E -02	-6.66E -03
3.30E +00	2.70E +00	2.92E +00	1.56E +01	5.78E -03	1.28E -02
3.50E +00	2.01E +00	2.26E +00	1.65E +01	1.35E -02	2.24E -02
3.71E +00	1.70E +00	1.90E +00	1.75E +01	1.39E -03	5.54E -03
3.91E +00	1.56E +00	1.74E +00	1.85E +01	-9.00E -04	2.12E -03
4.15E +00	1.49E +00	1.66E +00	1.95E +01	4.51E -04	3.53E -03
4.45E +00	1.52E +00	1.67E +00	2.05E +01	-2.16E -03	2.22E -03
4.75E +00	1.54E +00	1.68E +00	2.16E +01	-3.27E -03	1.39E -03
5.04E +00	1.42E +00	1.54E +00	2.26E +01	-2.09E -03	1.15E -03
5.34E +00	1.20E +00	1.32E +00	2.35E +01	-1.40E -03	1.32E -03
5.64E +00	9.77E -01	1.10E +00			

E1 (MeV)	E2 (MeV)	Integral neutrons $cm^{-2}kW^{-1}s^{-1}$	Error neutrons $cm^{-2}kW^{-1}s^{-1}$
0.811	1.000	5.31E +01	2.27E -01
1.000	1.200	3.95E +01	1.28E -01
1.200	1.600	3.87E +01	1.79E -01
1.600	2.000	1.71E +01	1.09E -01
2.000	3.000	1.21E +01	1.66E -01
3.000	4.000	2.45E +00	1.14E -01
4.000	6.000	2.75E +00	1.36E -01
6.000	8.000	1.19E +00	9.24E -02
8.000	10.000	4.25E -01	4.84E -02
10.000	12.000	1.67E -01	2.40E -02
12.000	16.000	4.68E -02	2.03E -02
16.000	20.000	2.21E -02	9.43E -03
3.000	10.000	6.81E +00	3.91E -01
1.500	15.000	4.30E +01	7.43E -01
3.000	12.000	6.98E +00	4.15E -01

Table 31. Neutron fluxes (50 keV to 1.4 MeV) on centerline at 25 cm behind the lead slab (Item IIB) Runs 1577.B, 1577.A, 1576.A

N	Energy Boundary (MeV)		Flux (neutrons $cm^{-2}MeV^{-1}kW^{-1}s^{-1}$)	Error (%)
		RUN 1577.B		
1	0.0382	0.0463	1.72E +04	1.55
2	0.0463	0.0544	1.51E +04	1.95
3	0.0544	0.0626	1.41E +04	2.26
4	0.0626	0.0739	1.37E +04	1.71
5	0.0739	0.0869	9.57E +03	2.26
6	0.0869	0.1032	6.15E +03	2.97
7	0.1032	0.1210	6.98E +03	2.59
8	0.1210	0.1422	6.53E +03	2.45
9	0.1422	0.1682	4.32E +03	3.09
10	0.1682	0.1974	3.54E +03	3.60
11	0.1974	0.2332	2.92E +03	3.68
		RUN 1577.A		
1	0.1665	0.1968	3.51E +03	1.31
2	0.1968	0.2332	2.92E +03	1.43
3	0.2332	0.2755	2.89E +03	1.33
4	0.2755	0.3240	2.57E +03	1.38
5	0.3240	0.3785	1.71E +03	1.91
6	0.3785	0.4451	1.21E +03	2.31
7	0.4451	0.5238	1.03E +03	2.38
8	0.5238	0.6207	8.61E +02	2.31
9	0.6207	0.7297	5.18E +02	3.45
		RUN 1576.A		
1	0.5243	0.6216	8.34E +02	1.19
2	0.6216	0.7297	5.66E +02	1.57
3	0.7297	0.8595	3.70E +02	1.96
4	0.8595	1.0108	2.63E +02	2.31
5	1.0108	1.1838	1.80E +02	2.85
6	1.1838	1.4000	1.10E +02	3.41

Table 32. 3-in Bonner ball radial traverses at 30 cm behind the removable radial shield mockups

Distance from centerline (cm)	Bonner ball count rates ($s^{-1}W^{-1}$)										
	Item IIB[a]	Item IIC	Item IID	Item IIE	Item IIH	Item II I	Item IIJ	Item IIK	Item IIL	Item IIN	Item IIO
100 S	2.31 (0)[b]		3.39 (-1)	3.57 (-1)		2.16 (-3)	2.60 (-3)	2.96 (-3)	5.00 (-3)	7.32 (-4)	9.11 (-4)
90	3.26 (0)								6.70 (-3)	1.01 (-3)	1.13 (-3)
85											
80	4.69 (0)	2.35 (-1)	5.65 (-1)	6.04 (-1)	3.10 (-2)	3.21 (-3)	4.19 (-3)	4.65 (-3)	9.53 (-3)	1.01 (-3)	1.37 (-3)
70	6.31 (0)				3.06 (-2)				1.25 (-2)		1.70 (-3)
65		3.83 (-1)									
60	8.37 (0)		1.17 (0)	1.22 (0)		5.68 (-3)	8.30 (-3)	8.92 (-3)	1.52 (-2)	1.54 (-3)	2.29 (-3)
55											
50	1.05 (1)	6.35 (-1)		1.81 (0)	4.21 (-2)	7.63 (-3)	1.21 (-2)	1.26 (-2)	1.78 (-2)	1.96 (-3)	3.08 (-3)
40	1.26 (1)	8.29 (-1)	2.67 (0)	2.32 (0)		9.59 (-3)	1.61 (-2)	1.62 (-2)	1.97 (-2)	2.38 (-3)	4.03 (-3)
30	1.43 (1)	9.96 (-1)	3.29 (0)	2.72 (0)	5.18 (-2)	1.14 (-2)	1.93 (-2)	1.87 (-2)	2.18 (-2)	2.77 (-3)	4.74 (-3)
25											
20	1.56 (1)	1.14 (0)	3.90 (0)	3.02 (0)		1.28 (-2)	2.16 (-2)	2.05 (-2)	2.33 (-2)	3.02 (-3)	5.14 (-3)
15											5.36 (-3)
10	1.63 (1)	1.22 (0)	4.02 (0)		5.55 (-2)	1.36 (-2)	2.32 (-2)	2.17 (-2)	2.42 (-2)	3.22 (-3)	5.38 (-3)
5			4.19 (0)	3.20 (0)							
0	1.66 (1)	1.24 (0)	4.26 (0)		5.51 (-2)	1.36 (-2)	2.34 (-2)	2.20 (-2)	2.42 (-2)	3.27 (-3)	5.44 (-3)
5			4.32 (0)	3.27 (0)							
10	1.62 (1)	1.19 (0)	4.27 (0)		5.35 (-2)	1.31 (-2)	2.32 (-2)	2.13 (-2)	2.31 (-2)	3.19 (-3)	5.31 (-3)
15			4.22 (0)	3.17 (0)							
20	1.52 (1)	1.09 (0)	4.10 (0)			1.21 (-2)	2.18 (-2)	2.01 (-2)	2.23 (-2)	2.93 (-3)	4.99 (-3)
25			3.87 (0)	2.98 (0)							
30	1.38 (1)	9.50 (-1)	3.26 (0)	2.65 (0)	4.65 (-2)	1.07 (-2)	1.89 (-2)	1.85 (-2)	2.07 (-2)	2.60 (-3)	4.44 (-3)
40	1.19 (1)	7.73 (-1)	2.65 (0)	2.26 (0)		8.79 (-3)	1.57 (-2)	1.56 (-2)	1.87 (-2)	2.20 (-3)	3.76 (-3)
50	9.87 (0)	5.74 (-1)		1.75 (0)	3.61 (-2)	6.77 (-3)	1.16 (-2)	1.19 (-2)	1.63 (-2)	1.79 (-3)	2.95 (-3)
55											
60	7.78 (0)	4.18 (-1)	1.20 (0)	1.17 (0)		5.00 (-3)	7.81 (-3)	8.29 (-3)	1.42 (-2)	1.41 (-3)	2.14 (-3)
70	5.90 (0)			7.94 (-1)	2.58 (-2)	3.72 (-3)		5.87 (-3)	1.16 (-2)		1.66 (-3)
75		2.44 (-1)									
78.8					2.27 (-2)						
80	4.26 (0)		5.65 (-1)	5.76 (-1)		2.87 (-3)	3.94 (-3)		8.61 (-3)		
85											
90	2.97 (0)	1.52 (-1)				2.28 (-3)					
100 N	2.12 (0)										

[a]See experimental program plan in Appendix A for description of configurations.
[b]Read: 2.31×10^{0}.

Table 33. 10-in Bonner ball radial traverses at 30 cm behind the removable radial shield mockups

Distance from centerline (cm)	Bonner ball count rates ($s^{-1}W^{-1}$)										
	Item IIB[a]	Item IIC	Item IID	Item IIE	Item IIH	Item II I	Item IIJ	Item IIK	Item IIL	Item IIN	Item IIO
100 S	7.39 (-1)[b]					3.26 (-3)	3.15 (-3)	3.56 (-3)		9.11 (-4)	9.46 (-4)
90									1.04 (-2)		1.43 (-3)
85	1.28 (0)										
80		5.79 (-1)				5.93 (-3)	6.02 (-3)	6.88 (-3)		1.64 (-3)	1.96 (-3)
76					5.54 (-2)						
75				1.01 (0)							
70	2.09 (0)		9.22 (-1)		6.42 (-2)				2.22 (-2)		2.76 (-3)
65		1.05 (0)									
60			1.41 (0)	1.81 (0)		1.28 (-2)	1.35 (-2)	1.51 (-2)	2.64 (-2)	3.32 (-3)	4.09 (-3)
55	3.05 (0)										
50		1.83 (0)	2.09 (0)	2.58 (0)	9.38 (-2)	1.79 (-2)	2.00 (-2)	2.20 (-2)	3.16 (-2)		6.09 (-3)
40	4.07 (0)	2.44 (0)	2.81 (0)	3.40 (0)		2.35 (-2)	2.69 (-2)	2.89 (-2)	3.73 (-2)	6.09 (-3)	8.15 (-3)
30		3.02 (0)	3.54 (0)	4.11 (0)	1.20 (-1)	2.83 (-2)	3.31 (-2)	3.49 (-2)	4.13 (-2)	7.42 (-3)	9.95 (-3)
25	4.87 (0)										
20		3.47 (0)	4.09 (0)	4.66 (0)		3.21 (-2)	3.80 (-2)	3.89 (-2)	4.34 (-2)	8.13 (-3)	1.15 (-2)
10	5.34 (0)	3.75 (0)	4.41 (0)	4.98 (0)	1.33 (-1)	3.40 (-2)	4.09 (-2)	4.18 (-2)	4.59 (-2)	8.90 (-3)	1.23 (-2)
0	5.43 (0)	3.83 (0)	4.52 (0)	5.10 (0)	1.34 (-1)	3.40 (-2)	4.20 (-2)	4.25 (-2)	4.60 (-2)	9.10 (-3)	1.23 (-2)
10	5.30 (0)	3.71 (0)	4.40 (0)	4.96 (0)	1.29 (-1)	3.30 (-2)	4.13 (-2)	4.16 (-2)	4.49 (-2)	8.79 (-3)	1.20 (-2)
20		3.38 (0)	4.07 (0)	4.62 (0)		3.03 (-2)	3.79 (-2)	3.85 (-2)	4.23 (-2)	8.18 (-3)	1.12 (-2)
25	4.78 (0)										
30		2.92 (0)	3.51 (0)	4.03 (0)	1.12 (-1)	2.58 (-2)	3.29 (-2)	3.39 (-2)	3.86 (-2)	7.13 (-3)	9.59 (-3)
40	3.97 (0)	2.32 (0)	2.83 (0)	3.32 (0)		2.08 (-2)	2.66 (-2)	2.81 (-2)	3.42 (-2)	5.79 (-3)	7.79 (-3)
50		1.73 (0)	2.12 (0)	2.49 (0)	8.29 (-2)	1.54 (-2)	1.93 (-2)	2.15 (-2)	2.97 (-2)		5.79 (-3)
55	2.93 (0)										
60		1.20 (0)	1.45 (0)	1.74 (0)		1.07 (-2)	1.31 (-2)	1.47 (-2)	2.44 (-2)	3.16 (-3)	4.00 (-3)
70	1.99 (0)		9.61 (-1)	1.16 (0)	5.38 (-2)	7.35 (-3)		9.70 (-3)	1.96 (-2)		2.73 (-3)
75		6.72 (-1)									
76.3					4.58 (-2)						
80							5.85 (-3)				
85	1.21 (0)										
90		3.88 (-1)									
100 N	7.21 (-1)										

[a]See experimental program plan in Appendix A for description of configurations.
[b]Read: 7.39×10^{-1}.

Table 34. Bare fission chamber radial traverse at 30 cm behind the removable radial shield mockups

Distance from centerline (cm)	count rates ($s^{-1}W^{-1}$)										
	Item IIB[a]	Item IIC	Item IID	Item IIE	Item IIH	Item II I	Item IIJ	Item IIK	Item IIL	Item IIN	Item IIO
125 S					1.15 (-4)						
100	9.84 (-3)[b]		2.61 (-3)	2.64 (-3)	1.33 (-4)		4.26 (-5)	5.12 (-5)	5.56 (-5)	2.44 (-5)	2.56 (-5)
95						4.42 (-5)					
90	1.22 (-2)	1.34 (-3)							5.33 (-5)		
80	1.63 (-2)		2.80 (-3)	3.13 (-3)	1.20 (-4)	3.81 (-5)	3.73 (-5)	4.72 (-5)	5.05 (-5)	2.34 (-5)	2.61 (-5)
75		1.21 (-3)									
70	1.97 (-2)				1.19 (-4)				4.90 (-5)		
60	2.45 (-2)	1.18 (-3)	4.16 (-3)	4.05 (-3)		3.69 (-5)	3.75 (-5)	4.15 (-5)	4.78 (-5)	2.04 (-5)	2.33 (-5)
50	2.96 (-2)	1.29 (-3)		5.30 (-3)	1.10 (-4)	3.70 (-5)	4.18 (-5)	4.36 (-5)	4.84 (-5)		
40	3.46 (-2)	1.45 (-3)	8.16 (-3)	6.36 (-3)		3.61 (-5)	4.84 (-5)	4.82 (-5)	4.87 (-5)	1.84 (-5)	2.26 (-5)
30	3.91 (-2)	1.53 (-3)	9.74 (-3)	6.83 (-3)	1.07 (-4)	3.74 (-5)	5.09 (-5)	4.74 (-5)	4.82 (-5)	1.88 (-5)	2.30 (-5)
20	4.23 (-2)	1.63 (-3)	1.09 (-2)	7.11 (-3)		3.66 (-5)	5.18 (-5)	4.72 (-5)	4.93 (-5)	1.80 (-5)	2.34 (-5)
15			1.12 (-2)				5.15 (-5)				2.36 (-5)
10	4.38 (-2)	1.68 (-3)	1.15 (-2)	7.24 (-3)	1.04 (-4)	3.64 (-5)	5.13 (-5)	4.79 (-5)	4.80 (-5)	1.80 (-5)	2.31 (-5)
5			1.14 (-2)				5.01 (-5)				2.24 (-5)
0	4.47 (-2)	1.70 (-3)	1.15 (-2)	7.31 (-3)	1.03 (-4)	3.71 (-5)	5.08 (-5)	4.70 (-5)	4.83 (-5)	1.80 (-5)	2.21 (-5)
5			1.15 (-2)				5.09 (-5)				2.29 (-5)
10	4.35 (-2)	1.66 (-3)	1.15 (-2)	7.15 (-3)	1.02 (-4)	3.66 (-5)	5.08 (-5)	4.60 (-5)	4.75 (-5)	1.80 (-5)	2.23 (-5)
15			1.13 (-2)				5.12 (-5)				2.24 (-5)
20	4.15 (-2)	1.57 (-3)	1.09 (-2)	6.91 (-3)		3.62 (-5)	5.16 (-5)	4.66 (-5)	4.73 (-5)	1.75 (-5)	2.26 (-5)
30	3.77 (-2)	1.46 (-3)	9.66 (-3)	6.53 (-3)	1.01 (-4)	3.64 (-5)	5.03 (-5)	4.64 (-5)	4.57 (-5)	1.88 (-5)	2.31 (-5)
40	3.22 (-2)	1.34 (-3)	8.20 (-3)	5.95 (-3)		3.56 (-5)	4.85 (-5)	4.42 (-5)	4.59 (-5)	1.87 (-5)	2.32 (-5)
50	2.78 (-2)	1.19 (-3)		4.91 (-3)	9.86 (-5)	3.57 (-5)	4.12 (-5)	4.10 (-5)	4.60 (-5)		
60	2.25 (-2)	1.06 (-3)	4.18 (-3)	3.75 (-3)		3.46 (-5)	3.69 (-5)	3.93 (-5)	4.61 (-5)	2.06 (-5)	2.38 (-5)
70	1.82 (-2)			3.14 (-3)	1.04 (-4)			4.01 (-5)	4.44 (-5)		2.53 (-5)
75		8.96 (-4)									
80	1.41 (-2)		2.68 (-3)	2.78 (-3)	1.01 (-4)	3.66 (-5)	3.53 (-5)				
90	1.09 (-2)	8.75 (-4)									
92						4.00 (-5)					
100 N	8.73 (-3)										

[a]See experimental program plan in Appendix A for description of configurations.
[b]Read: 9.84×10^{-3}.

Table 35. Cd-covered fission chamber radial traverse at 30 cm behind the removable radial shield mockups

Distance from centerline (cm)	count rates ($s^{-1}W^{-1}$)										
	Item IIB[a]	Item IIC	Item IID	Item IIE	Item IIH	Item II I	Item IIJ	Item IIK	Item IIL	Item IIN	Item IIO
125 S					9.77 (-6)						
100	4.25 (-3)[b]		5.66 (-4)	5.53 (-4)	1.53 (-5)	2.80 (-6)	3.82 (-6)	4.09 (-6)	6.04 (-6)	1.19 (-6)	1.43 (-6)
90		2.21 (-4)							7.54 (-6)		
85	7.26 (-3)										
80			9.14 (-4)	8.96 (-4)	2.93 (-5)	3.59 (-6)	4.82 (-6)	5.71 (-6)		1.49 (-6)	1.98 (-6)
75		3.19 (-4)									
70	1.18 (-2)				2.89 (-5)				1.33 (-5)		
60		5.00 (-4)	1.99 (-3)	1.79 (-3)		5.78 (-6)	8.71 (-6)	9.03 (-6)		1.78 (-6)	2.52 (-6)
55	1.79 (-2)								1.55 (-5)		
50		6.81 (-4)		2.75 (-3)	3.31 (-5)	7.26 (-6)	1.26 (-5)	1.29 (-5)			
40	2.44 (-2)	8.64 (-4)	4.85 (-3)	3.44 (-3)		8.40 (-6)	1.72 (-5)	1.59 (-5)	1.77 (-5)	2.44 (-6)	4.12 (-6)
30		1.02 (-3)	6.11 (-3)	3.98 (-3)	3.85 (-5)	9.52 (-6)	1.93 (-5)	1.83 (-5)	1.87 (-5)	2.62 (-6)	4.77 (-6)
25	2.94 (-2)										
20		1.14 (-3)	7.18 (-3)	4.36 (-3)		1.03 (-5)	2.07 (-5)	1.90 (-5)	1.94 (-5)	2.90 (-6)	5.01 (-6)
15			7.55 (-3)								4.98 (-6)
10	3.18 (-2)	1.21 (-3)	7.67 (-3)	4.58 (-3)	4.17 (-5)	1.05 (-5)	2.08 (-5)	1.95 (-5)	1.98 (-5)	2.80 (-6)	5.18 (-6)
5			7.81 (-3)								4.88 (-6)
0	3.21 (-2)	1.24 (-3)	7.77 (-3)	4.63 (-3)	4.25 (-5)	1.05 (-5)	2.10 (-5)	1.89 (-5)	1.98 (-5)	2.89 (-6)	4.87 (-6)

Table 35. (continued)

Distance from centerline (cm)	count rates ($s^{-1}W^{-1}$)										
	Item IIB	Item IIC	Item IID	Item IIE	Item IIH	Item II I	Item IIJ	Item IIK	Item IIL	Item IIN	Item IIO
5			7.78 (-3)								4.89 (-6)
10	3.14 (-2)	1.17 (-3)	7.61 (-3)	4.60 (-3)	4.15 (-5)	1.00 (-5)	2.05 (-5)	1.88 (-5)	1.95 (-5)	2.80 (-6)	4.95 (-6)
15			7.35 (-3)	4.23 (-3)							4.89 (-6)
20		1.08 (-3)	7.00 (-3)			9.46 (-6)	2.09 (-5)	1.90 (-5)	1.88 (-5)	2.71 (-6)	4.98 (-6)
25	2.84 (-2)										
30		9.40 (-4)	5.91 (-3)	3.82 (-3)	3.68 (-5)	9.11 (-6)	1.86 (-5)	1.80 (-5)	1.75 (-5)	2.51 (-6)	4.43 (-6)
40	2.30 (-2)	7.91 (-4)	4.63 (-3)	3.30 (-3)		7.59 (-6)	1.56 (-5)	1.57 (-5)	1.65 (-5)	2.22 (-6)	3.95 (-6)
50		6.11 (-4)		2.59 (-3)	3.18 (-5)	6.01 (-6)	1.30 (-5)	1.20 (-5)			
55	1.69 (-2)								1.48 (-5)		
60		4.57 (-4)	1.88 (-3)	1.70 (-3)		4.91 (-6)	9.08 (-6)	9.04 (-6)		1.77 (-6)	2.54 (-6)
70	1.11 (-2)			1.14 (-3)	2.35 (-5)			6.43 (-6)	1.17 (-5)		
75		2.71 (-4)									
80			8.72 (-4)	8.29 (-4)	2.10 (-5)	3.18 (-6)	4.95 (-6)				
85	6.52 (-3)										
89						2.77 (-6)					
90		1.80 (-4)									
100 N	3.77 (-3)										

[a]See experimental program plan in Appendix A for description of configurations.
[b]Read: 4.25×10^{-3}.

Table 36. Bare fission chamber radial traverse at 30 cm behind the removable radial shield mockups (Cd cover over face of mockup)

Distance from centerline (cm)	count rates ($s^{-1}W^{-1}$)										
	Item IIB[a]	Item IIC	Item IID	Item IIE	Item IIH	Item II I	Item IIJ	Item IIK	Item IIL	Item IIN	Item IIO
100 S	8.36 (-3)[b]		2.17 (-3)	2.25 (-3)	1.25 (-4)		4.06 (-5)	4.63 (-5)		2.30 (-5)	2.43 (-5)
95						4.02 (-5)					
90		1.23 (-3)									
85	1.14 (-2)										
80			2.04 (-3)	2.42 (-3)	1.10 (-4)	3.39 (-5)	3.23 (-5)	4.00 (-5)		2.04 (-5)	2.28 (-5)
75		1.04 (-3)									
70	1.52 (-2)				1.02 (-4)				4.19 (-5)		
60		8.91 (-4)	2.82 (-3)	2.93 (-3)		2.89 (-5)	2.82 (-5)	3.11 (-5)	4.20 (-5)	1.66 (-5)	1.75 (-5)
55	2.08 (-2)										
50		9.61 (-4)		3.72 (-3)	9.09 (-5)	2.89 (-5)	3.02 (-5)	3.18 (-5)	3.98 (-5)		
40	2.68 (-2)	1.12 (-3)	5.50 (-3)	4.29 (-3)		2.94 (-5)	3.27 (-5)	3.32 (-5)	3.97 (-5)	1.49 (-5)	1.70 (-5)
30		1.26 (-3)	6.65 (-3)	4.83 (-3)	8.86 (-5)	2.96 (-5)	3.56 (-5)	3.40 (-5)	3.89 (-5)	1.47 (-5)	1.72 (-5)
25	3.14 (-2)										
20		1.38 (-3)	7.72 (-3)	5.12 (-3)		2.96 (-5)	3.62 (-5)	3.36 (-5)	3.88 (-5)	1.41 (-5)	1.72 (-5)
15			8.04 (-3)								1.67 (-5)
10	3.46 (-2)	1.44 (-3)	8.33 (-3)	5.35 (-3)	8.84 (-5)	3.07 (-5)	3.59 (-5)	3.47 (-5)	3.97 (-5)	1.48 (-5)	1.66 (-5)
5			8.40 (-3)								1.73 (-5)
0	3.45 (-2)	1.45 (-3)	8.39 (-3)	5.35 (-3)	8.71 (-5)	3.02 (-5)	3.62 (-5)	3.41 (-5)	4.01 (-5)	1.43 (-5)	1.72 (-5)

Table 36. (continued)

Distance from centerline (cm)	count rates ($s^{-1}W^{-1}$)										
	Item IIB	Item IIC	Item IID	Item IIE	Item IIH	Item II I	Item IIJ	Item IIK	Item IIL	Item IIN	Item IIO
5			8.40 (-3)								1.75 (-5)
10	3.41 (-2)	1.42 (-3)	8.28 (-3)	5.29 (-3)	8.73 (-5)	2.98 (-5)	3.53 (-5)	3.44 (-5)	3.83 (-5)	1.41 (-5)	1.72 (-5)
15			8.11 (-3)								1.74 (-5)
20		1.33 (-3)	7.73 (-3)	4.98 (-3)		2.95 (-5)	3.62 (-5)	3.39 (-5)	3.67 (-5)	1.49 (-5)	1.77 (-5)
25	3.02 (-2)										
30		1.20 (-3)	6.65 (-3)	4.61 (-3)	8.34 (-5)	2.89 (-5)	3.45 (-5)	3.23 (-5)	3.63 (-5)	1.47 (-5)	1.72 (-5)
40	2.54 (-2)	1.04 (-3)	5.43 (-3)	4.13 (-3)		2.96 (-5)	3.33 (-5)	3.26 (-5)	3.46 (-5)	1.50 (-5)	1.70 (-5)
50		8.96 (-4)		3.47 (-3)	8.23 (-5)	2.89 (-5)	2.94 (-5)	3.08 (-5)	3.43 (-5)		
55	1.95 (-2)										
60		7.99 (-4)	2.82 (-3)	2.62 (-3)		2.87 (-5)	2.74 (-5)	3.09 (-5)	3.56 (-5)	1.66 (-5)	1.82 (-5)
70	1.39 (-2)			2.26 (-3)	9.01 (-5)			3.44 (-5)	3.60 (-5)		2.01 (-5)
75		7.28 (-4)									
80			1.94 (-3)	2.07 (-3)	9.01 (-5)	3.22 (-5)	2.93 (-5)				
85	9.53 (-3)										
90		7.61 (-4)									
92						3.71 (-5)					
100 N	7.10 (-3)										

[a]See experimental program plan in Appendix A for description of configurations.
[b]Read: 8.36×10^{-3}.

Table 37. Fast neutron fluxes (>0.8 MeV) on centerline at 178 cm behind the shield mockup (Item IIC) Run 7914

Neutron Energy (MeV)	Flux (neutrons $cm^{-2}MeV^{-1}kW^{-1}s^{-1}$) Lower Limit	Upper Limit	Neutron Energy (MeV)	Flux (neutrons $cm^{-2}MeV^{-1}kW^{-1}s^{-1}$) Lower Limit	Upper Limit
8.11E -01	1.28E +02	1.30E +02	5.94E +00	1.90E +00	2.01E +00
9.07E -01	1.18E +02	1.19E +02	6.25E +00	1.55E +00	1.70E +00
1.01E +00	9.15E +01	9.25E +01	6.55E +00	1.30E +00	1.42E +00
1.11E +00	7.37E +01	7.46E +01	6.84E +00	1.06E +00	1.13E +00
1.20E +00	6.60E +01	6.68E +01	7.24E +00	7.31E -01	7.89E -01
1.31E +00	6.07E +01	6.15E +01	7.74E +00	4.41E -01	5.03E -01
1.41E +00	5.53E +01	5.61E +01	8.24E +00	2.98E -01	3.52E -01
1.51E +00	5.04E +01	5.11E +01	8.76E +00	2.18E -01	2.52E -01
1.61E +00	4.58E +01	4.65E +01	9.26E +00	1.74E -01	2.04E -01
1.71E +00	4.20E +01	4.26E +01	9.74E +00	1.36E -01	1.59E -01
1.81E +00	3.88E +01	3.94E +01	1.03E +01	8.60E -02	1.06E -01
1.93E +00	3.59E +01	3.65E +01	1.08E +01	5.87E -02	7.57E -02
2.10E +00	3.25E +01	3.31E +01	1.12E +01	4.87E -02	6.34E -02
2.30E +00	2.93E +01	2.98E +01	1.18E +01	3.26E -02	4.42E -02
2.50E +00	2.62E +01	2.67E +01	1.24E +01	1.07E -02	2.11E -02
2.70E +00	2.27E +01	2.31E +01	1.32E +01	4.89E -03	1.15E -02
2.90E +00	1.92E +01	1.96E +01	1.40E +01	3.47E -03	7.71E -03
3.10E +00	1.57E +01	1.61E +01	1.48E +01	-6.25E -04	2.55E -03
3.30E +00	1.27E +01	1.30E +01	1.56E +01	-2.56E -03	5.57E -04
3.50E +00	1.03E +01	1.07E +01	1.65E +01	-1.61E -03	9.67E -04
3.71E +00	8.67E +00	8.95E +00	1.75E +01	-6.95E -04	1.83E -03
3.91E +00	7.49E +00	7.73E +00	1.85E +01	-7.76E -04	1.42E -03
4.15E +00	6.46E +00	6.68E +00	1.95E +01	-1.17E -03	9.46E -04
4.45E +00	5.42E +00	5.60E +00	2.05E +01	-2.51E -03	6.03E -04
4.75E +00	4.46E +00	4.62E +00	2.16E +01	-2.37E -03	7.55E -04
5.04E +00	3.72E +00	3.86E +00	2.26E +01	-1.04E -03	1.34E -03
5.34E +00	3.02E +00	3.15E +00	2.35E +01	-4.90E -04	1.47E -03
5.64E +00	2.37E +00	2.50E +00			

E1 (MeV)	E2 (MeV)	Integral neutrons $cm^{-2}kW^{-1}s^{-1}$	Error neutrons $cm^{-2}kW^{-1}s^{-1}$
0.811	1.000	2.20E +01	1.27E -01
1.000	1.200	1.54E +01	9.24E -02
1.200	1.600	2.26E +01	1.55E -01
1.600	2.000	1.59E +01	1.27E -01
2.000	3.000	2.62E +01	2.36E -01
3.000	4.000	1.12E +01	1.61E -01
4.000	6.000	8.19E +00	1.55E -01
6.000	8.000	2.02E +00	8.64E -02
8.000	10.000	4.50E -01	3.52E -02
10.000	12.000	1.30E -01	1.60E -02
12.000	16.000	2.52E -02	1.10E -02
16.000	20.000	4.06E -04	4.78E -03
3.000	10.000	2.18E +01	4.38E -01
1.500	15.000	6.90E +01	8.63E -01
3.000	12.000	2.19E +01	4.54E -01

Table 38. Neutron fluxes (50 keV to 1.4 MeV) on centerline at 178 cm behind the shield mockup (Item IIC) Runs 1579.D, 1579.A, 1578.A

N	Energy Boundary (MeV)		Flux (neutrons $cm^{-2}MeV^{-1}kW^{-1}s^{-1}$)	Error (%)
		RUN 1579.D		
1	0.0381	0.0448	1.58E +03	2.82
2	0.0448	0.0533	1.32E +03	3.05
3	0.0533	0.0634	1.07E +03	3.51
4	0.0634	0.0736	1.11E +03	3.85
5	0.0736	0.0871	1.14E +03	3.03
6	0.0871	0.1-23	8.90E +02	3.84
7	0.1023	0.1192	8.17E +02	4.19
8	0.1192	0.1412	9.12E +02	3.06
9	0.1412	0.1666	7.54E +02	3.50
10	0.1666	0.1954	6.59E +02	3.85
11	0.1954	0.2309	5.64E +02	3.84
12	0.2309	0.2715	5.06E +02	4.02
		RUN 1579.A		
1	0.1956	0.2306	5.35E +02	1.76
2	0.2306	0.2715	5.23E +02	1.70
3	0.2715	0.3240	4.64E +02	1.62
4	0.3240	0.3765	3.13E +02	2.73
5	0.3765	0.4466	2.20E +02	3.15
6	0.4466	0.5225	2.55E +02	2.85
7	0.5225	0.6159	2.92E +02	2.13
8	0.6159	0.7268	2.36E +02	2.32
9	0.7268	0.8553	1.69E +02	3.01
		RUN 1578.A		
1	0.6156	0.7245	2.26E +02	1.38
2	0.7245	0.8553	1.65E +02	1.61
3	0.8553	1.0078	8.82E +01	2.70
4	1.0078	1.1821	6.08E +01	3.69
5	1.1821	1.4000	5.48E +01	3.39

Table 39. Fission chamber measurements on centerline at 0.7 cm behind the removable radial shield mockup

	Bonner ball count rates ($s^{-1}W^{-1}$)												
Detector	Item IID[a]	Item IIE	Item IIH	Item II I	Item II IA*	Item IIJ	Item IIK	Item IIL	Item IIM	Item IIN	Item IIO	Item IIP	Item IIQ
bare	7.37 (-3)[b]	9.55 (-3)	1.16 (-4)	3.88 (-5)	4.75 (-5)	4.11 (-5)	4.76 (-5)	5.45 (-5)	3.05 (-5)	1.67 (-5)	1.70 (-5)	1.56 (-5)	1.40 (-5)
Cd covered	5.44 (-3)	7.66 (-3)	6.40 (-5)	1.79 (-5)	1.96 (-5)	2.27 (-5)	2.79 (-5)	3.02 (-5)	1.27 (-5)	4.20 (-6)	5.27 (-6)	8.56 (-7)	1.33 (-6)
detector face bare, Cd wrapped around cylinder of detector	6.07 (-3)		6.52 (-5)	1.91 (-5)	2.03 (-5)			3.16 (-5)	1.34 (-5)	4.77 (-6)	5.97 (-6)	1.09 (-6)	2.44 (-6)
bare detector inside Cd hut	6.74 (-3)	8.98 (-3)		2.01 (-5)	2.40 (-5)	2.64 (-5)	3.30 (-5)	3.37 (-5)	1.43 (-5)	5.17 (-6)	6.31 (-6)	8.76 (-7)	1.80 (-6)
detector Cd covered inside Cd hut				1.78 (-5)									
detector bare inside Cd hut, repeat run after doing IIQ and IIP				1.89 (-5)									

[a]See experimental program plan in Appendix A for description of configurations.
[b]Read: 7.37×10^{-3}.
*Item II IA is the same as II I, except the lithiated paraffin bricks around the IVFS vessel have been removed.

Table 40. Fast neutron fluxes (>0.8 MeV) on centerline at 25 cm behind the lead slab (Item IIF) Run 7916

Neutron Energy (MeV)	Flux (neutrons $cm^{-2}MeV^{-1}kW^{-1}s^{-1}$) Lower Limit	Upper Limit	Neutron Energy (MeV)	Flux (neutrons $cm^{-2}MeV^{-1}kW^{-1}s^{-1}$) Lower Limit	Upper Limit
8.11E -01	1.68E +02	1.71E +02	5.94E +00	7.57E -01	8.48E -01
9.07E -01	1.74E +02	1.75E +02	6.25E +00	6.79E -01	7.86E -01
1.01E +00	1.45E +02	1.46E +02	6.55E +00	5.89E -01	6.79E -01
1.11E +00	1.09E +02	1.09E +02	6.84E +00	5.27E -01	5.93E -01
1.20E +00	7.82E +01	7.87E +01	7.24E +00	4.50E -01	5.06E -01
1.31E +00	5.57E +01	5.63E +01	7.74E +00	3.13E -01	3.81E -01
1.41E +00	4.25E +01	4.30E +01	8.24E +00	2.11E -01	2.81E -01
1.51E +00	3.49E +01	3.54E +01	8.76E +00	1.80E -01	2.19E -01
1.61E +00	2.96E +01	3.00E +01	9.26E +00	1.62E -01	1.97E -01
1.71E +00	2.52E +01	2.56E +01	9.74E +00	1.49E -01	1.79E -01
1.81E +00	2.12E +01	2.16E +01	1.03E +01	1.33E -01	1.61E -01
1.93E +00	1.73E +01	1.76E +01	1.08E +01	1.17E -01	1.41E -01
2.10E +00	1.28E +01	1.31E +01	1.12E +01	9.48E -02	1.16E -01
2.30E +00	9.22E +00	9.47E +00	1.18E +01	6.23E -02	7.96E -02
2.50E +00	6.50E +00	6.70E +00	1.24E +01	4.10E -02	5.63E -02
2.70E +00	4.38E +00	4.57E +00	1.32E +01	2.80E -02	3.89E -02
2.90E +00	3.25E +00	3.44E +00	1.40E +01	-7.51E -04	8.00E -03
3.10E +00	2.52E +00	2.73E +00	1.48E +01	-7.65E -03	1.05E -03
3.30E +00	1.95E +00	2.11E +00	1.56E +01	5.87E -03	1.20E -02
3.50E +00	1.61E +00	1.79E +00	1.65E +01	1.07E -02	1.79E -02
3.71E +00	1.56E +00	1.70E +00	1.75E +01	8.47E -04	5.10E -03
3.91E +00	1.52E +00	1.65E +00	1.85E +01	-9.02E -04	2.32E -03
4.15E +00	1.41E +00	1.53E +00	1.95E +01	4.77E -04	3.67E -03
4.45E +00	1.28E +00	1.39E +00	2.05E +01	-2.57E -03	2.15E -03
4.75E +00	1.14E +00	1.24E +00	2.16E +01	-3.73E -03	1.25E -03
5.04E +00	1.00E +00	1.09E +00	2.26E +01	-2.03E -03	1.40E -03
5.34E +00	8.94E -01	9.83E -01	2.35E +01	-1.12E -03	1.79E -03
5.64E +00	8.05E -01	9.06E -01			

E1 (MeV)	E2 (MeV)	Integral neutrons $cm^{-2}kW^{-1}s^{-1}$	Error neutrons $cm^{-2}kW^{-1}s^{-1}$
0.811	1.000	3.20E +01	1.43E -01
1.000	1.200	2.24E +01	7.14E -02
1.200	1.600	1.90E +01	1.05E -01
1.600	2.000	8.87E +00	6.92E -02
2.000	3.000	7.37E +00	1.12E -01
3.000	4.000	1.91E +00	8.23E -02
4.000	6.000	2.21E +00	1.02E -01
6.000	8.000	1.07E +00	7.50E -02
8.000	10.000	3.96E -01	4.30E -02
10.000	12.000	2.27E -01	2.26E -02
12.000	16.000	7.43E -02	2.00E -02
16.000	20.000	1.86E -02	8.88E -03
3.000	10.000	5.59E +00	3.03E -01
1.500	15.000	2.54E +01	5.45E -01
3.000	12.000	5.81E +00	3.25E -01

Table 41. Neutron fluxes (50 keV to 1.4 MeV) on centerline at 25 cm behind the lead slab (Item IIF) Runs 1581.C, 1581.B, 1581.A

N	Energy Boundary (MeV)		Flux (neutrons $cm^{-2}MeV^{-1}kW^{-1}s^{-1}$)	Error (%)
		RUN 1581.C		
1	0.0387	0.0456	6.63E +03	1.81
2	0.0456	0.0542	5.32E +03	1.96
3	0.0542	0.0628	4.45E +03	2.57
4	0.0628	0.0732	4.22E +03	2.42
5	0.0732	0.0869	3.70E +03	2.15
6	0.0869	0.1024	2.45E +03	3.12
7	0.1024	0.1196	2.30E +03	3.26
8	0.1196	0.1420	2.44E +03	2.43
9	0.1420	0.1661	1.68E +03	3.54
10	0.1661	0.1954	1.41E +03	3.63
11	0.1954	0.2315	1.12E +03	3.79
		RUN 1581.B		
1	0.1714	0.1954	1.39E +03	1.83
2	0.1954	0.2315	1.10E +03	1.63
3	0.2315	0.2736	1.04E +03	1.60
4	0.2736	0.3217	9.42E +02	1.66
5	0.3217	0.3819	6.24E +02	2.09
6	0.3819	0.4480	4.24E +02	3.06
7	0.4480	0.5262	3.97E +02	2.95
8	0.5262	0.6164	3.97E +02	2.66
9	0.6164	0.7307	2.97E +02	2.70
		RUN 1581.A		
1	0.5299	0.6191	3.66E +02	1.66
2	0.6191	0.7307	2.84E +02	1.71
3	0.7307	0.8534	2.05E +02	2.16
4	0.8534	1.0096	1.50E +02	2.19
5	1.0096	1.1880	9.85E +01	2.76
6	1.1880	1.4000	5.07E +01	4.18

Table 42. Fast neutron fluxes (>0.8 MeV) on centerline at 25 cm behind the lead slab (Item IIG) Run 7917.A

Neutron Energy (MeV)	Flux (neutrons $cm^{-2}MeV^{-1}kW^{-1}s^{-1}$) Lower Limit	Upper Limit	Neutron Energy (MeV)	Flux (neutrons $cm^{-2}MeV^{-1}kW^{-1}s^{-1}$) Lower Limit	Upper Limit
8.11E -01	5.55E +01	5.61E +01	5.94E +00	6.23E -01	6.49E -01
9.07E -01	5.13E +01	5.17E +01	6.25E +00	4.63E -01	4.97E -01
1.01E +00	4.12E +01	4.15E +01	6.55E +00	3.74E -01	4.03E -01
1.11E +00	3.44E +01	3.47E +01	6.84E +00	3.19E -01	3.37E -01
1.20E +00	3.02E +01	3.05E +01	7.24E +00	2.48E -01	2.62E -01
1.31E +00	2.71E +01	2.73E +01	7.74E +00	1.67E -01	1.82E -01
1.41E +00	2.46E +01	2.49E +01	8.24E +00	1.17E -01	1.30E -01
1.51E +00	2.25E +01	2.26E +01	8.76E +00	8.49E -02	9.26E -02
1.61E +00	2.02E +01	2.04E +01	9.26E +00	5.60E -02	6.25E -02
1.71E +00	1.81E +01	1.83E +01	9.74E +00	3.53E -02	4.06E -02
1.81E +00	1.63E +01	1.65E +01	1.03E +01	2.41E -02	2.85E -02
1.93E +00	1.48E +01	1.49E +01	1.08E +01	1.79E -02	2.17E -02
2.10E +00	1.32E +01	1.33E +01	1.12E +01	1.24E -02	1.56E -02
2.30E +00	1.17E +01	1.18E +01	1.18E +01	8.13E -03	1.06E -02
2.50E +00	1.00E +01	1.01E +01	1.24E +01	4.28E -03	6.57E -03
2.70E +00	8.20E +00	8.30E +00	1.32E +01	1.35E -03	3.06E -03
2.90E +00	6.70E +00	6.79E +00	1.40E +01	7.11E -04	2.30E -03
3.10E +00	5.40E +00	5.50E +00	1.48E +01	1.15E -03	2.33E -03
3.30E +00	4.32E +00	4.40E +00	1.56E +01	9.67E -04	2.15E -03
3.50E +00	3.51E +00	3.60E +00	1.65E +01	1.78E -04	1.02E -03
3.71E +00	2.94E +00	3.01E +00	1.75E +01	-2.92E -04	5.13E -04
3.91E +00	2.52E +00	2.58E +00	1.85E +01	-4.15E -04	2.47E -04
4.15E +00	2.14E +00	2.20E +00	1.95E +01	-4.59E -04	1.92E -04
4.45E +00	1.83E +00	1.87E +00	2.05E +01	-5.78E -04	3.67E -04
4.75E +00	1.51E +00	1.55E +00	2.16E +01	-5.58E -04	4.34E -04
5.04E +00	1.20E +00	1.23E +00	2.26E +01	-3.60E -04	3.72E -04
5.34E +00	9.69E -01	1.00E +00	2.35E +01	-2.67E -04	3.29E -04
5.64E +00	7.98E -01	8.28E -01			

E1 (MeV)	E2 (MeV)	Integral neutrons $cm^{-2}kW^{-1}s^{-1}$	Error neutrons $cm^{-2}kW^{-1}s^{-1}$
0.811	1.000	9.57E +00	3.84E -02
1.000	1.200	7.09E +00	2.43E -02
1.200	1.600	1.01E +01	4.03E -02
1.600	2.000	6.74E +00	3.21E -02
2.000	3.000	1.00E +01	5.77E -02
3.000	4.000	3.78E +00	3.85E -02
4.000	6.000	2.70E +00	3.66E -02
6.000	8.000	6.32E -01	2.06E -02
8.000	10.000	1.56E -01	8.08E -03
10.000	12.000	3.51E -02	3.48E -03
12.000	16.000	1.00E -02	3.15E -03
16.000	20.000	5.81E -04	1.51E -03
3.000	10.000	7.27E +00	1.04E -01
1.500	15.000	2.62E +01	2.09E -01
3.000	12.000	7.31E +00	1.07E -01

Table 43. Neutron fluxes (50 keV to 1.4 MeV) on centerline at 25 cm behind the lead slab (Item IIG) Runs 1582.C, 1582.B, 1582.A

N	Energy Boundary (MeV)		Flux (neutrons $cm^{-2}MeV^{-1}kW^{-1}s^{-1}$)	Error (%)
		RUN 1582.C		
1	0.0385	0.0450	1.19E +03	3.39
2	0.0450	0.0532	1.03E +03	3.46
3	0.0532	0.0630	8.90E +02	3.70
4	0.0630	0.0745	9.36E +02	3.31
5	0.0745	0.0876	7.96E +02	3.72
6	0.0876	0.1023	6.12E +02	4.70
7	0.1023	0.1220	5.88E +02	3.88
8	0.1220	0.1432	5.84E +02	3.99
9	0.1432	0.1678	4.67E +02	4.64
10	0.1678	0.1973	4.28E +02	4.47
11	0.1973	0.2316	3.55E +02	4.89
12	0.2316	0.2742	2.90E +02	4.97
		RUN 1582.B		
1	0.2003	0.2311	3.33E +02	2.01
2	0.2311	0.2742	3.04E +02	1.68
3	0.2742	0.3235	2.61E +02	1.89
4	0.3235	0.3790	1.72E +02	2.80
5	0.3790	0.4467	1.31E +02	3.28
6	0.4467	0.5269	1.53E +02	2.60
7	0.5269	0.6193	1.60E +02	2.26
8	0.6193	0.7302	1.19E +02	2.49
		RUN 1582.A		
1	0.5216	0.6204	1.52E +02	1.45
2	0.6204	0.7302	1.21E +02	1.70
3	0.7302	0.8510	8.73 +012	2.19
4	0.8510	1.0047	4.64E +01	3.25
5	1.0047	1.1804	3.09E +01	4.55
6	1.1804	1.4000	2.88E +01	3.97

Table 44. Fast neutron fluxes (>0.8 MeV) on centerline at 25 cm behind the lead slab (Item IIN) Run 7919

Neutron Energy (MeV)	Flux (neutrons $cm^{-2}MeV^{-1}kW^{-1}s^{-1}$) Lower Limit	Upper Limit	Neutron Energy (MeV)	Flux (neutrons $cm^{-2}MeV^{-1}kW^{-1}s^{-1}$) Lower Limit	Upper Limit
8.11E -01	2.69E +00	2.73E +00	5.94E +00	2.30E -02	2.46E -02
9.07E -01	2.37E +00	2.39E +00	6.25E +00	1.83E -02	2.02E -02
1.01E +00	1.70E +00	1.72E +00	6.55E +00	1.53E -02	1.70E -02
1.11E +00	1.27E +00	1.28E +00	6.84E +00	1.32E -02	1.44E -02
1.20E +00	1.04E +00	1.05E +00	7.24E +00	1.10E -02	1.19E -02
1.31E +00	8.94E -01	9.05E -01	7.74E +00	8.60E -03	9.62E -03
1.41E +00	7.96E -01	8.06E -01	8.24E +00	6.28E -03	7.23E -03
1.51E +00	7.29E -01	7.39E -01	8.76E +00	4.52E -03	5.07E -03
1.61E +00	6.69E -01	6.78E -01	9.26E +00	3.34E -03	3.82E -03
1.71E +00	6.09E -01	6.17E -01	9.74E +00	2.51E -03	2.91E -03
1.81E +00	5.51E -01	5.59E -01	1.03E +01	1.70E -03	2.04E -03
1.93E +00	4.92E -01	5.00E -01	1.08E +01	1.08E -03	1.37E -03
2.10E +00	4.27E -01	4.34E -01	1.12E +01	7.69E -04	1.01E -03
2.30E +00	3.70E -01	3.77E -01	1.18E +01	6.34E -04	8.31E -04
2.50E +00	3.17E -01	3.23E -01	1.24E +01	3.72E -04	5.72E -04
2.70E +00	2.61E -01	2.66E -01	1.32E +01	9.34E -05	2.51E -04
2.90E +00	2.16E -01	2.21E -01	1.40E +01	1.08E -04	2.60E -04
3.10E +00	1.74E -01	1.79E -01	1.48E +01	1.72E -04	2.86E -04
3.30E +00	1.37E -01	1.41E -01	1.56E +01	1.31E -04	2.43E -04
3.50E +00	1.11E -01	1.16E -01	1.65E +01	2.84E -05	1.07E -04
3.71E +00	9.62E -02	9.95E -02	1.75E +01	-2.20E -05	5.43E -05
3.91E +00	8.57E -02	8.86E -02	1.85E +01	-3.57E -05	2.67E -05
4.15E +00	7.22E -02	7.50E -02	1.95E +01	-4.43E -05	1.76E -05
4.45E +00	5.56E -02	5.78E -02	2.05E +01	-5.63E -05	3.18E -05
4.75E +00	4.47E -02	4.68E -02	2.16E +01	-5.33E -05	3.96E -05
5.04E +00	3.82E -02	4.01E -02	2.26E +01	-3.38E -05	3.61E -05
5.34E +00	3.30E -02	3.47E -02	2.35E +01	-2.44E -05	3.15E -05
5.64E +00	2.79E -02	2.97E -02			

E1 (MeV)	E2 (MeV)	Integral neutrons $cm^{-2}kW^{-1}s^{-1}$	Error neutrons $cm^{-2}kW^{-1}s^{-1}$
0.811	1.000	4.40E -01	2.09E -03
1.000	1.200	2.68E -01	1.24E -03
1.200	1.600	3.32E -01	2.04E -03
1.600	2.000	2.26E -01	1.63E -03
2.000	3.000	3.21E -01	2.98E -03
3.000	4.000	1.23E -01	1.97E -03
4.000	6.000	8.83E -02	2.03E -03
6.000	8.000	2.72E -02	1.28E -03
8.000	10.000	8.93E -03	5.85E -04
10.000	12.000	2.37E -03	2.70E -04
12.000	16.000	9.92E -04	2.91E -04
16.000	20.000	7.78E -05	1.43E -04
3.000	10.000	2.48E -01	5.87E -03
1.500	15.000	8.69E -01	1.15E -02
3.000	12.000	2.50E -01	6.14E -03

Table 45. Neutron fluxes (50 keV to 1.4 MeV) on centerline at 25 cm behind the lead slab (Item IIN) Runs 1585.A, 1584.A, 1583.B

N	Energy Boundary (MeV)		Flux (neutrons $cm^{-2}MeV^{-1}kW^{-1}s^{-1}$)	Error (%)
		RUN 1585.A		
1	0.0385	0.0450	5.11E +01	5.59
2	0.0450	0.0532	4.18E +01	6.04
3	0.0532	0.0630	3.52E +01	6.64
4	0.0630	0.0728	3.74E +01	7.00
5	0.0728	0.0859	3.41E +01	6.11
6	0.0859	0.1023	2.53E +01	7.09
7	0.1023	0.1186	2.46E +01	8.26
8	0.1186	0.1399	2.57E +01	6.34
9	0.1399	0.1661	2.05E +01	6.80
		RUN 1584.A		
1	0.1222	0.1410	2.39E +01	2.32
2	0.1410	0.1661	2.04E +01	2.28
3	0.1661	0.1974	1.75E +01	2.36
4	0.1974	0.2350	1.44E +01	2.64
5	0.2350	0.2726	1.35E +01	3.13
6	0.2726	0.3228	1.15E +01	2.92
7	0.3228	0.3792	7.76E +00	4.23
8	0.3792	0.4481	5.34E +00	5.50
9	0.4481	0.5234	7.02E +00	4.25
10	0.5234	0.6174	7.26E +00	3.30
11	0.6174	0.7302	4.99E +00	3.86
		RUN 1583.B		
1	0.5216	0.6204	6.85E +00	1.56
2	0.6204	0.7302	5.28E +00	1.84
3	0.7302	0.8510	3.65E +00	2.39
4	0.8510	1.0047	1.72E +00	3.86
5	1.0047	1.1804	1.04E +00	5.88
6	1.1804	1.4000	8.40E -01	5.91

Table 46. Fast neutron fluxes (>0.8 MeV) on centerline at 25 cm behind the lead slab (Item IIO) Run 7920

Neutron Energy (MeV)	Flux (neutrons $cm^{-2}MeV^{-1}kW^{-1}s^{-1}$) Lower Limit	Upper Limit	Neutron Energy (MeV)	Flux (neutrons $cm^{-2}MeV^{-1}kW^{-1}s^{-1}$) Lower Limit	Upper Limit
8.11E -01	2.67E +00	2.71E +00	5.94E +00	2.73E -02	2.92E -02
9.07E -01	2.56E +00	2.58E +00	6.25E +00	2.41E -02	2.65E -02
1.01E +00	1.99E +00	2.00E +00	6.55E +00	2.00E -02	2.19E -02
1.11E +00	1.48E +00	1.50E +00	6.84E +00	1.64E -02	1.78E -02
1.20E +00	1.18E +00	1.19E +00	7.24E +00	1.42E -02	1.53E -02
1.31E +00	9.88E -01	9.99E -01	7.74E +00	1.28E -02	1.42E -02
1.41E +00	8.81E -01	8.94E -01	8.24E +00	1.01E -02	1.15E -02
1.51E +00	8.13E -01	8.23E -01	8.76E +00	7.20E -03	7.93E -03
1.61E +00	7.44E -01	7.53E -01	9.26E +00	5.21E -03	5.86E -03
1.71E +00	6.73E -01	6.82E -01	9.74E +00	4.13E -03	4.65E -03
1.81E +00	6.12E -01	6.21E -01	1.03E +01	3.08E -03	3.54E -03
1.93E +00	5.53E -01	5.62E -01	1.08E +01	2.26E -03	2.66E -03
2.10E +00	4.75E -01	4.83E -01	1.12E +01	1.70E -03	2.02E -03
2.30E +00	3.91E -01	3.98E -01	1.18E +01	1.23E -03	1.49E -03
2.50E +00	3.21E -01	3.26E -01	1.24E +01	6.25E -04	8.69E -04
2.70E +00	2.61E -01	2.66E -01	1.32E +01	1.74E -04	3.51E -04
2.90E +00	2.18E -01	2.24E -01	1.40E +01	2.13E -04	3.78E -04
3.10E +00	1.80E -01	1.86E -01	1.48E +01	2.55E -04	3.84E -04
3.30E +00	1.45E -01	1.50E -01	1.56E +01	1.36E -04	2.46E -04
3.50E +00	1.20E -01	1.25E -01	1.65E +01	2.13E -05	9.80E -05
3.71E +00	1.06E -01	1.10E -01	1.75E +01	-3.29E -05	3.96E -05
3.91E +00	9.42E -02	9.76E -02	1.85E +01	-4.43E -05	1.53E -05
4.15E +00	8.18E -02	8.48E -02	1.95E +01	-4.04E -05	1.69E -05
4.45E +00	6.72E -02	6.97E -02	2.05E +01	-6.16E -05	2.43E -05
4.75E +00	5.27E -02	5.51E -02	2.16E +01	-6.33E -05	2.68E -05
5.04E +00	4.26E -02	4.47E -02	2.26E +01	-3.32E -05	3.07E -05
5.34E +00	3.51E -02	3.71E -02	2.35E +01	-1.91E -05	3.45E -05
5.64E +00	2.99E -02	3.20E -02			

E1 (MeV)	E2 (MeV)	Integral neutrons $cm^{-2}kW^{-1}s^{-1}$	Error neutrons $cm^{-2}kW^{-1}s^{-1}$
0.811	1.000	4.73E -01	2.05E -03
1.000	1.200	3.11E -01	1.34E -03
1.200	1.600	3.69E -01	2.24E -03
1.600	2.000	2.52E -01	1.73E -03
2.000	3.000	3.36E -01	3.14E -03
3.000	4.000	1.31E -01	2.19E -03
4.000	6.000	1.01E -01	2.31E -03
6.000	8.000	3.57E -02	1.59E -03
8.000	10.000	1.41E -02	8.01E -04
10.000	12.000	4.52E -03	3.62E -04
12.000	16.000	1.47E -03	3.27E -04
16.000	20.000	4.78E -05	1.36E -04
3.000	10.000	2.82E -01	6.90E -03
1.500	15.000	9.55E -01	1.29E -02
3.000	12.000	2.87E -01	7.26E -03

Table 47. Neutron fluxes (50 keV to 1.4 MeV) on centerline at 25 cm behind the lead slab (Item IIO) Runs 1588.A, 1587.A, 1586.A

N	Energy Boundary (MeV)		Flux (neutrons $cm^{-2}MeV^{-1}kW^{-1}s^{-1}$)	Error (%)
		RUN 1588.A		
1	0.0385	0.0467	5.61E +01	4.57
2	0.0467	0.0549	6.14E +01	4.73
3	0.0549	0.0631	7.36E +01	4.32
4	0.0631	0.0745	7.11E +01	3.29
5	0.0745	0.0876	4.54E +01	4.79
6	0.0876	0.1040	2.40E +01	7.79
7	0.1040	0.1220	3.17E +01	5.99
8	0.1220	0.1433	3.07E +01	5.57
9	0.1433	0.1695	1.82E +01	8.11
10	0.1695	0.1990	1.91E +01	7.56
11	0.1990	0.2350	1.68E +01	7.37
		RUN 1587.A		
1	0.1661	0.1974	1.86E +01	3.76
2	0.1974	0.2350	1.77E +01	3.70
3	0.2350	0.2726	1.88E +01	3.89
4	0.2726	0.3228	1.52E +01	3.81
5	0.3228	0.3792	1.14E +01	4.96
6	0.3792	0.4481	8.86E +00	5.60
7	0.4481	0.5234	9.16E +00	5.40
8	0.5234	0.6174	8.47E +00	4.69
9	0.6174	0.7302	6.01E +00	5.40
		RUN 1586.A		
1	0.5216	0.6204	7.81E +00	1.91
2	0.6204	0.7302	5.72E +00	2.39
3	0.7302	0.8510	4.12E +00	3.04
4	0.8510	1.0047	2.47E +00	3.89
5	1.0047	1.1804	1.44E +00	5.97
6	1.1804	1.4000	9.14E -01	7.60

Table 48. Fission chamber measurements in void at 0.7 cm behind the fuel pins

	count rates ($s^{-1}W^{-1}$)		
Detector	Item IIP[a]	Item IIQ	Item IIIF
bare	7.75 (-5)[b]	9.15 (-5)	3.68 (-2)
Cd-covered	3.66 (-5)	4.40 (-5)	2.25 (-2)
bare detector with Cd covering cylinder of detector housing	3.91 (-5)	4.64 (-5)	

[a]See experimental program plan in Appendix A for description of configurations.
[b]Read: 7.75×10^{-5}.

Table 49. Bonner ball measurements on centerline at 30 cm behind the ALMR shield mockups

Configuration[a]	Bonner ball count rates ($s^{-1}W^{-1}$)					
	3-inch Diam Ball	4-inch Diam Ball	5-inch Diam Ball	8-inch Diam Ball	10-inch Diam Ball	12-inch Diam Ball
IIIA	8.86 (0)[b]	1.89 (1)	2.28 (1)	1.52 (1)	8.71 (0)	4.78 (0)
IIIB	5.72 (0)	1.44 (1)	1.96 (1)	1.59 (1)	9.83 (0)	5.54 (0)
IIIC	7.12 (0)	1.40 (1)	1.60 (1)	9.81 (0)	5.54 (0))	2.96 (0)
IIID	8.18 (-1)	3.80 (0)	6.43 (0)	6.58 (0)	4.29 (0)	2.50 (0)
IIIE	1.28 (-1)	3.94 (-1)	5.34 (-1)	3.59 (-1)	1.88 (-1)	9.94 (-2)
IIIF	3.46 (-1)	1.53 (0)	2.59 (0)	2.52 (0)	1.55 (0)	8.87 (-1)

[a]See experimental program plan in Appendix A for description of configurations.
[b]Read: 8.86×10^{0}.

Table 50. Bonner ball measurements on centerline at 150 cm behind the ALMR shield mockups

	Bonner ball count rates ($s^{-1}W^{-1}$)											
	3-inch Diam ball		4-inch Diam ball		5-inch Diam ball		8-inch Diam ball		10-inch Diam ball		12-inch Diam ball	
Configuration[a]	Foreground[b]	Background[c]	Foreground	Background	Foreground	Background	Foreground	Background	Foreground	Background	Foreground	Background
IIIA	1.47 (0)[d]	9.68 (-2)	3.01 (0)	1.79 (-1)	3.44 (0)	1.97 (-1)	2.16 (0)	1.06 (-1)	1.19 (0)	5.61 (-2)	6.24 (-1)	2.93 (-2)
IIIB	9.91 (-1)	5.59 (-2)	2.23 (0)	1.11 (-1)	2.87 (0)	1.34 (-1)	2.20 (0)	7.49 (-1)	1.32 (0)	4.38 (-2)	7.30 (-1)	2.40 (-2)
IIIC	1.43 (0)	1.04 (-1)	2.74 (0)	1.81 (-1)	2.98 (0)	1.90 (-1)	1.73 (0)	9.09 (-2)	9.44 (-1)	4.43 (-2)	4.89 (-1)	2.23 (-2)
IIID	1.25 (-1)	1.49 (-2)	5.58 (-1)	3.38 (-2)	9.36 (-1)	4.36 (-2)	9.56 (-1)	2.98 (-2)	6.13 (-1)	1.74 (-2)	3.61 (-1)	9.53 (-3)
IIIE	2.41 (-2)	2.94 (-3)	6.89 (-2)	5.99 (-3)	8.72 (-2)	6.67 (-3)	5.73 (-2)	3.20 (-3)	3.03 (-2)	1.57 (-3)	1.57 (-2)	7.64 (-4)
IIIF	7.28 (-2)	1.22 (-2)	2.94 (-1)	3.04 (-2)	4.69 (-1)	3.79 (-2)	4.58 (-1)	2.49 (-2)	2.82 (-1)	1.50 (-2)	1.60 (-1)	7.84 (-3)

[a]See experimental program plan in Appendix A for description of configurations.
[b]Count rate without shadow shield between detector and configuration.
[c]Count rate with shadow shield between detector and configuration.
[d]Read: 1.47×10^{0}.

Table 51. 3-inch Bonner ball radial traverses at 30 cm behind the ALMR shield mockups

Distance from Centerline (cm)	count rates ($s^{-1}W^{-1}$) Item IIIA[a]	Item IIIB
100 S		6.11 (-1)[b]
90	8.79 (-1)	
80		1.11 (0)
70	1.71 (0)	
60		2.39 (0)
50	4.23 (0)	3.57 (0)
40	5.83 (0)	4.36 (0)
30	7.14 (0)	4.92 (0)
20	8.19 (0)	5.46 (0)
15	8.55 (0)	
10	8.77 (0)	5.74 (0)
5	8.86 (0)	
0	8.84 (0)	5.80 (0)
5	8.84 (0)	
10	8.67 (0)	5.68 (0)
15	8.38 (0)	
20	7.95 (0)	5.36 (0)
30	6.77 (0)	4.88 (0)
40	5.52 (0)	4.26 (0)
50	3.90 (0)	3.43 (0)
60		2.28 (0)
70	1.54 (0)	1.54 (0)
88 N	8.65 (-1)	

[a]See experimental program plan in Appendix A for description of configurations.
[b]Read: 6.11×10^{-1}.

Table 52. 10-inch Bonner ball radial traverses at 30 cm behind the ALMR shield mockups

Distance from Centerline (cm)	count rates ($s^{-1}W^{-1}$) Item IIIA[a]	Item IIIB
100 S		1.82 (0)[b]
80		1.79 (0)
79.5	1.36 (0)	
70	1.95 (0)	
60		3.96 (0)
50	4.21 (0)	5.52 (0)
40	5.55 (0)	6.99 (0)
30	6.87 (0)	8.24 (0)
20	7.89 (0)	9.22 (0)
15	8.31 (0)	
10	8.53 (0)	9.81 (0)
5	8.78 (0)	
0	8.72 (0)	9.93 (0)
5	8.76 (0)	
10	8.59 (0)	9.67 (0)
15	8.35 (0)	
20	7.93 (0)	9.03 (0)
30	6.97 (0)	8.00 (0)
40	5.74 (0)	6.65 (0)
50	4.30 (0)	5.18 (0)
60		3.71 (0)
70	1.97 (0)	2.55 (0)
80 N	1.33 (0)	

[a]See experimental program plan in Appendix A for description of configurations.
[b]Read: 1.82×10^{0}.

Table 53. Bare fission chamber radial traverses at 30 cm behind the ALMR shield mockups

Distance from Centerline (cm)	count rates ($s^{-1}W^{-1}$) Item IIIA[a]	Item IIIB
100 S		3.47 (-3)[b]
90	4.63 (-3)	
80		5.30 (-3)
70	6.78 (-3)	
60		7.82 (-3)
50	1.44 (-2)	1.14 (-2)
40	2.02 (-2)	1.30 (-2)
30	2.37 (-2)	1.40 (-2)
20	2.66 (-2)	1.44 (-2)
15	2.71 (-2)	
10	2.75 (-2)	1.46 (-2)
5	2.79 (-2)	
0	2.77 (-2)	1.46 (-2)
5	2.76 (-2)	
10	2.74 (-2)	1.46 (-2)
15	2.71 (-2)	
20	2.60 (-2)	1.42 (-2)
30	2.33 (-2)	1.37 (-2)
40	1.96 (-2)	1.28 (-2)
50	1.45 (-2)	1.07 (-2)
60		7.45 (-3)
70	6.77 (-3)	
78 N	5.66 (-3)	

[a]See experimental program plan in Appendix A for description of configurations.
[b]Read: 3.47×10^{-3}.

Table 54. Cd-covered fission chamber radial traverses at 30 cm behind the ALMR shield mockups

Distance from Centerline (cm)	count rates ($s^{-1}W^{-1}$) Item IIIA[a]	Item IIIB
100 S		9.30 (-4)[b]
90	1.42 (-3)	
80		1.77 (-3)
70	2.76 (-3)	
60		3.81 (-3)
50	7.52 (-3)	5.91 (-3)
40	1.08 (-2)	7.07 (-3)
30	1.34 (-2)	8.02 (-3)
20	1.55 (-2)	8.69 (-3)
15	1.63 (-2)	
10	1.67 (-2)	9.05 (-3)
5	1.68 (-2)	
0	1.68 (-2)	9.17 (-3)
5	1.69 (-2)	
10	1.65 (-2)	9.01 (-3)
15	1.61 (-2)	
20	1.52 (-2)	8.59 (-3)
30	1.30 (-2)	7.87 (-3)
40	1.06 (-2)	6.98 (-3)
50	7.39 (-3)	5.68 (-3)
60		3.64 (-3)
70	2.64 (-3)	
78 N	2.02 (-3)	

[a]See experimental program plan in Appendix A for description of configurations.
[b]Read: 9.30×10^{-4}.

Table 55. Bare fission chamber radial traverses at 30 cm behind the ALMR shield mockups (Cd over the face of the mockup)

	count rates ($s^{-1}W^{-1}$)	
Distance from Centerline (cm)	Item IIIA[a]	Item IIIB
100 S		2.62 (-3)[b]
90	3.09 (-3)	
80		3.64 (-3)
70	4.02 (-3)	
60		5.08 (-3)
50	8.54 (-3)	7.00 (-3)
40	1.17 (-2)	8.23 (-3)
30	1.43 (-2)	8.94 (-3)
20	1.66 (-2)	9.65 (-3)
15	1.73 (-2)	
10	1.78 (-2)	1.01 (-2)
5	1.80 (-2)	
0	1.78 (-2)	1.01 (-2)
5	1.80 (-2)	
10	1.77 (-2)	9.98 (-3)
15	1.73 (-2)	
20	1.67 (-2)	9.54 (-3)
30	1.42 (-2)	8.88 (-3)
40	1.19 (-2)	7.92 (-3)
50	8.78 (-3)	6.84 (-3)
60		4.90 (-3)
70	4.22 (-3)	
78 N	3.61 (-3)	

[a]See experimental program plan in Appendix A for description of configurations.
[b]Read: 2.62×10^{-3}.

Table 56. Fission chamber measurements on centerline at 30 cm behind the ALMR shield mockups

	count rates ($s^{-1}W^{-1}$)					
Detector	Item IIIA[a]	Item IIIB	Item IIIC	Item IIID	Item IIIE	Item IIIF
bare	2.81 (-2)[b]	1.39 (-2)	2.21 (-2	7.80 (-4)	2.67 (-4)	5.61 (-4)
Cd covered	1.69 (-2)	8.92 (-3)	1.44 (-2)	5.98 (-4)	1.19 (-4)	2.66 (-4)
bare Cd sheet over mockup	1.81 (-2)	9.78 (-3)	1.60 (-2)	7.35 (-4)	1.83 (-4)	4.49 (-4)
bare inside Cd hut	2.59 (-2)	1.30 (-2)	1.95 (-2)	6.08 (-4)	1.92 (-4)	3.08 (-4)

[a]See experimental program plan in Appendix A for description of configurations.
[b]Read: 2.81×10^{-2}.

Table 57. Fission chamber measurements on centerline at 150 cm behind the ALMR shield mockups

	count rates ($s^{-1}W^{-1}$)					
Detector	Item IIIA[a]	Item IIIB	Item IIIC	Item IIID	Item IIIE	Item IIIF
bare	6.53 (-3)[b]	3.79 (-3)	5.53 (-3)	2.73 (-4)	1.40 (-4)	3.05 (-4)
Cd covered	3.06 (-3)	1.75 (-3)	2.99 (-3)	1.08 (-4)	2.82 (-5)	7.21 (-5)
bare Cd sheet over mockup	4.18 (-3)	2.57 (-3)	4.16 (-3)	2.61 (-4)	1.16 (-4)	2.67 (-4)

[a]See experimental program plan in Appendix A for description of configurations.
[b]Read: 6.53×10^{-3}.

APPENDIX C

FIGURES

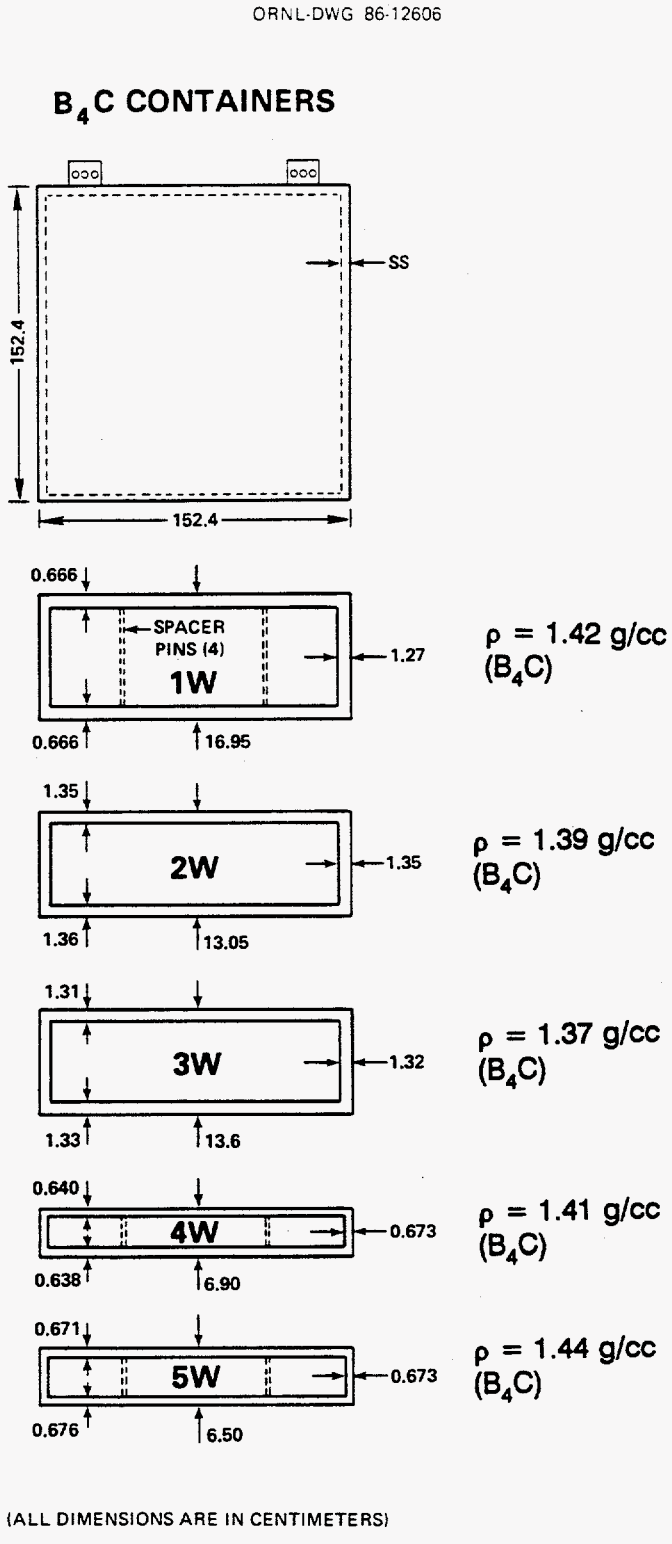

Figure 1. Schematic of stainless steel containers used for boron carbide shield slabs.

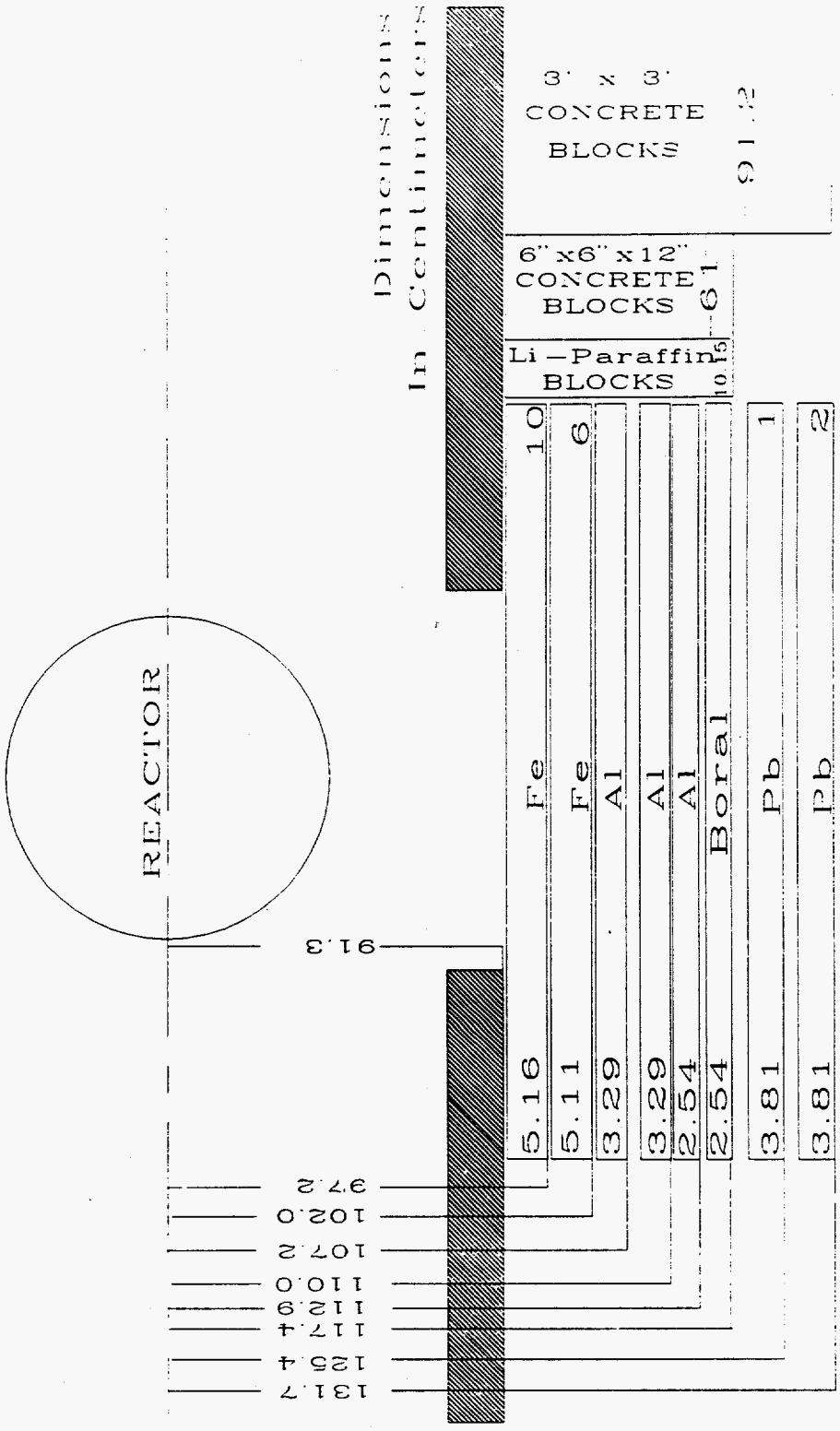

Figure 2. Schematic of SM-0 (Fe + Al + Boral) Item IA plus lead.

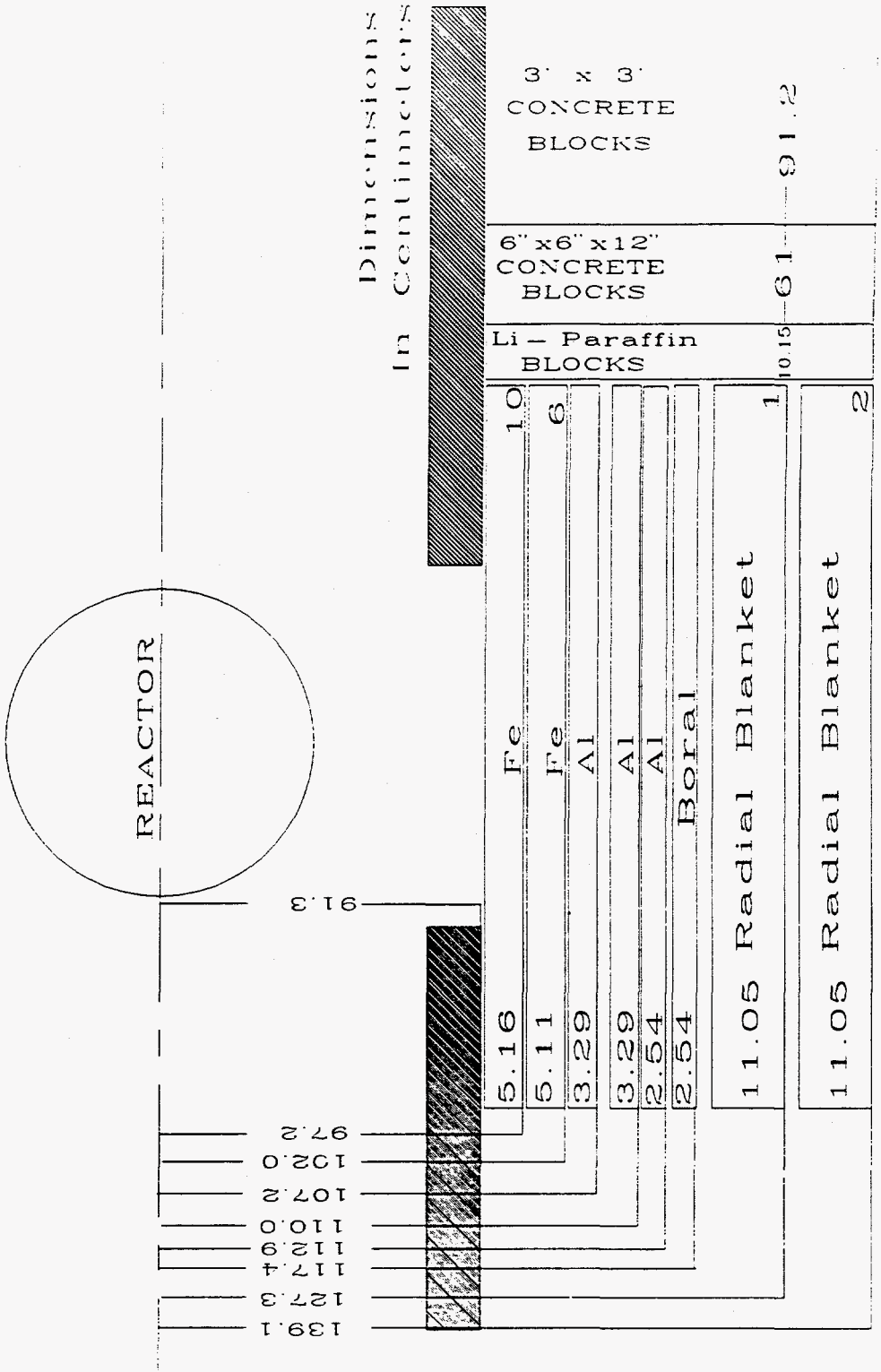

Figure 3. Schematic of SM-1 (Fe + Al + Boral + radial blankets) Item IB.

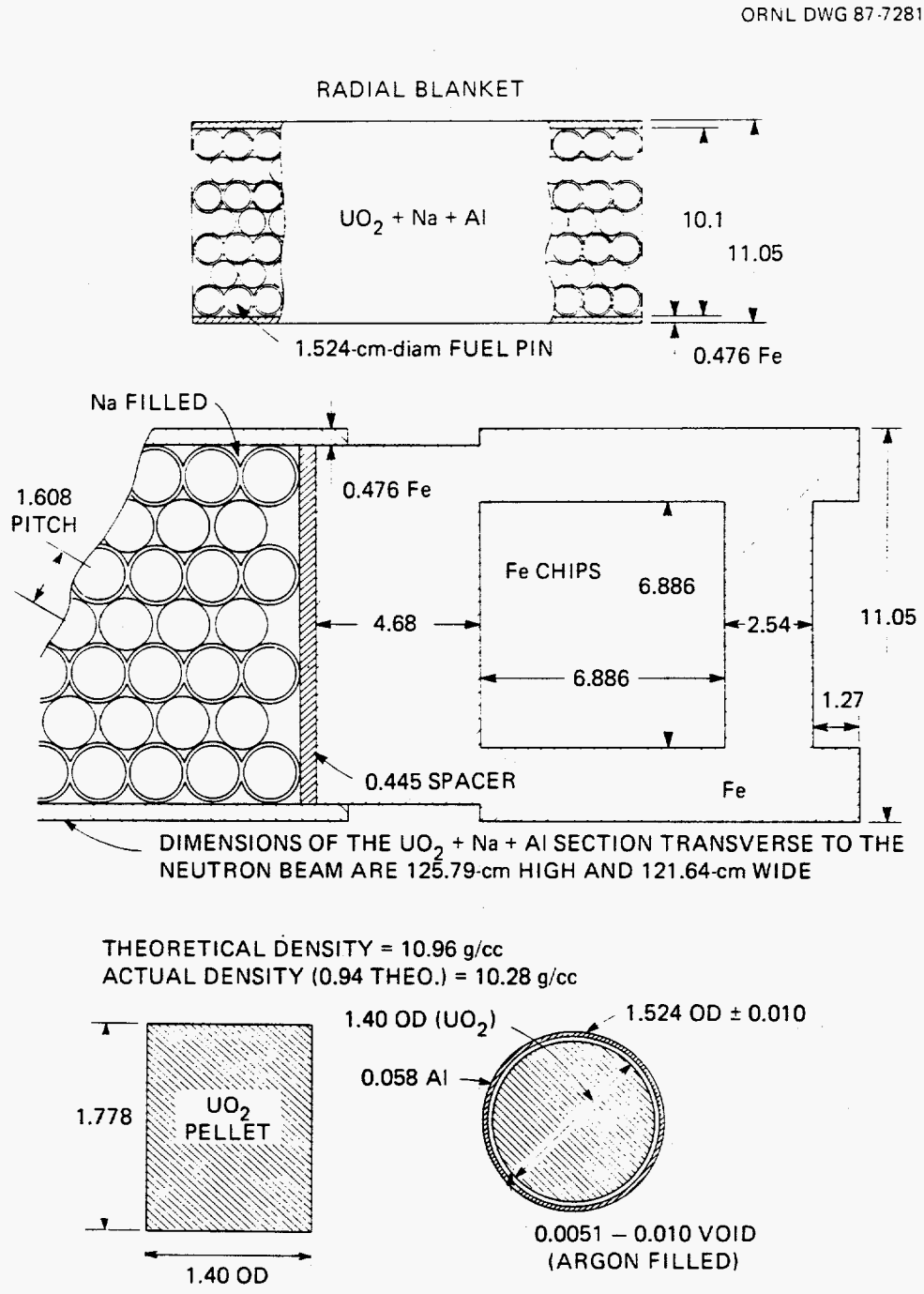

Figure 4. Schematic of radial blanket slab containing UO_2.

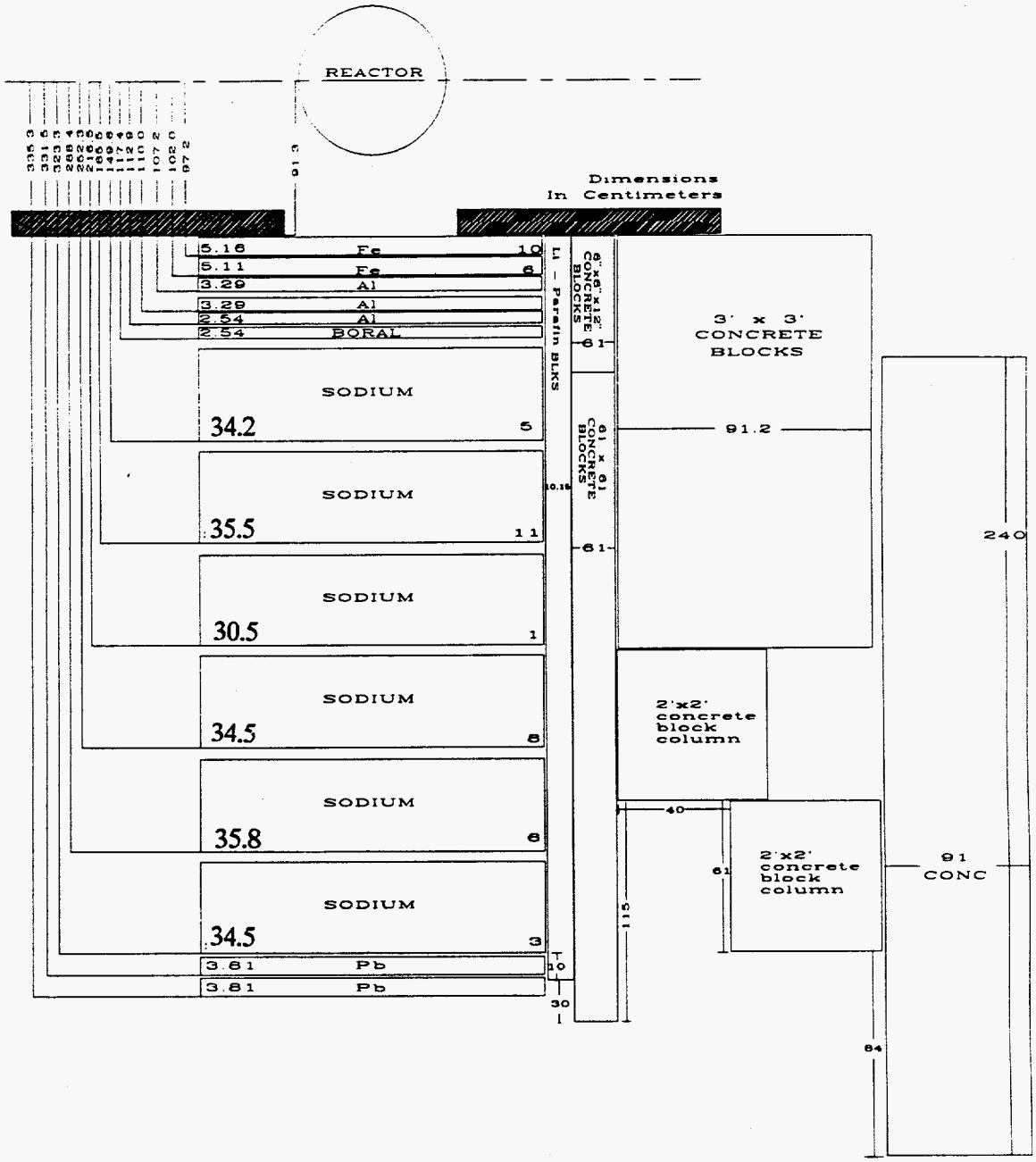

Figure 5. Schematic of SM-2 (Fe + Al + Boral + sodium) plus lead.

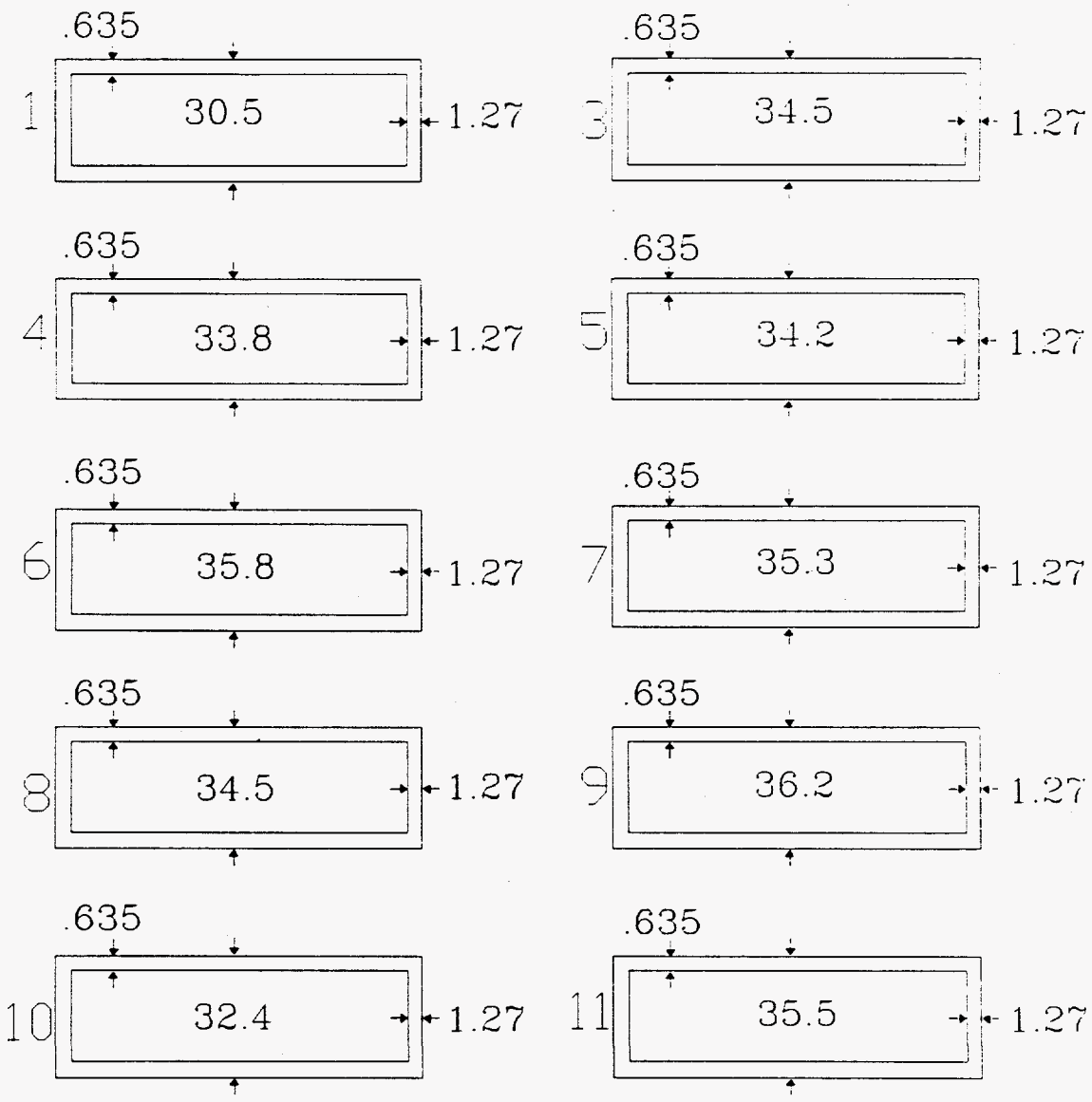

Figure 6. Schematic of sodium tanks.

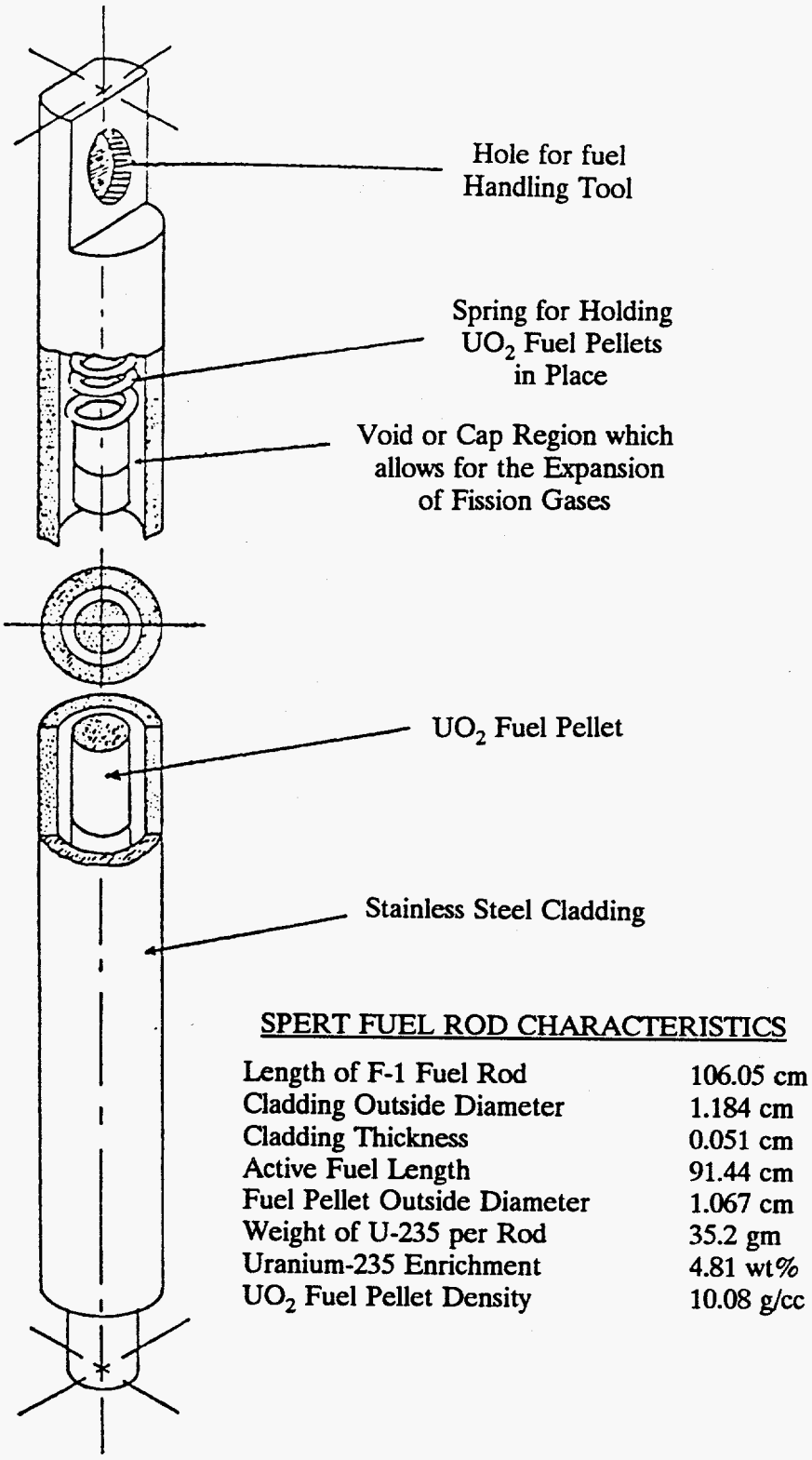

SPERT FUEL ROD CHARACTERISTICS

Length of F-1 Fuel Rod	106.05 cm
Cladding Outside Diameter	1.184 cm
Cladding Thickness	0.051 cm
Active Fuel Length	91.44 cm
Fuel Pellet Outside Diameter	1.067 cm
Weight of U-235 per Rod	35.2 gm
Uranium-235 Enrichment	4.81 wt%
UO_2 Fuel Pellet Density	10.08 g/cc

Figure 7. Isometric of the SPERT fuel rod containing uranium-dioxide fuel pellets.

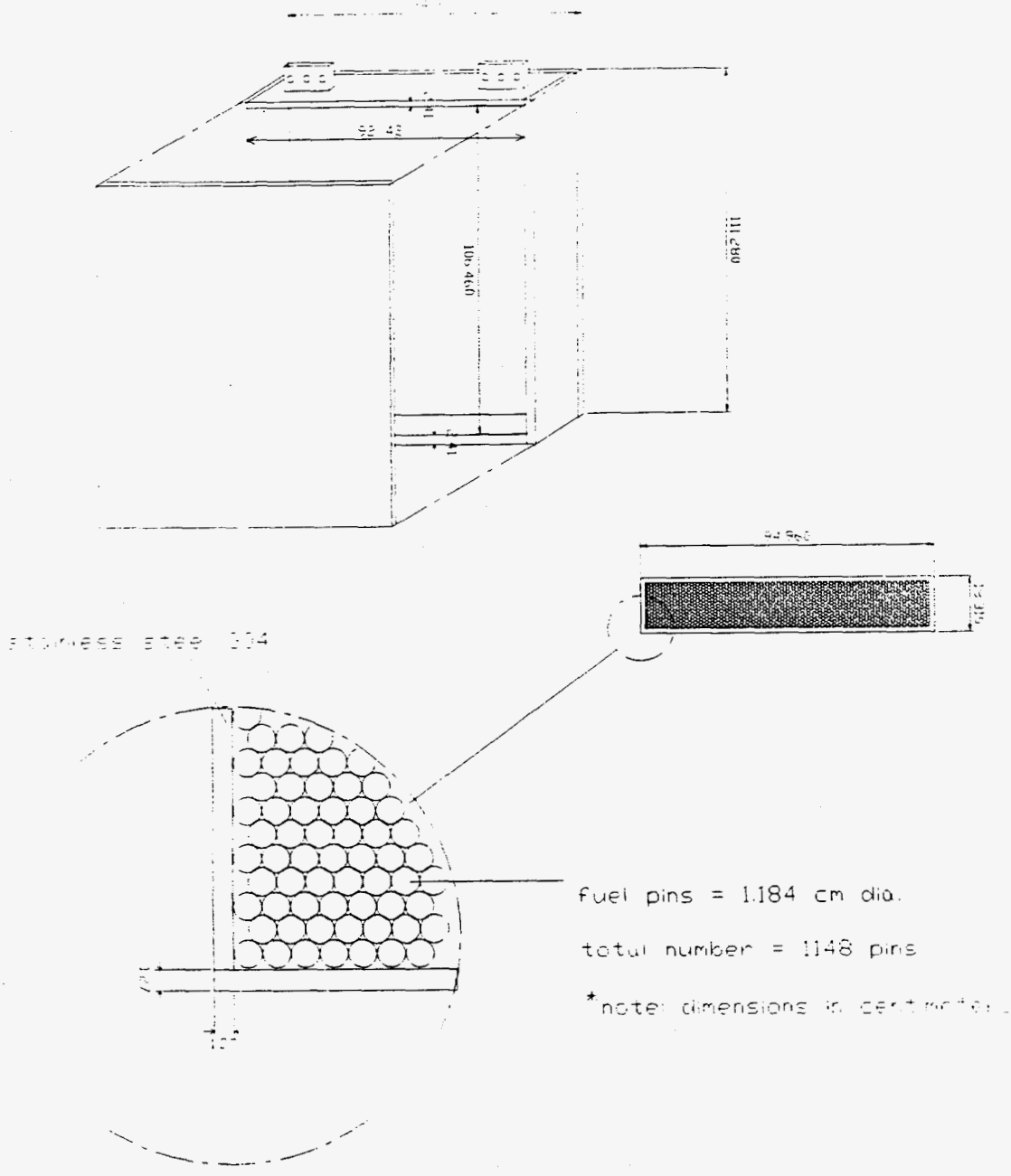

Figure 8. Schematic of thick IVFS mockup (slab #1).

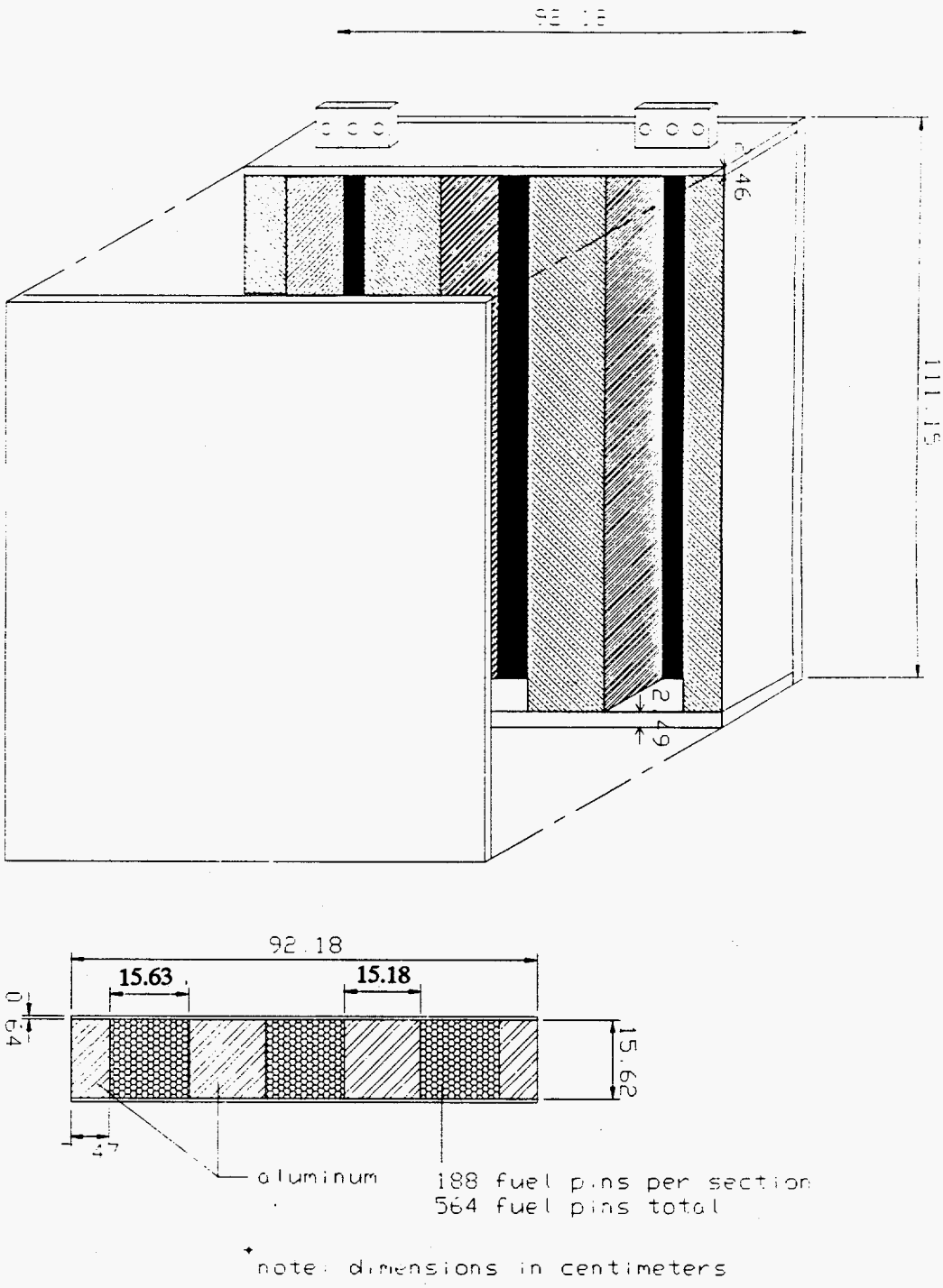

Figure 9. Schematic of heterogeneous IVFS mockup (slab #2).

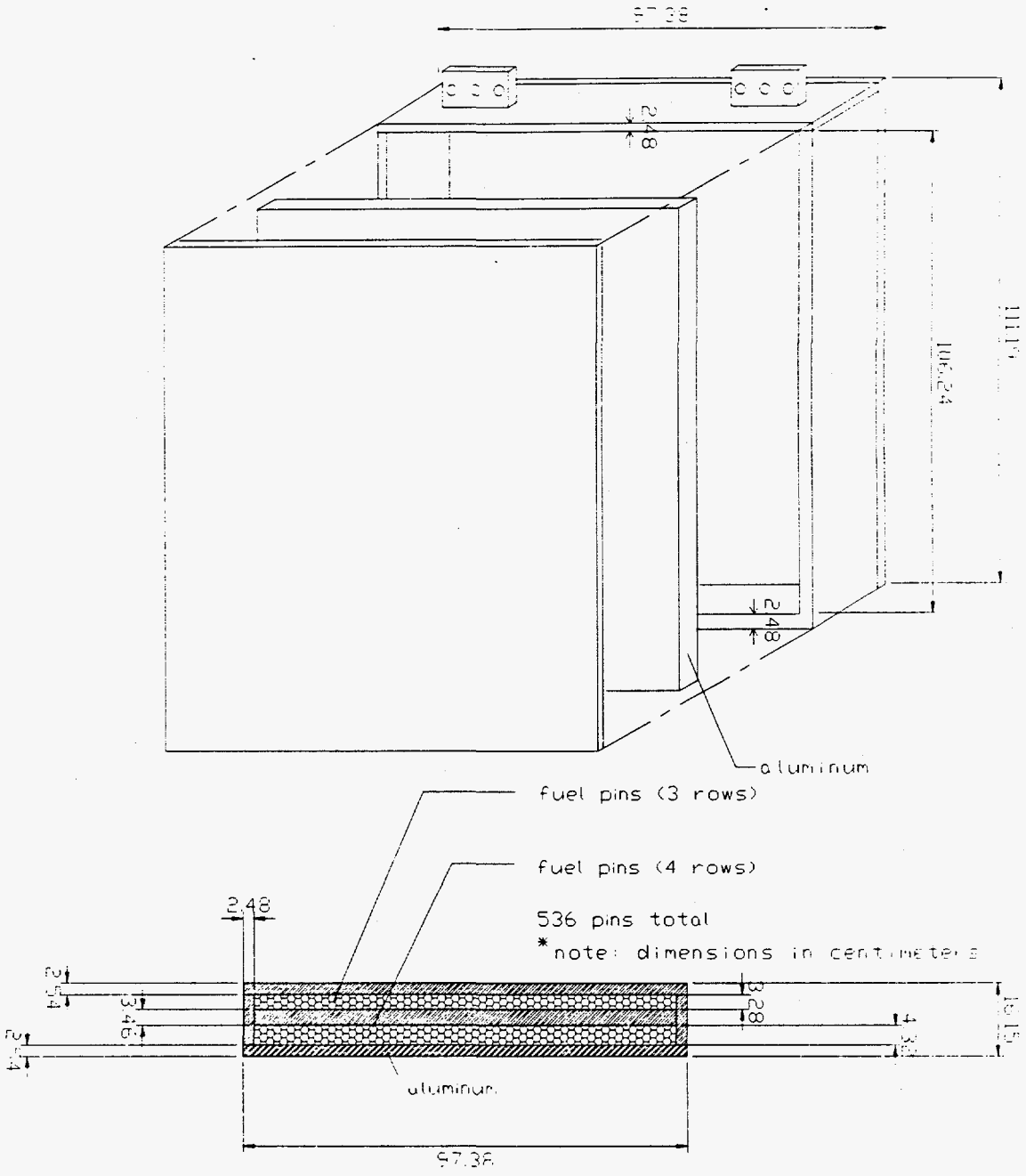

Figure 10. Schematic of homogeneous IVFS mockup (slab #3).

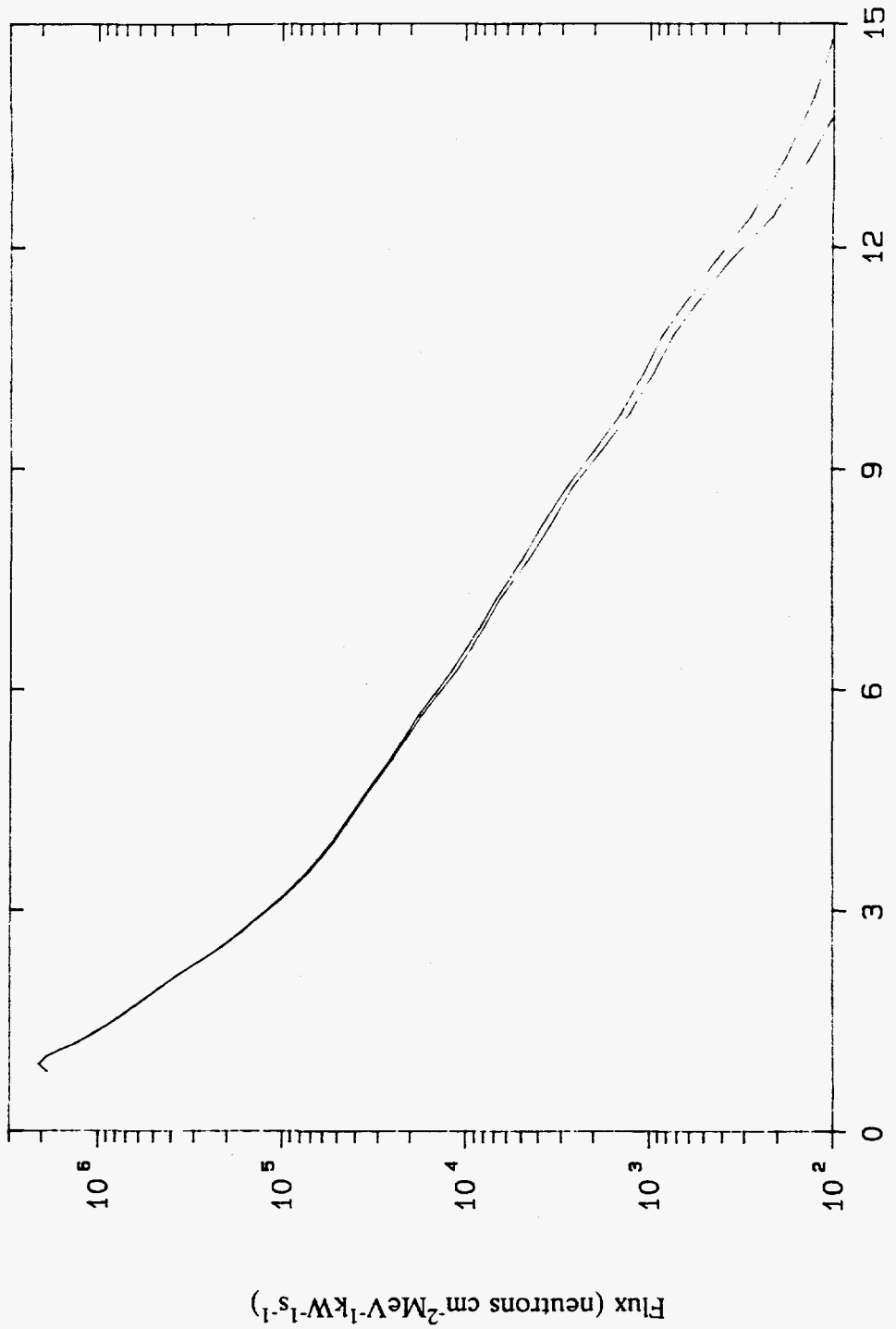

Figure 11. Spectrum of high-energy neutrons (>0.8 MeV) on centerline at 25 cm behind the lead slab (Item IA) Run 7900.A.

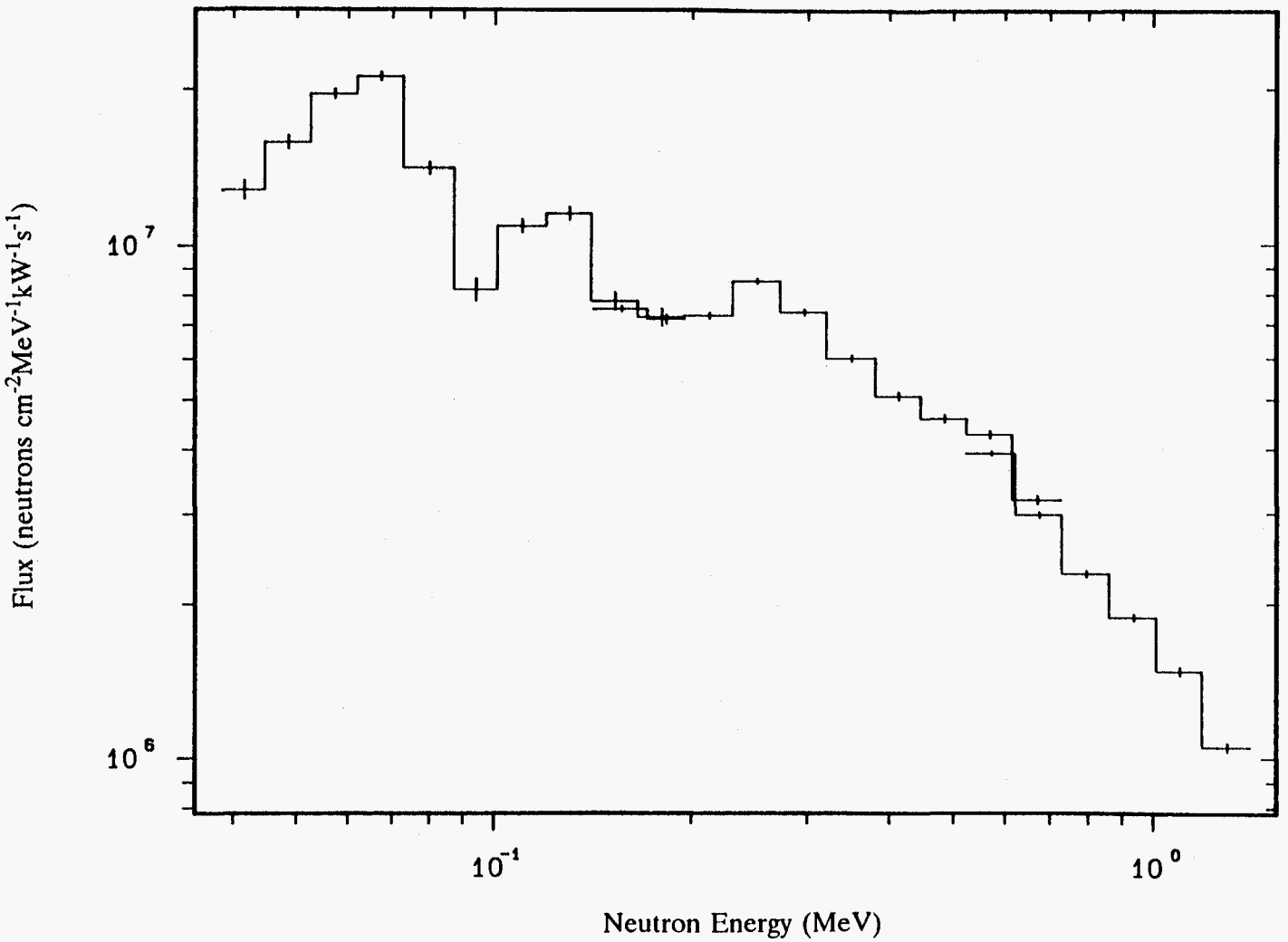

Figure 12. Neutron spectrum (50 keV to 1.4 MeV) on centerline at 25 cm behind the lead slab (Item IA) Runs 1573.D, 1573.B, 1573.A.

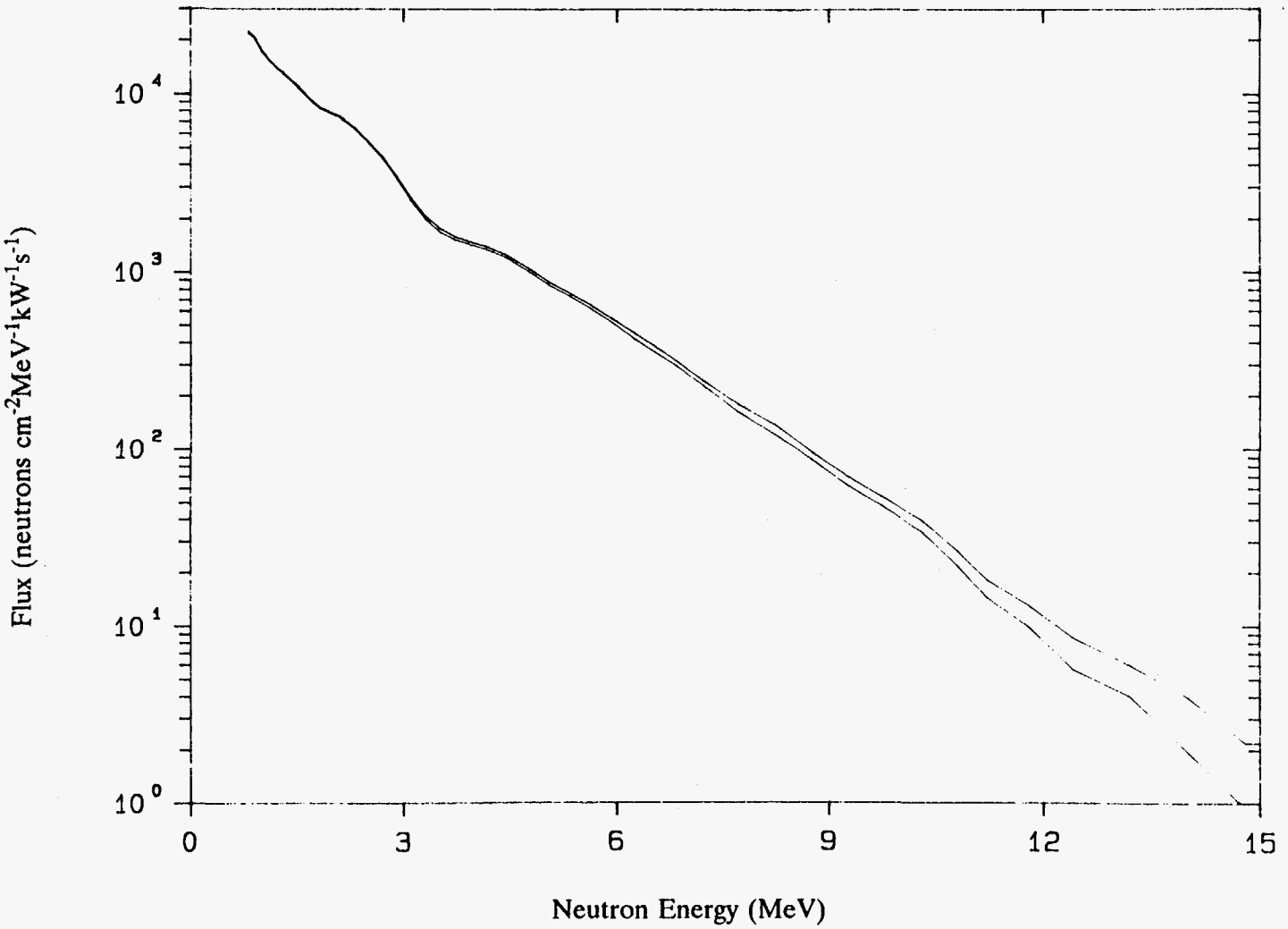

Figure 13. Spectrum of high-energy neutrons (>0.8 MeV) on centerline at 179.1 cm behind the mockup (Item IB) Run 7903.

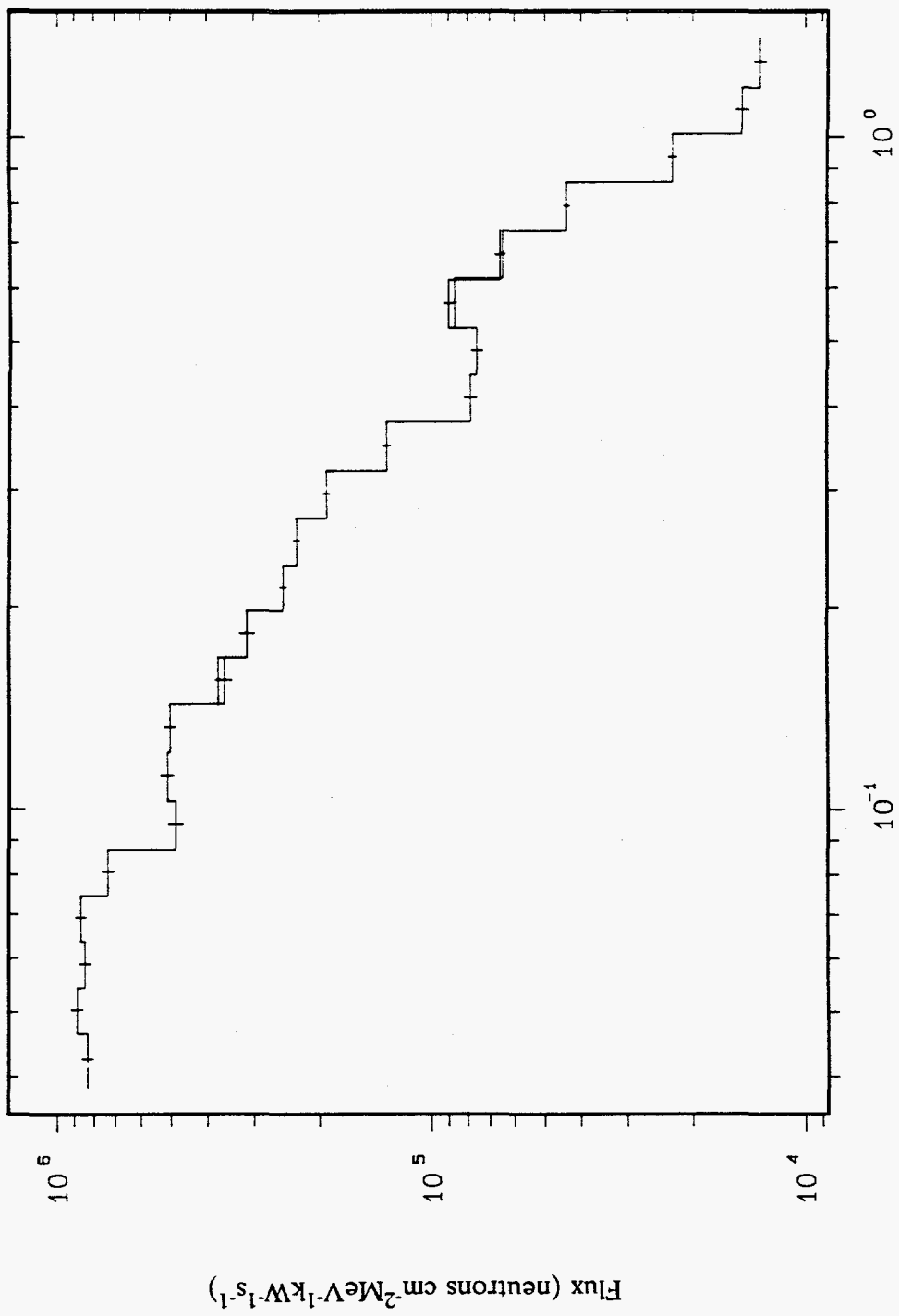

Figure 14. Neutron spectrum (50 keV to 1.4 MeV) on centerline at 179.1 cm behind the mockup (Item IB) Runs 1575.D, 1575.A, 1574.D.

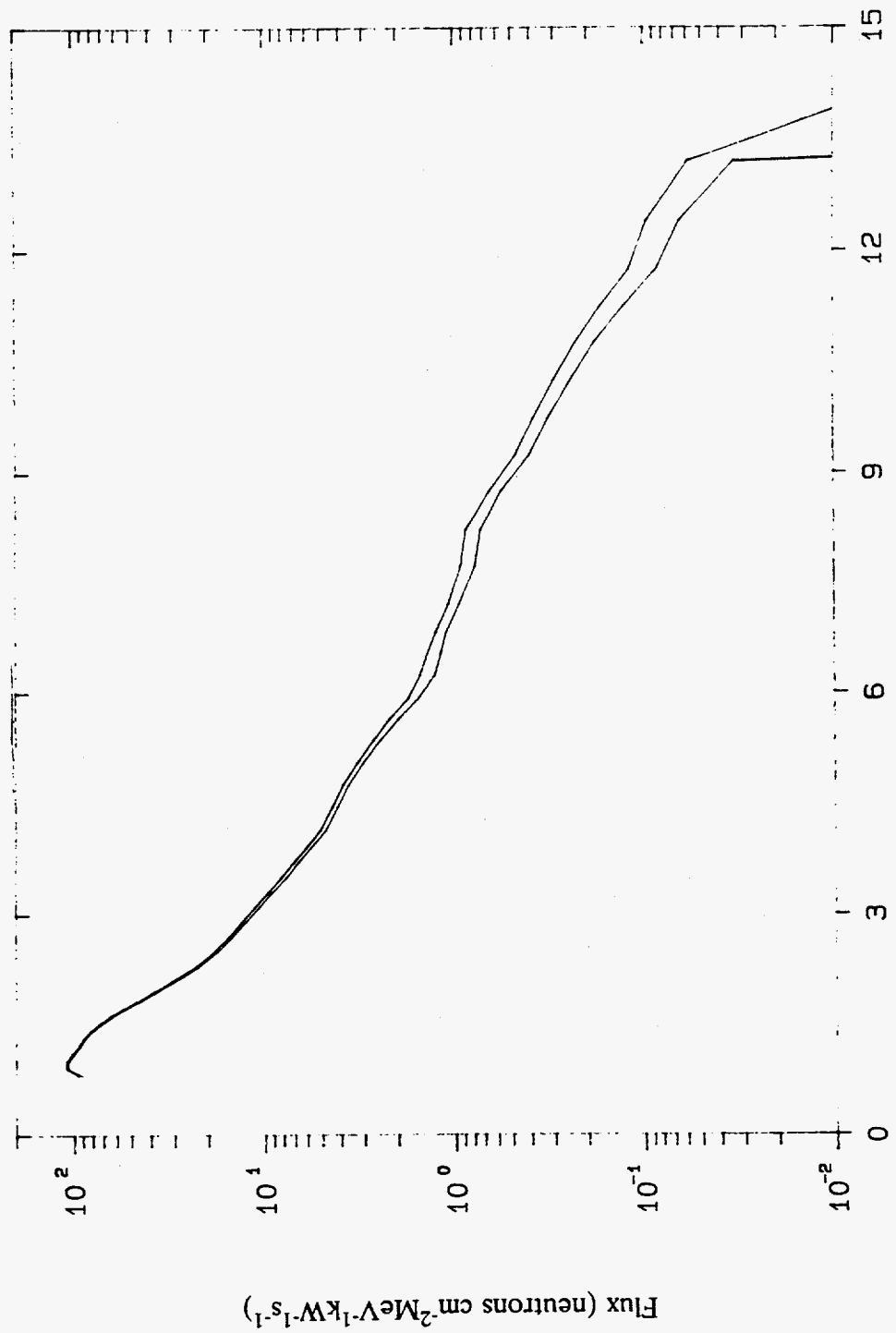

Figure 15. Spectrum of high-energy neutrons (>0.8 MeV) on centerline at 25 cm behind the lead slab (Item IC) Run 7922.

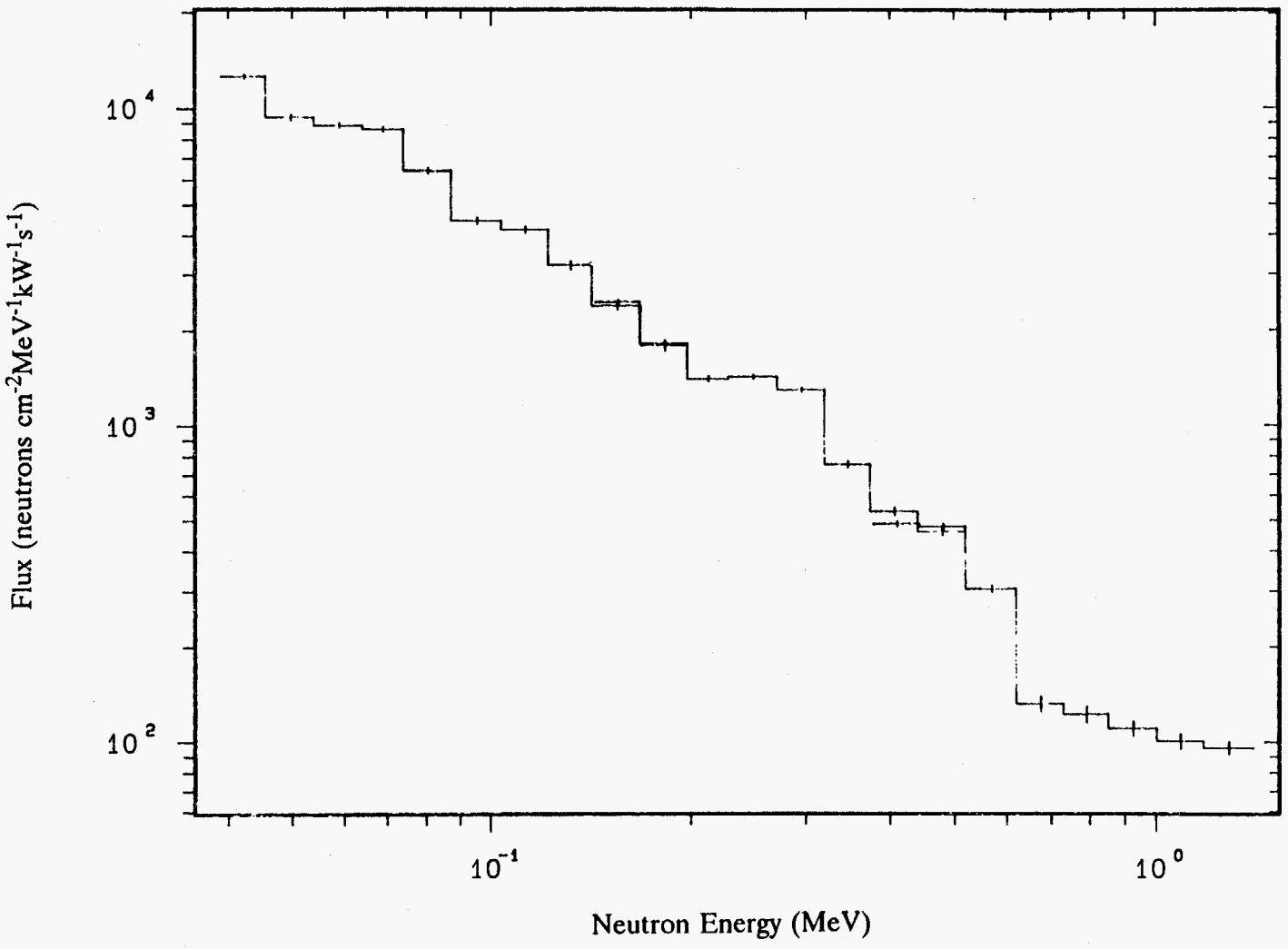

Figure 16. Neutron spectrum (50 keV to 1.4 MeV) on centerline at 25 cm behind the lead slab (Item IC) Runs 1591.A, 1590.A, 1589.A.

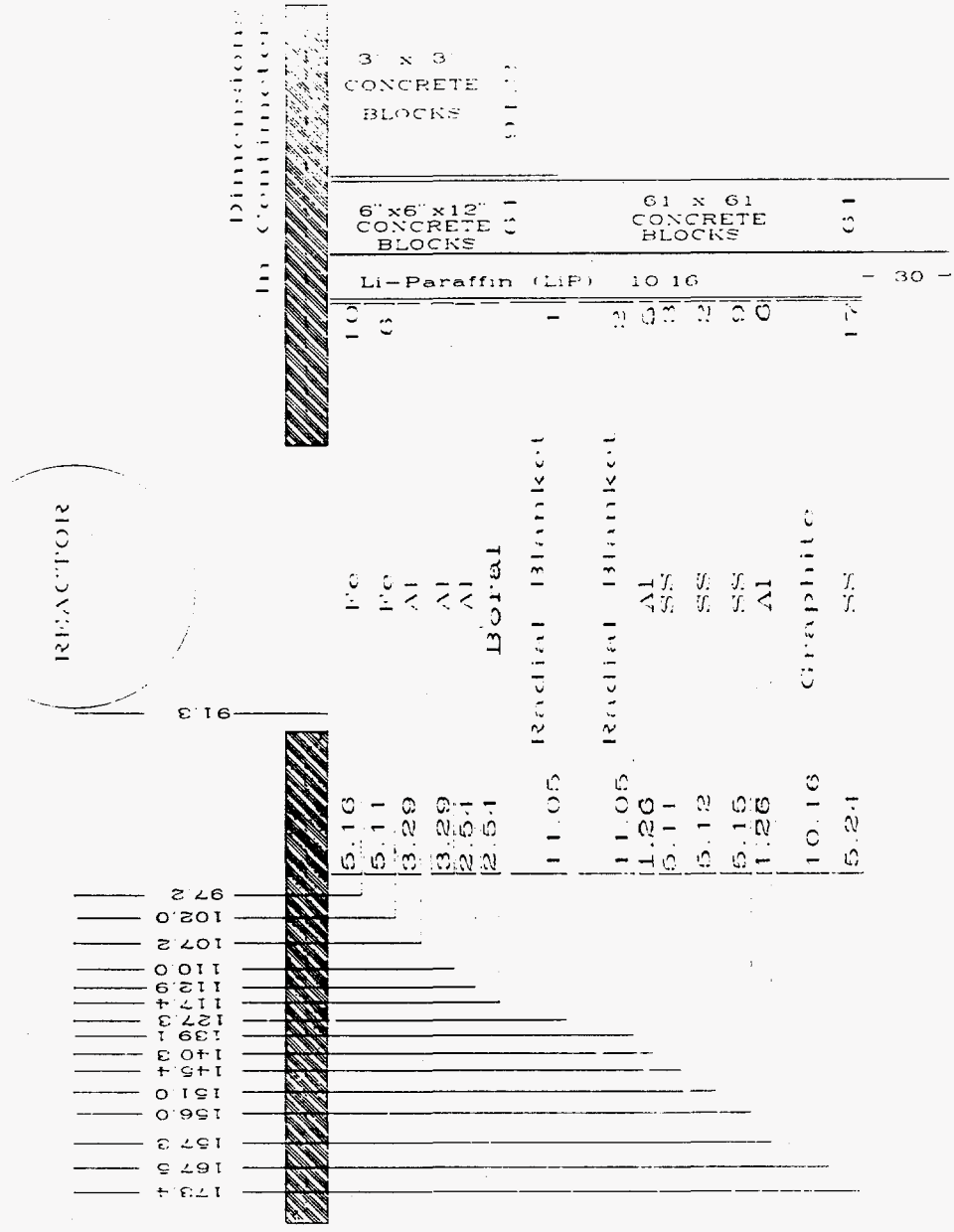

Figure 17. Schematic of SM-1 plus shield configuration for Item IIA.

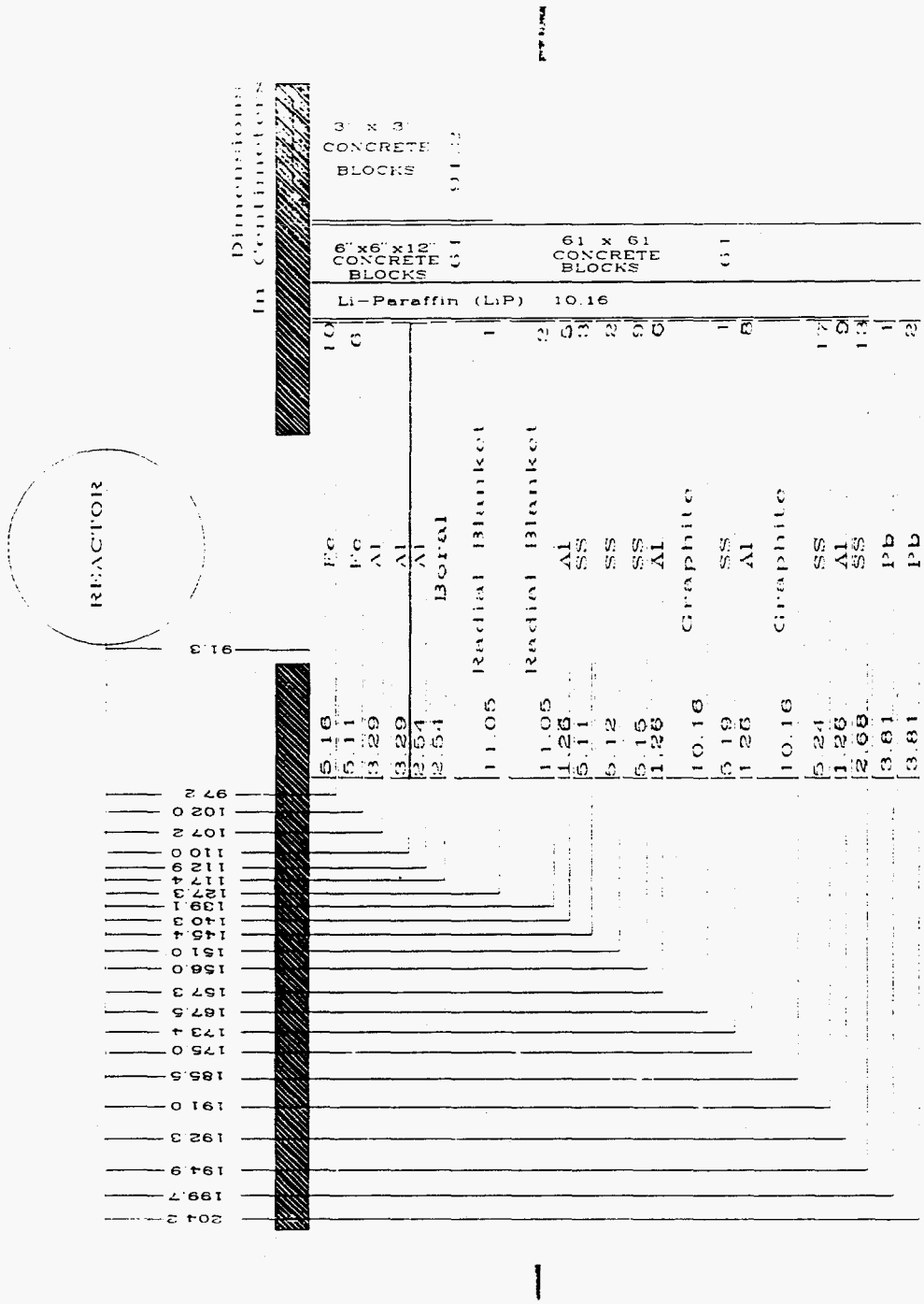

Figure 18. Schematic of SM-1 plus shield configuration for Item IIB plus lead.

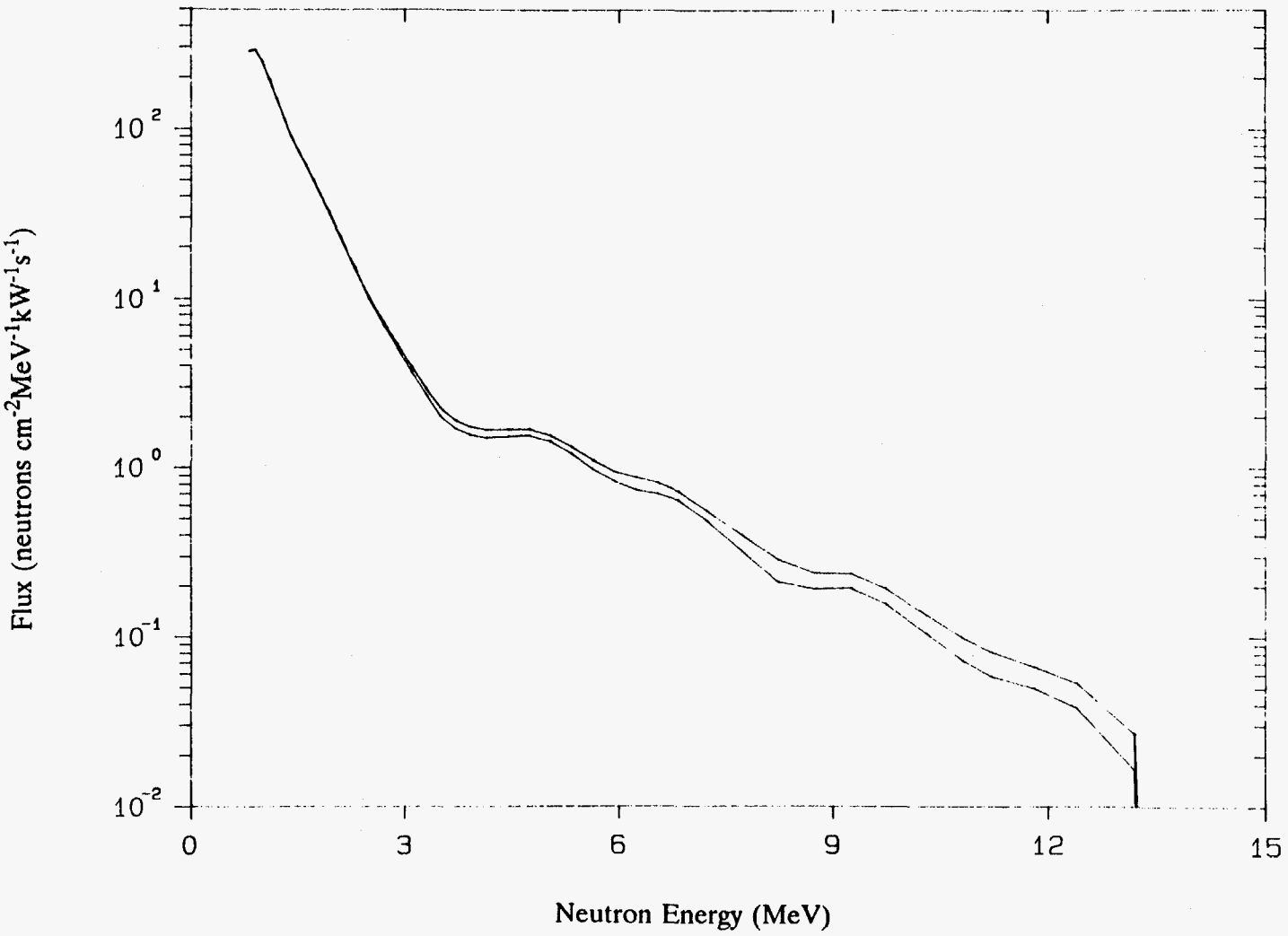

Figure 19. Spectrum of high-energy neutrons (>0.8 MeV) on centerline at 25 cm behind the lead slab (Item IIB) Run 7912.

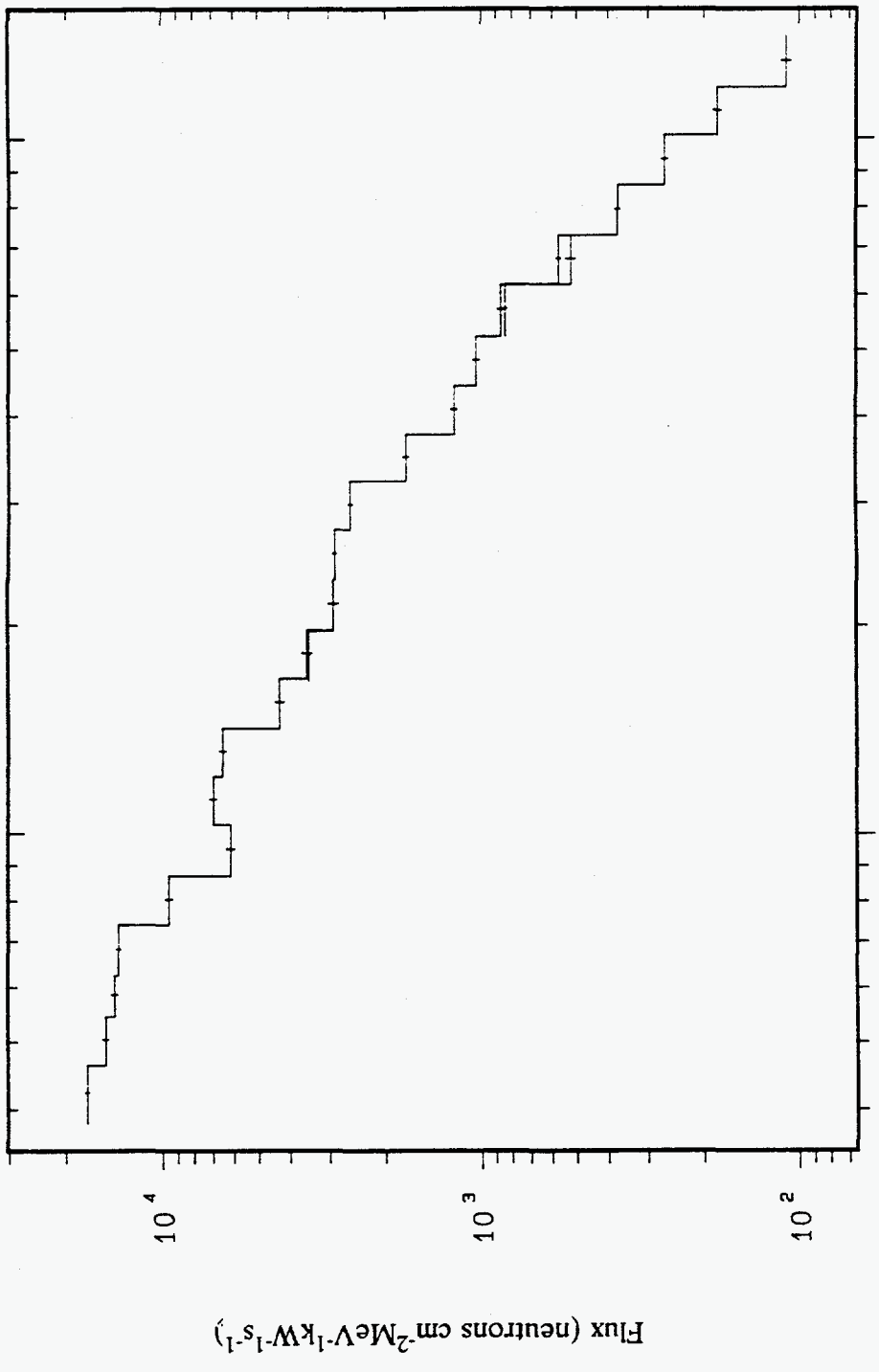

Figure 20. Neutron spectrum (50 keV to 1.4 MeV) on centerline at 25 cm behind the lead slab (Item IIB) Runs 1577.B, 1577.A, 1576.A.

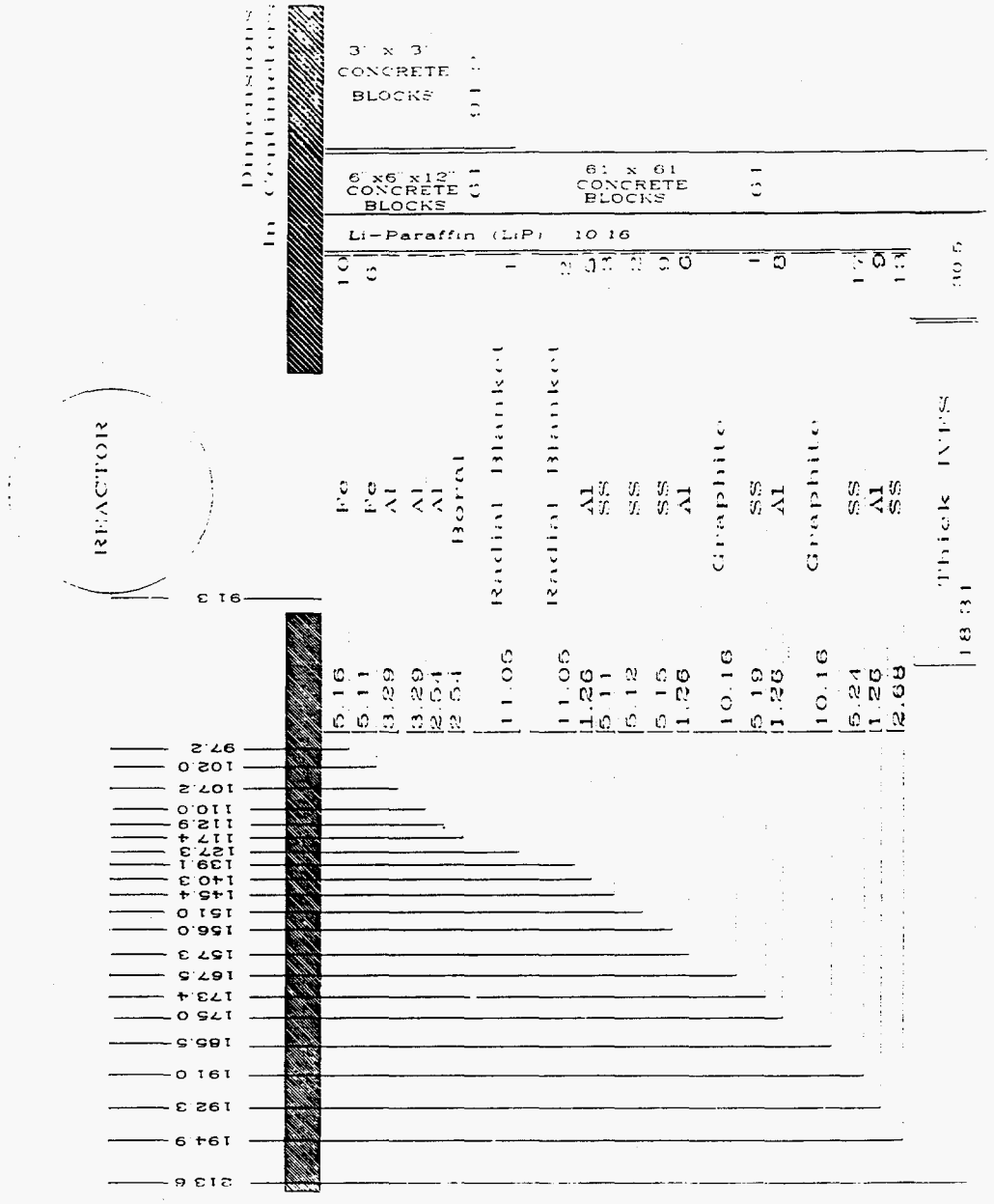

Figure 21. Schematic of SM-1 plus shield configuration for Item IIC.

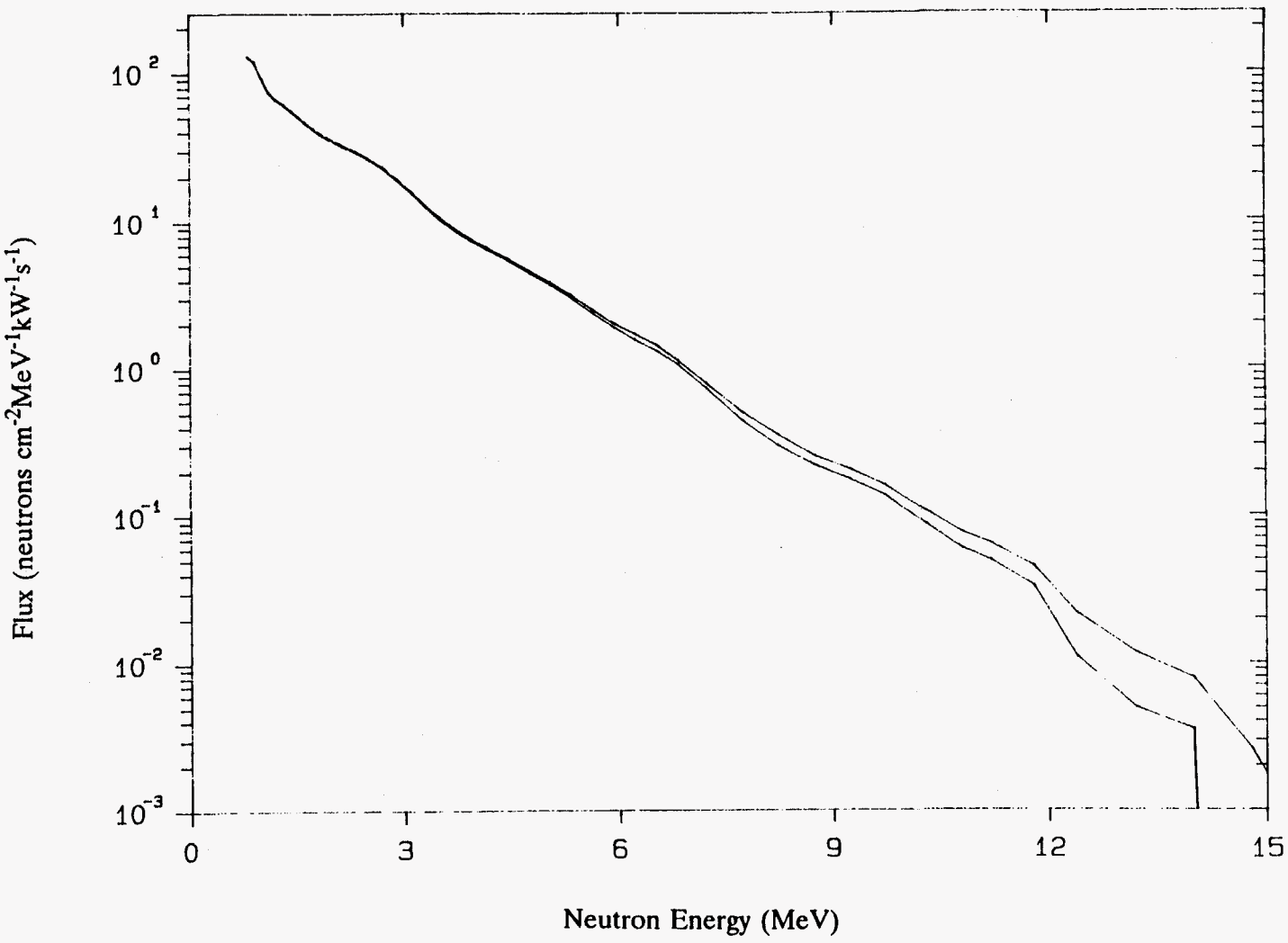

Figure 22. Spectrum of high-energy neutrons (>0.8 MeV) on centerline at 178 cm behind the mockup (Item IIC) Run 7914.

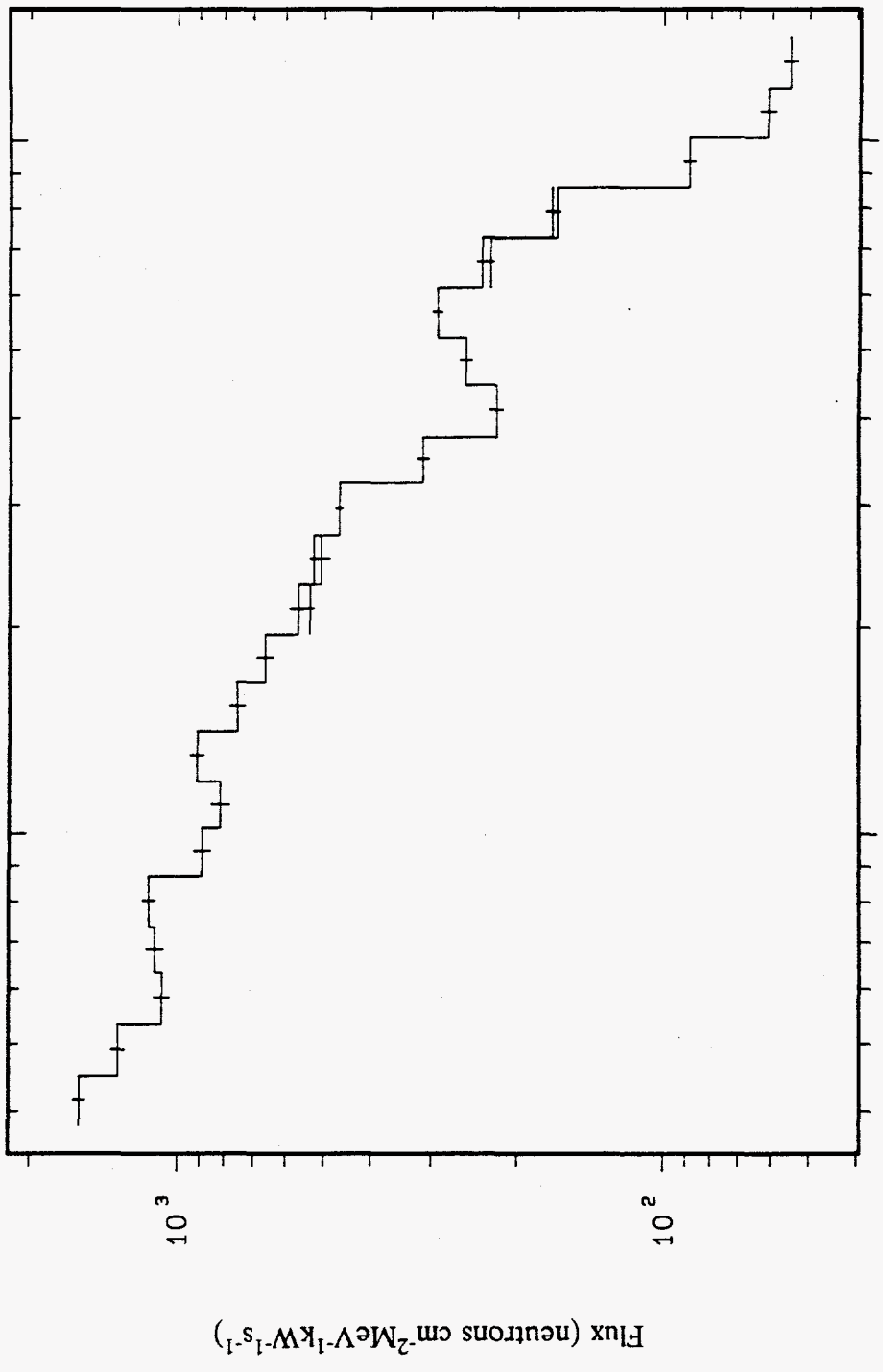

Figure 23. Neutron spectrum (50 keV to 1.4 MeV) on centerline at 178 cm behind the mockup (Item IIC) Runs 1579.D, 1579.A, 1578.A.

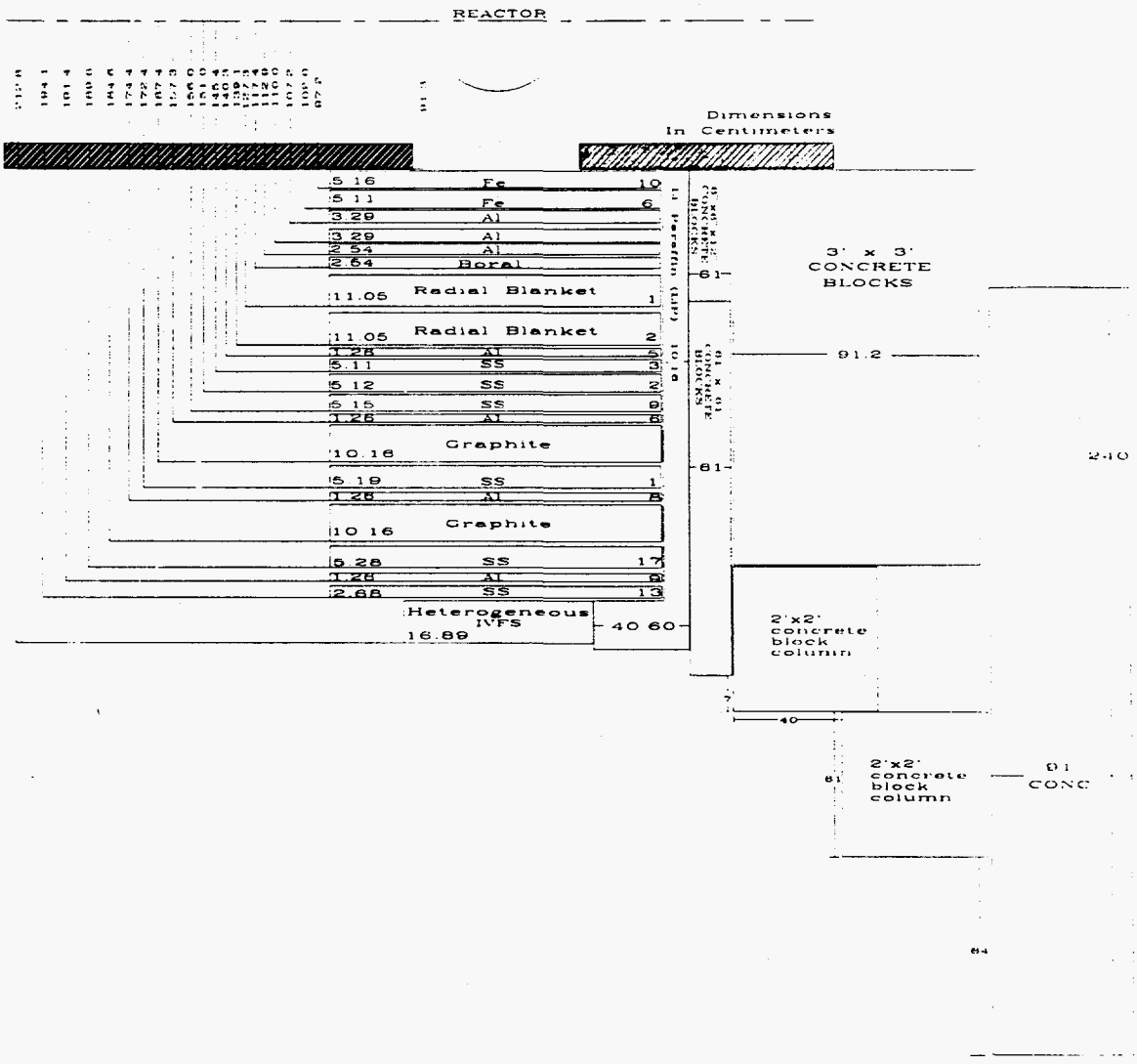

Figure 24. Schematic of SM-1 plus shield configuration for Item IID.

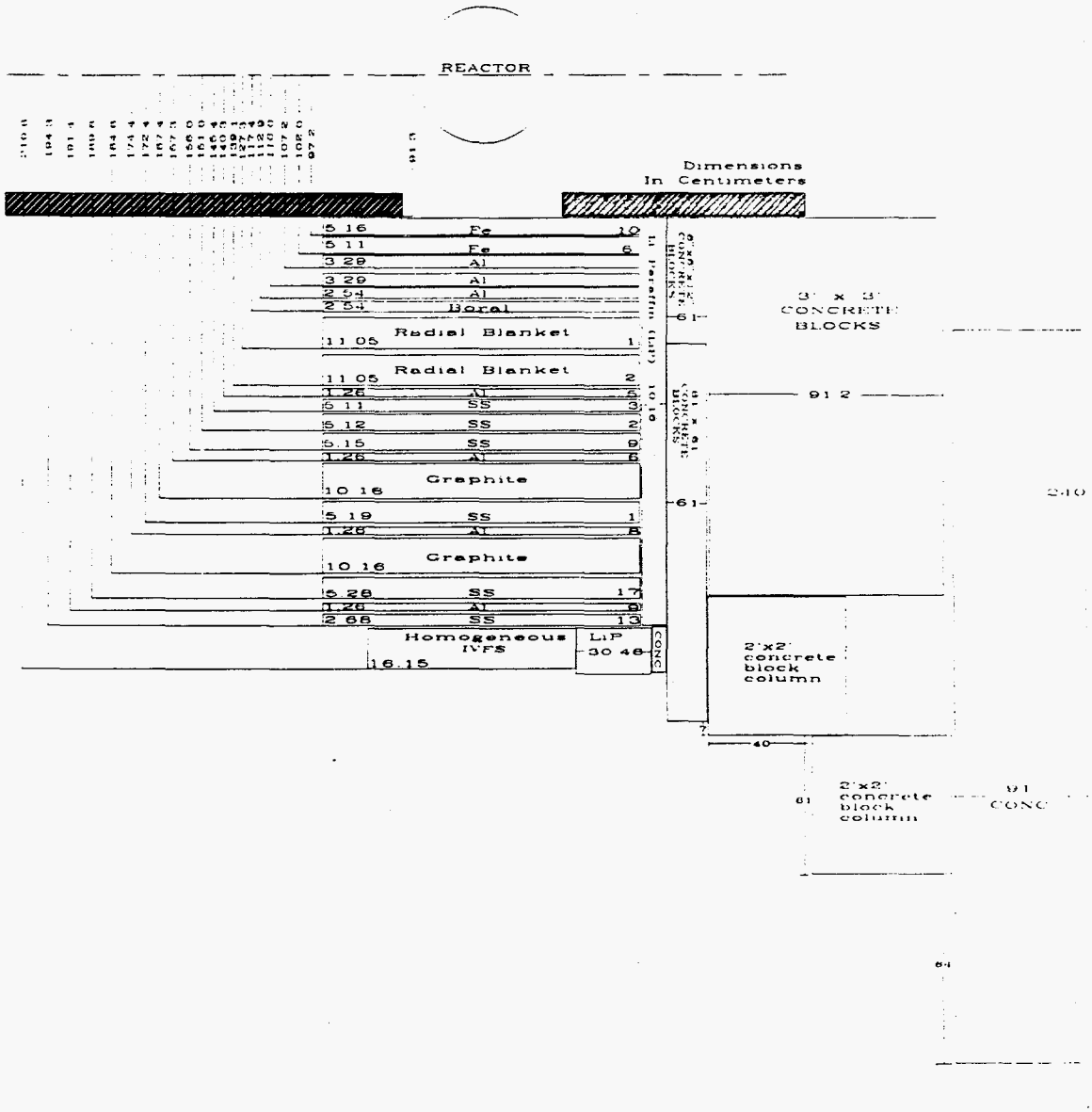

Figure 25. Schematic of SM-1 plus shield configuration for Item IIE.

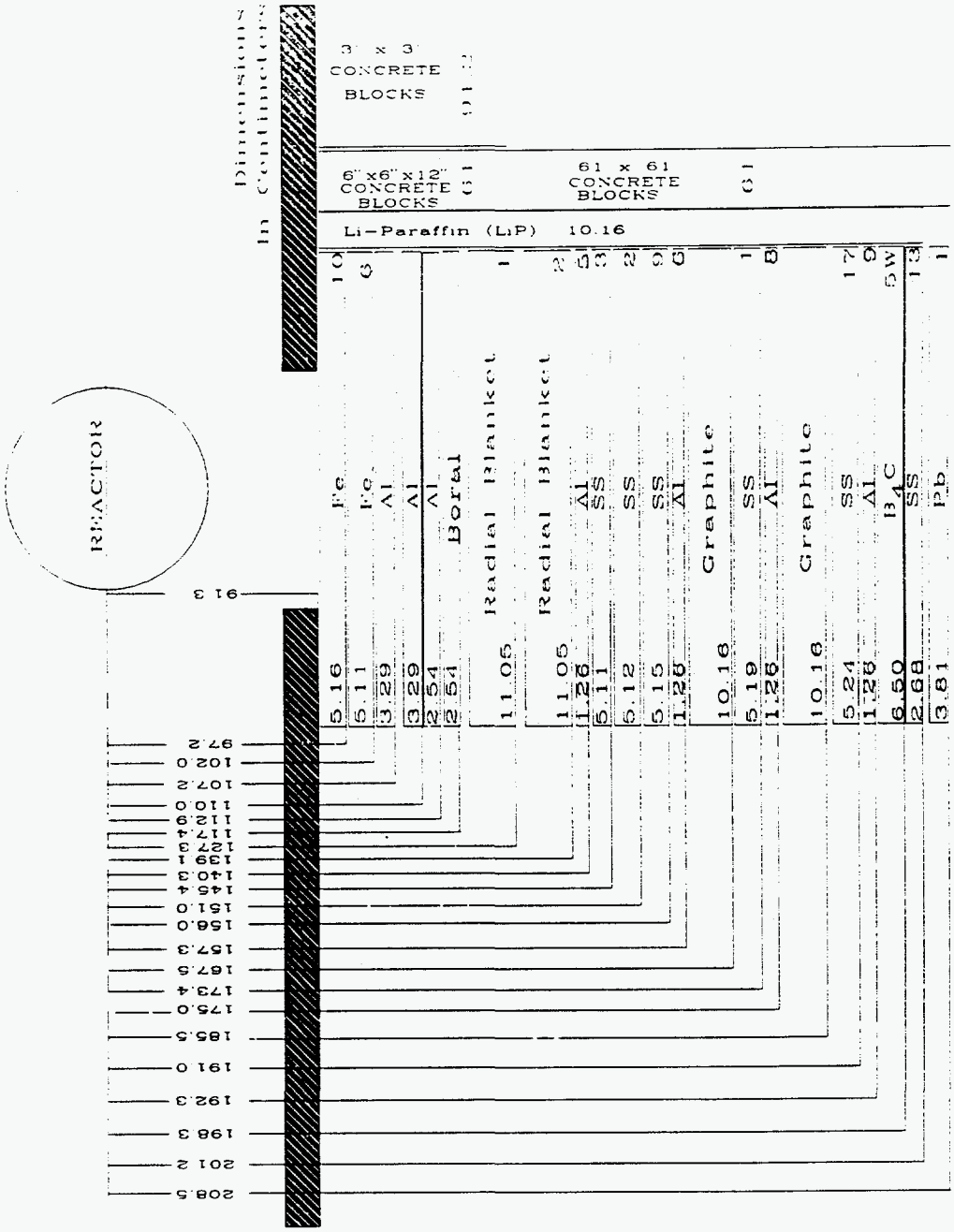

Figure 26. Schematic of SM-1 plus shield configuration for Item IIF plus lead.

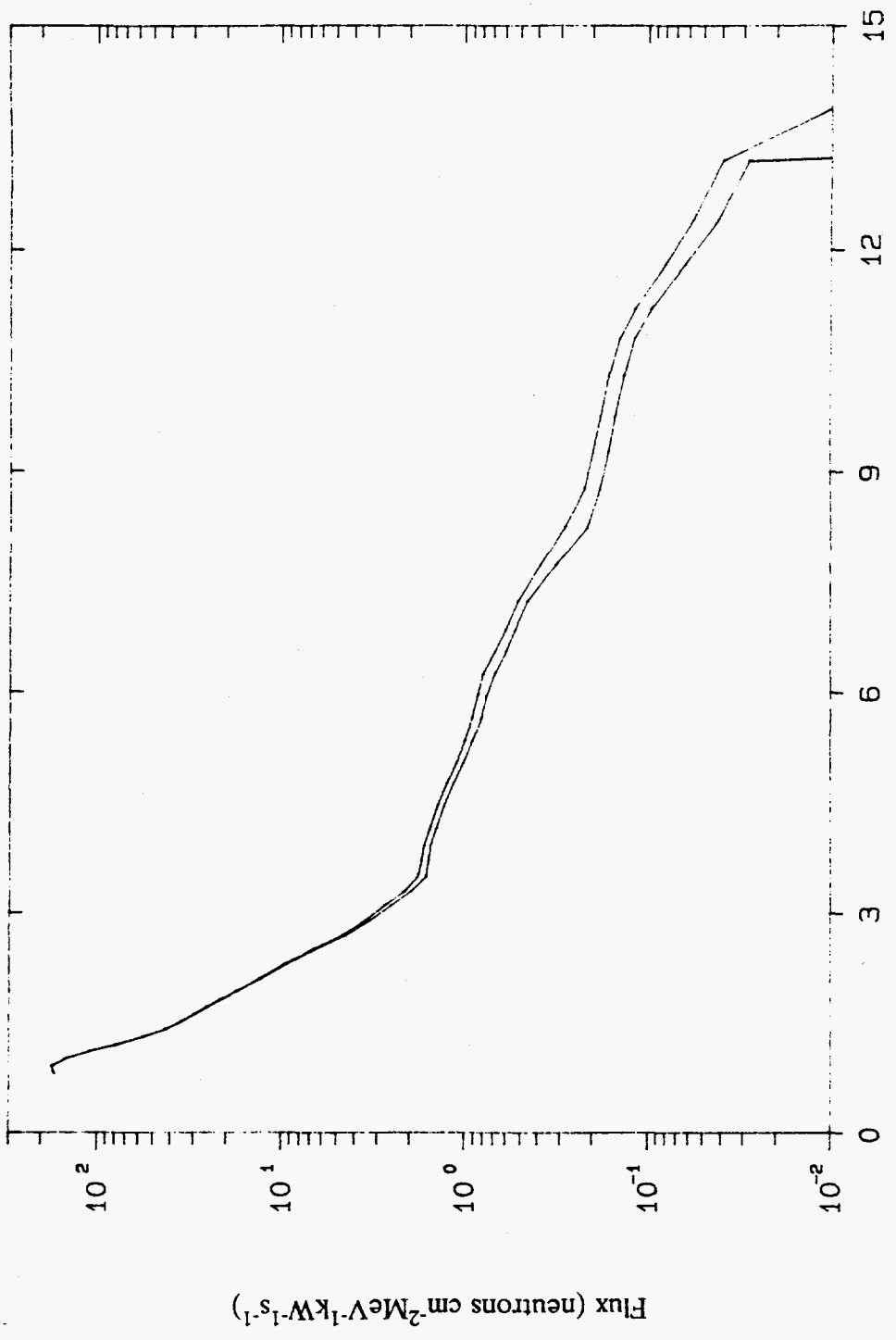

Figure 27. Spectrum of high-energy neutrons (>0.8 MeV) on centerline at 25 cm behind the lead slab (Item IIF) Run 7916.

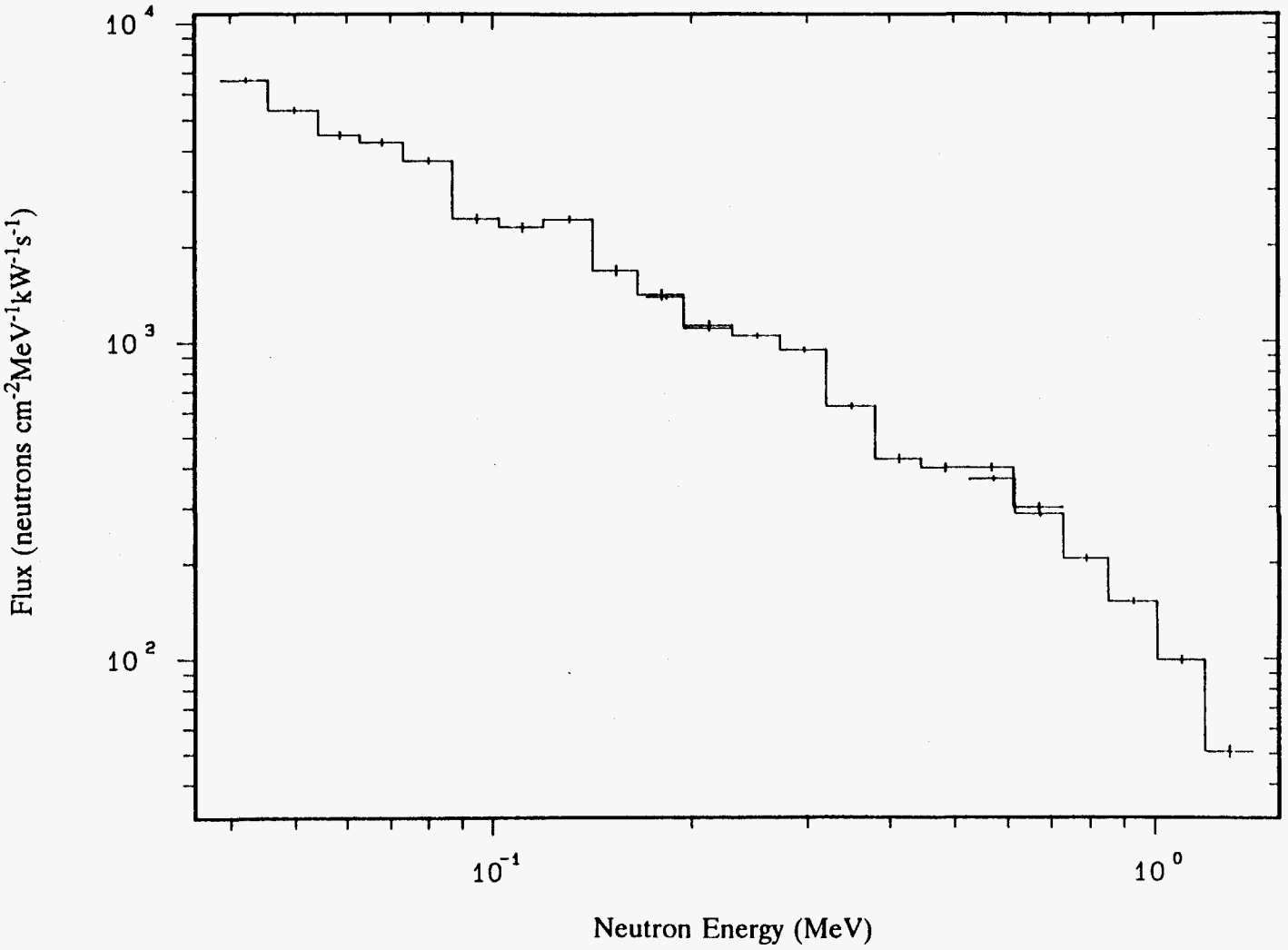

Figure 28. Neutron spectrum (50 keV to 1.4 MeV) on centerline at 25 cm behind the lead slab (Item IIF) Runs 1581.C, 1581.B, 1581.A.

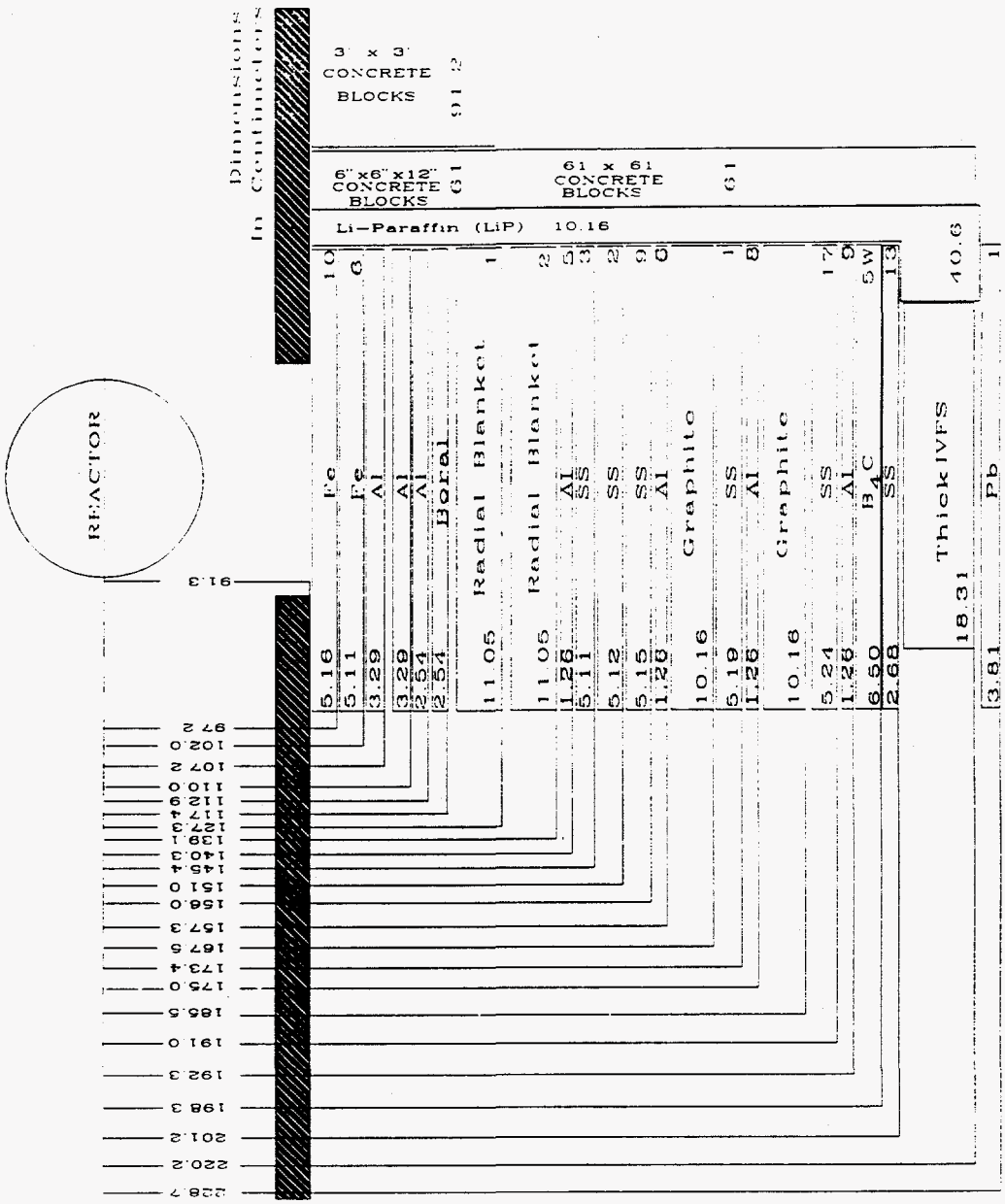

Figure 29. Schematic of SM-1 plus shield configuration for Item IIG plus lead.

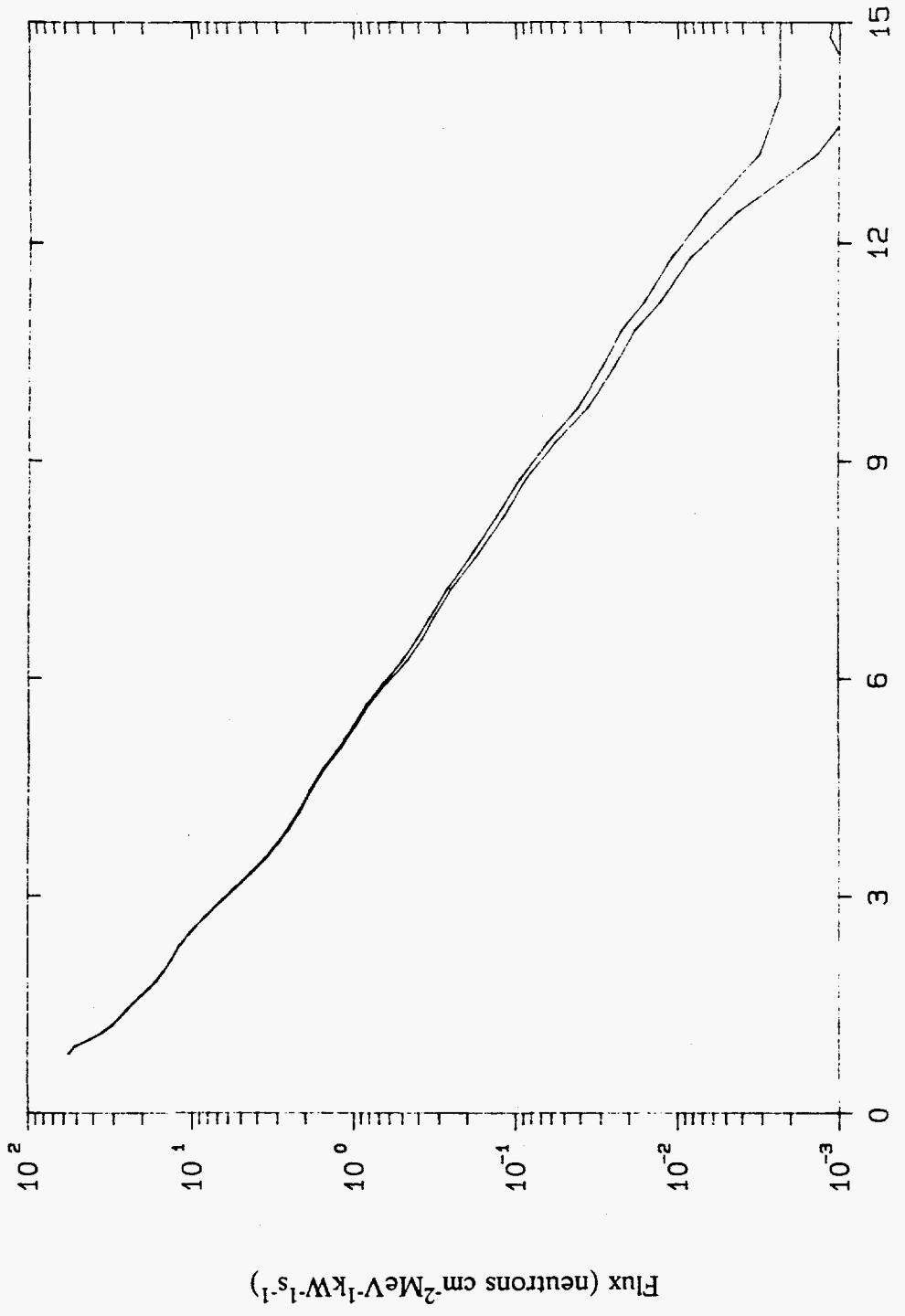

Figure 30. Spectrum of high-energy neutrons (>0.8 MeV) on centerline at 25 cm behind the lead slab (Item IIG) Run 7917.A.

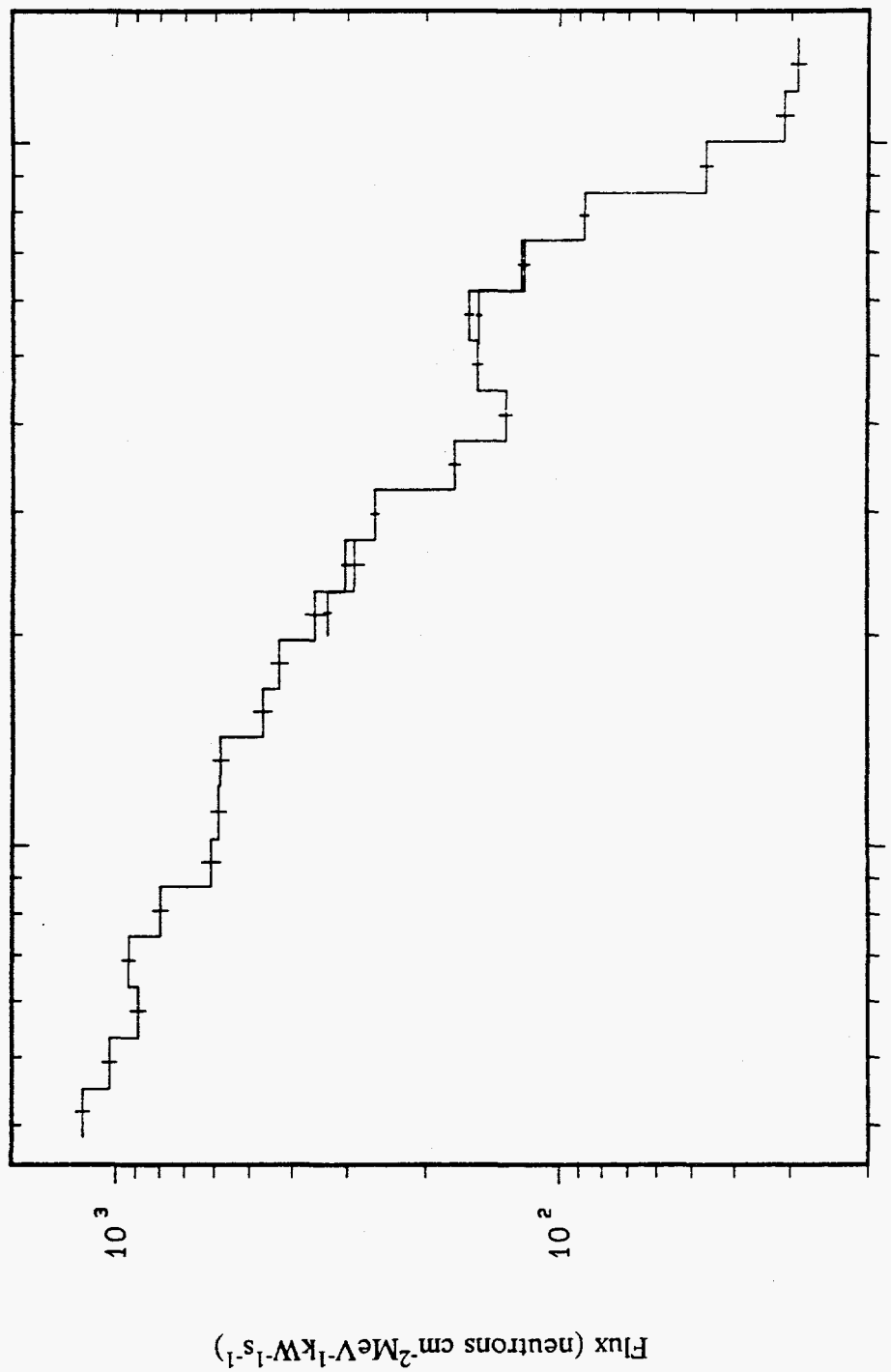

Figure 31. Neutron spectrum (50 keV to 1.4 MeV) on centerline at 25 cm behind the lead slab (Item IIG) Runs 1582.C, 1582.B, 1582.A.

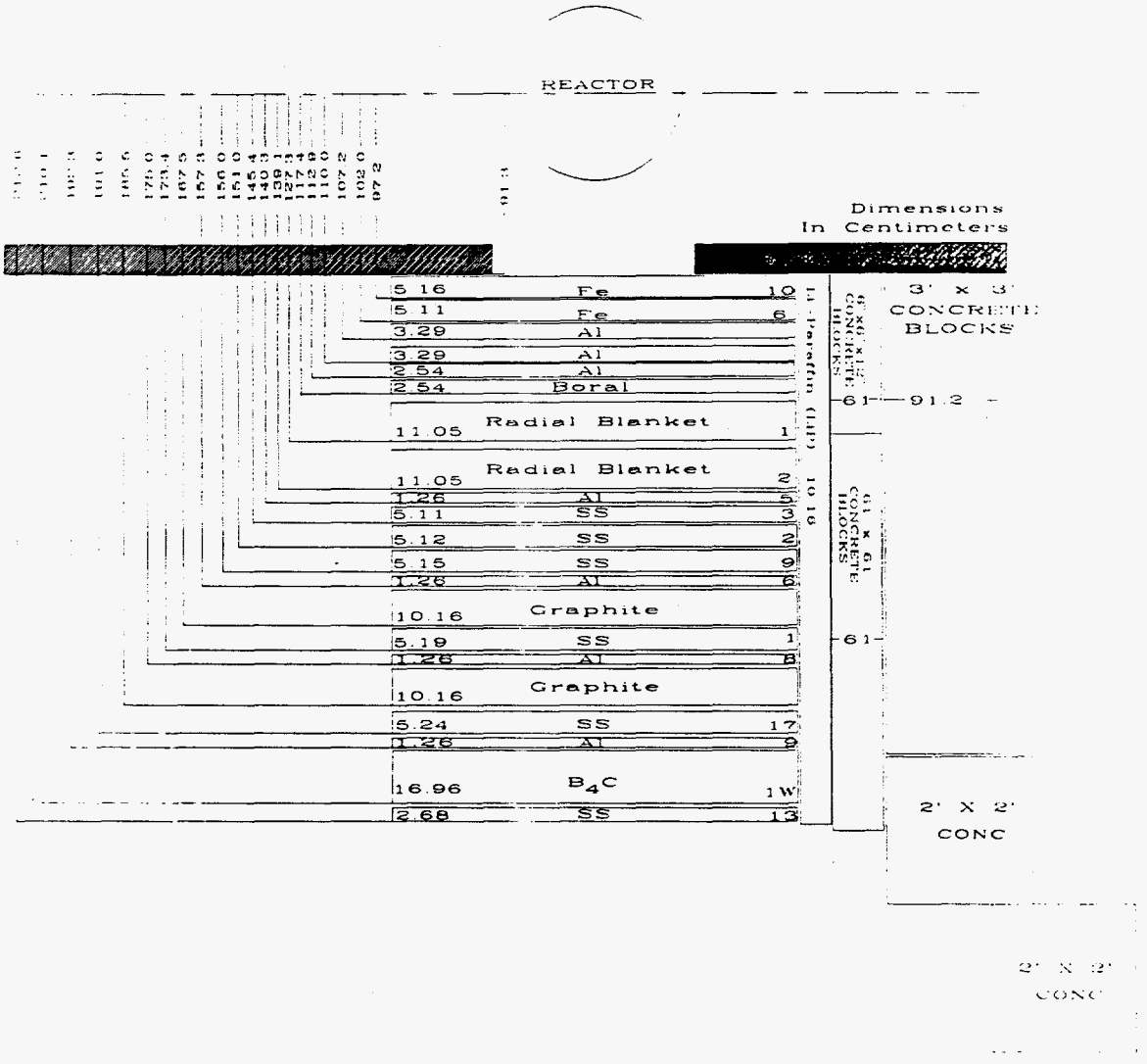

Figure 32. Schematic of SM-1 plus shield configuration for Item IIH.

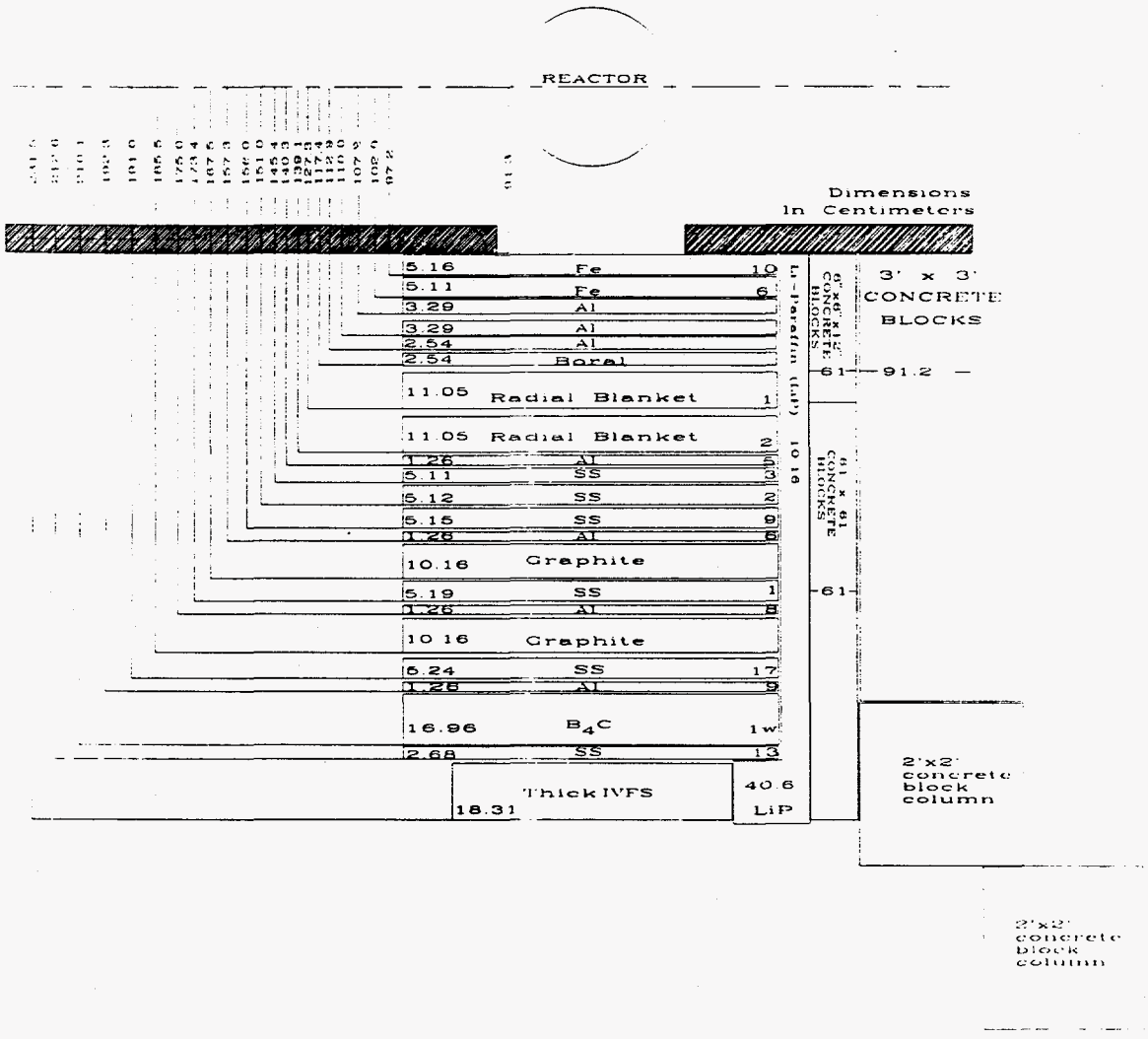

Figure 33. Schematic of SM-1 plus shield configuration for Item II I.

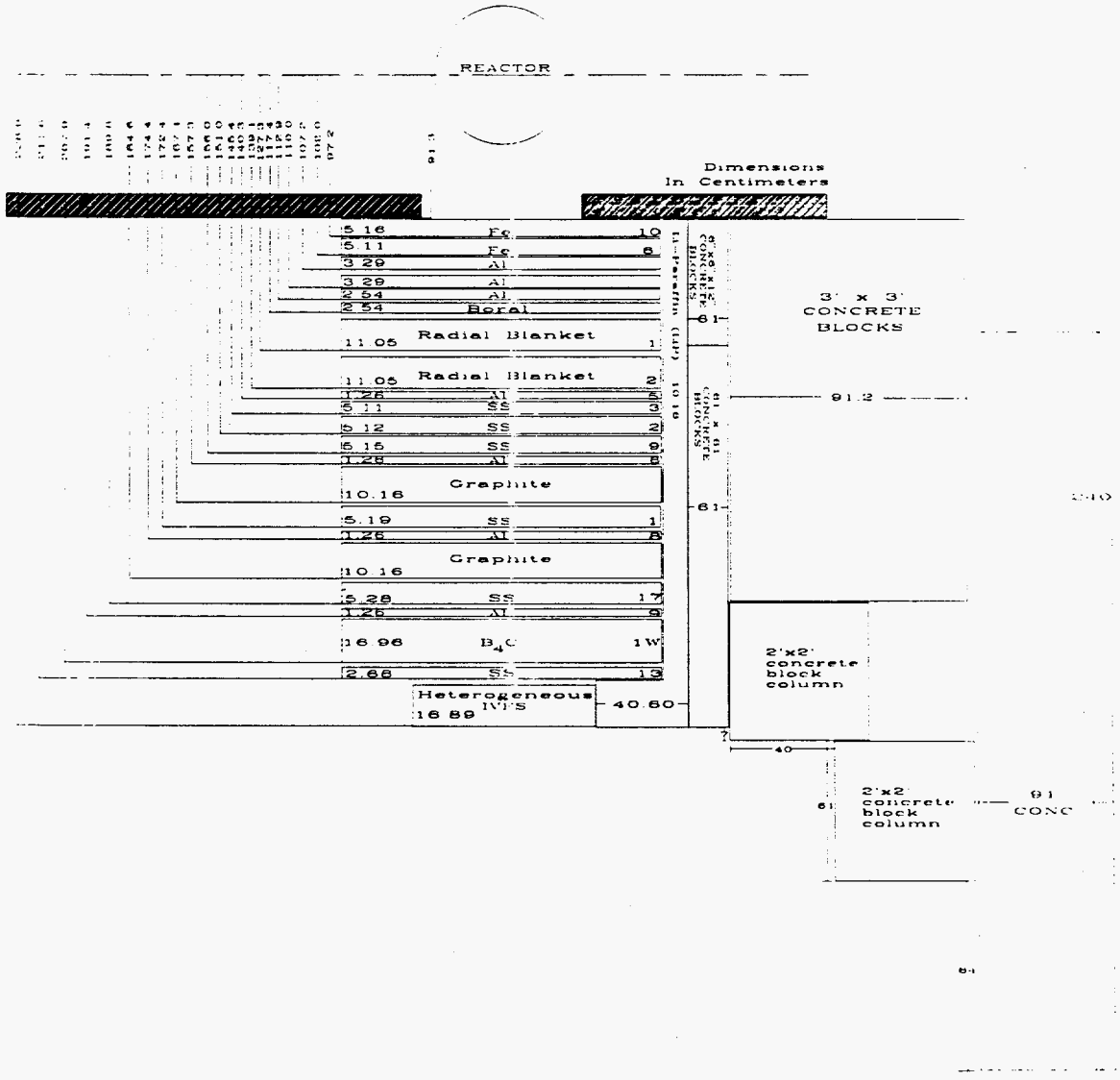

Figure 34. Schematic of SM-1 plus shield configuration for Item III.

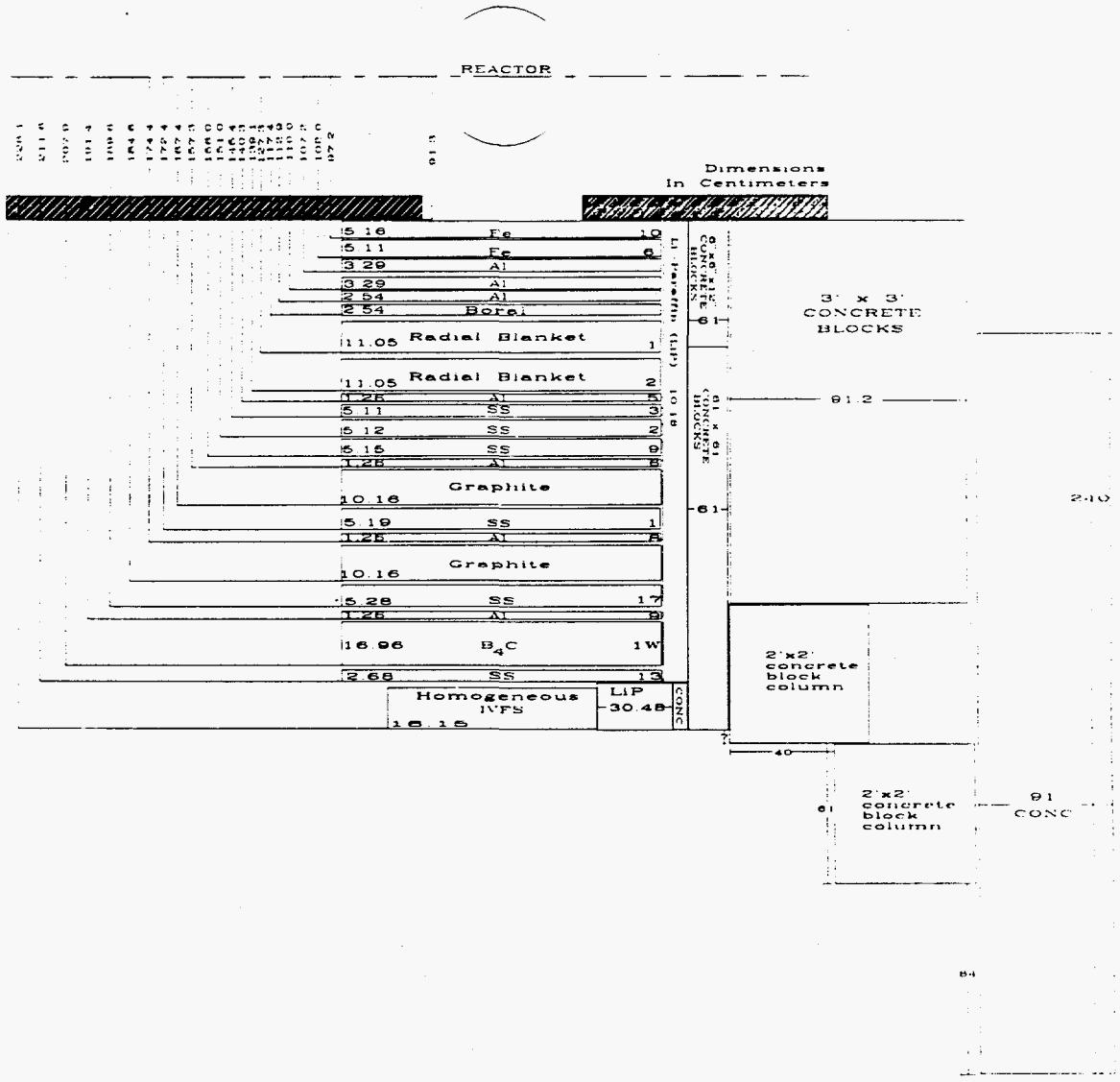

Figure 35. Schematic of SM-1 plus shield configuration for Item IIK.

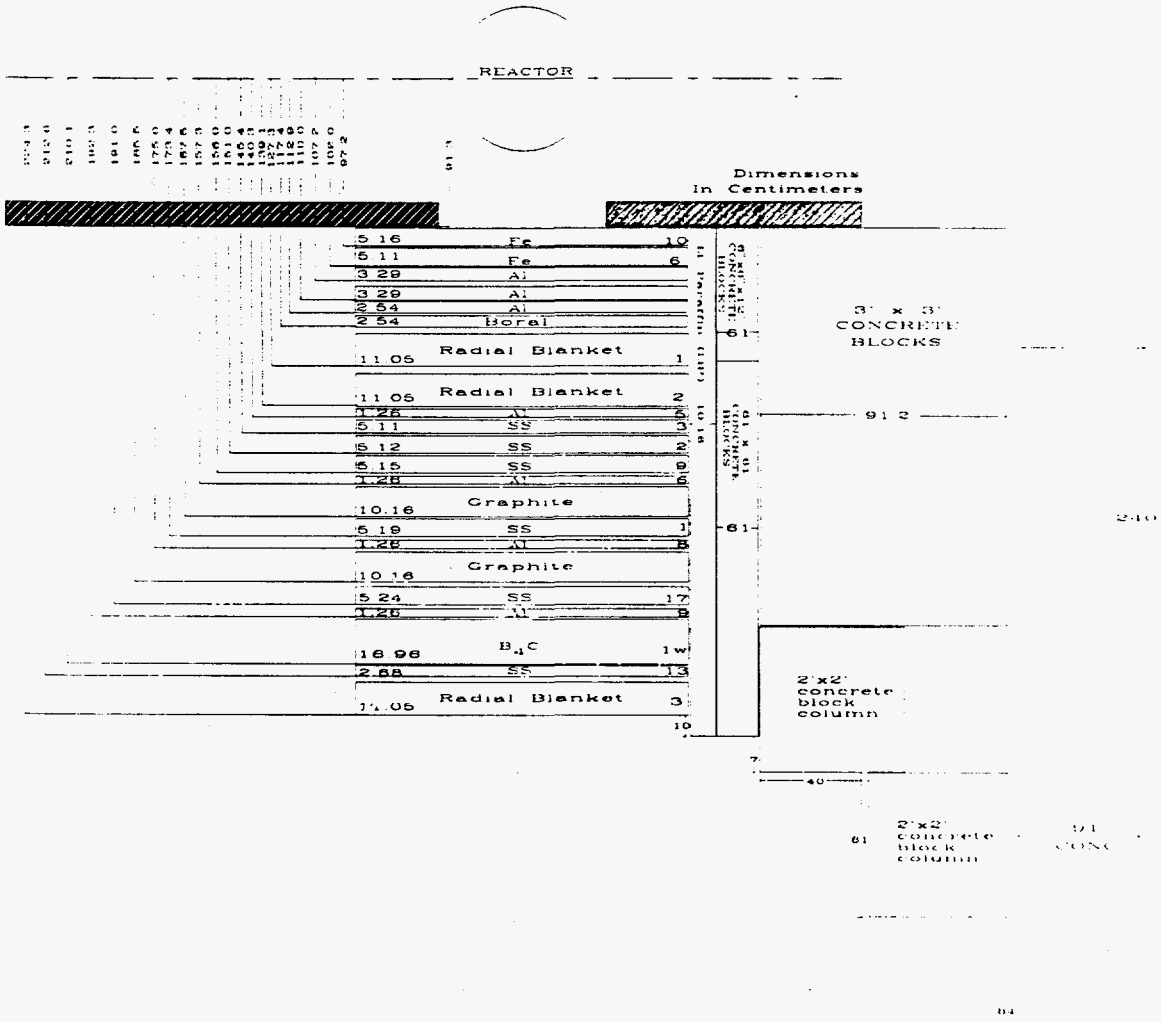

Figure 36. Schematic of SM-1 plus shield configuration for Item IIL.

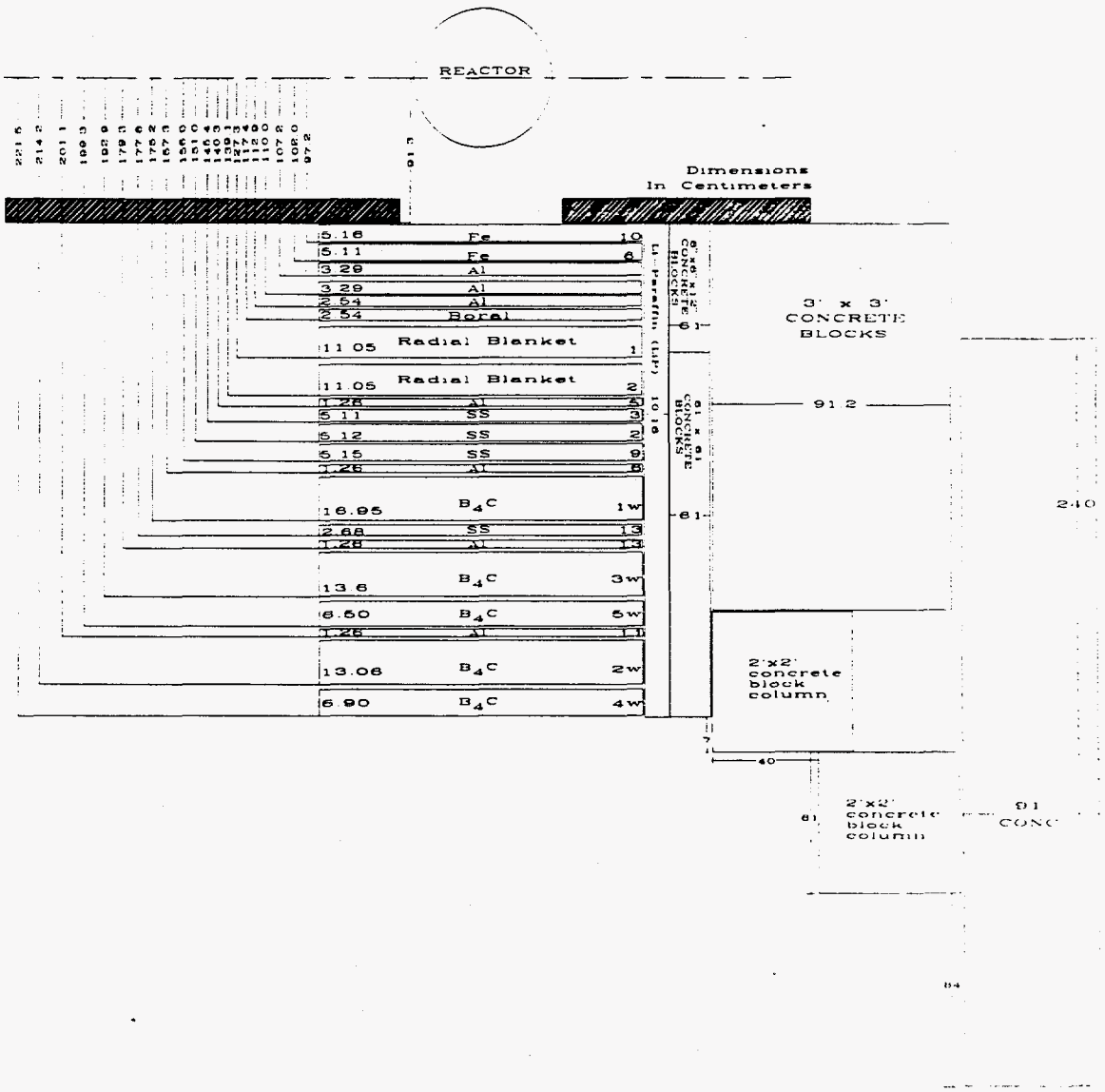

Figure 37. Schematic of SM-1 plus shield configuration for Item IIM.

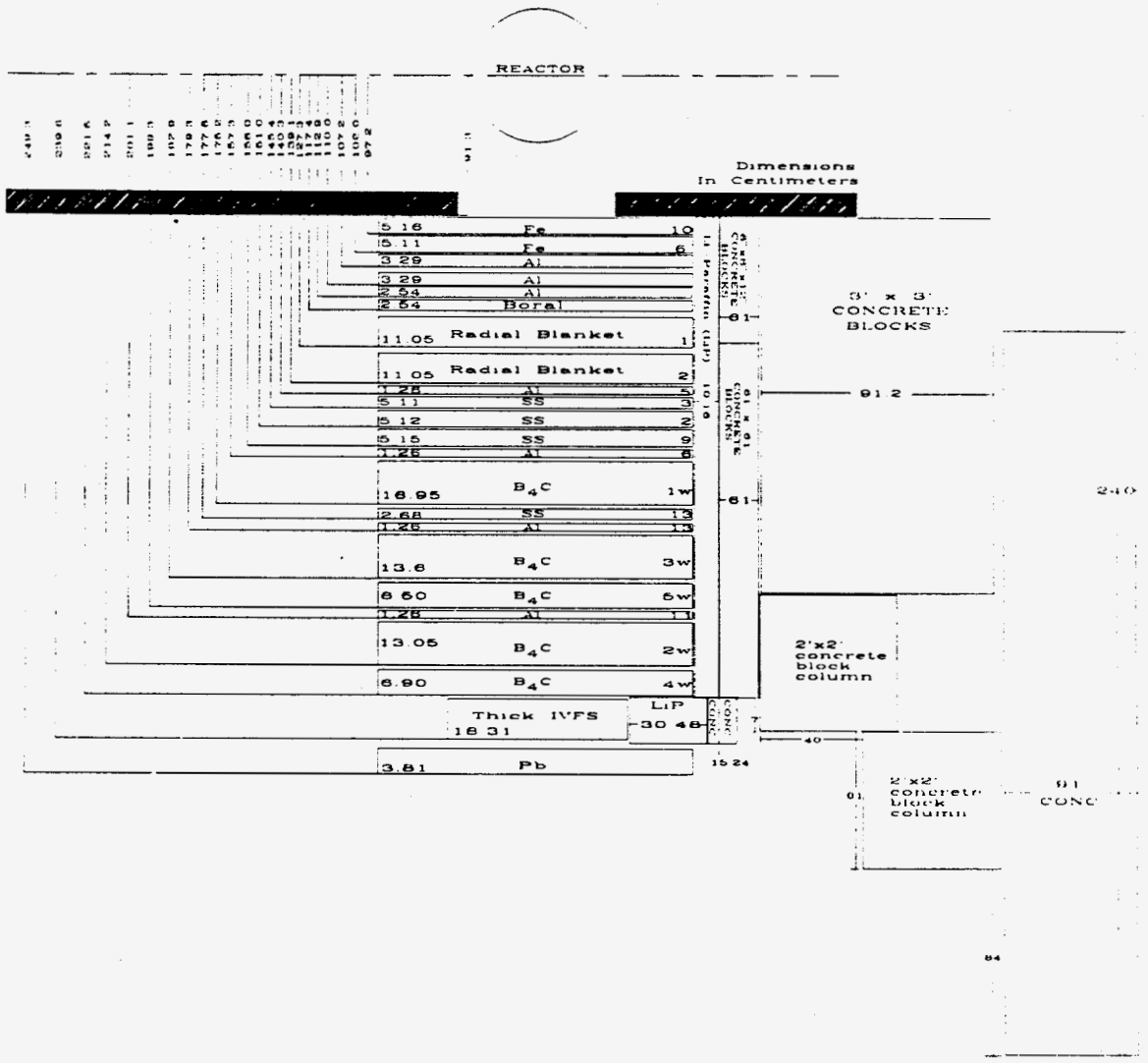

Figure 38. Schematic of SM-1 plus shield configuration for Item IIN plus lead.

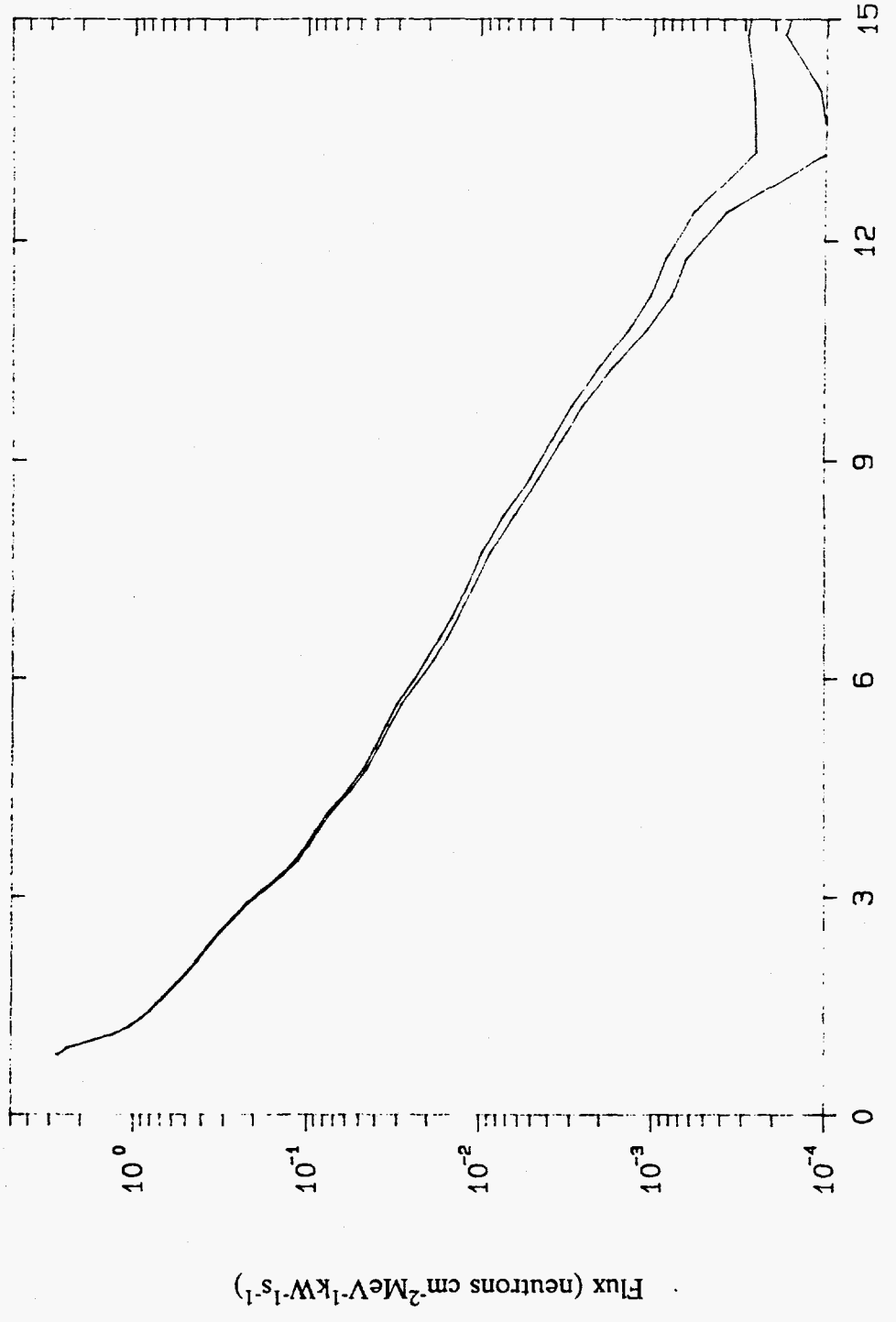

Figure 39. Spectrum of high-energy neutrons (>0.8 MeV) on centerline at 25 cm behind the lead slab (Item IIN) Run 7919.

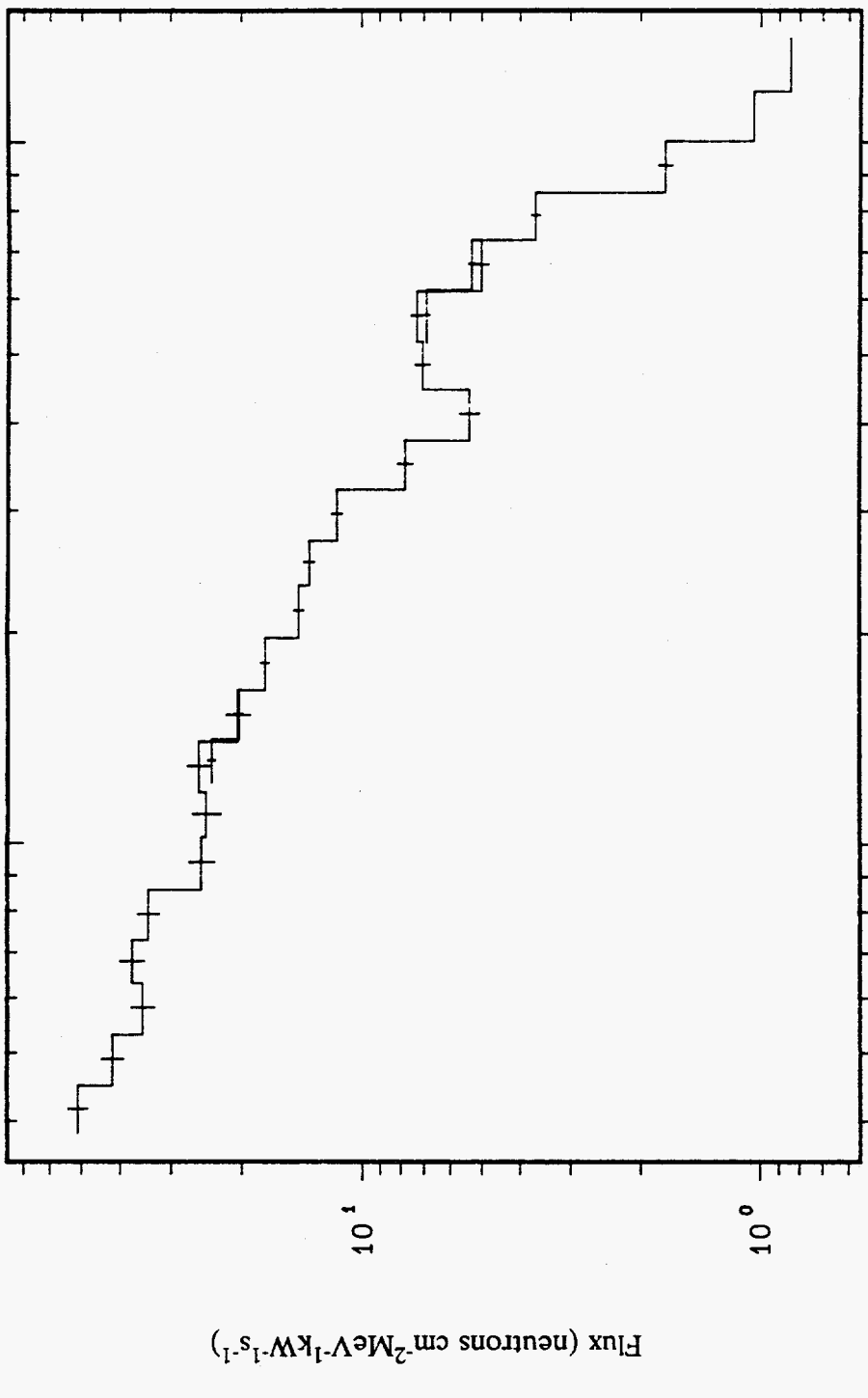

Figure 40. Neutron spectrum (50 keV to 1.4 MeV) on centerline at 25 cm behind the lead slab (Item IIN) Runs 1585.A, 1584.A, 1583.B.

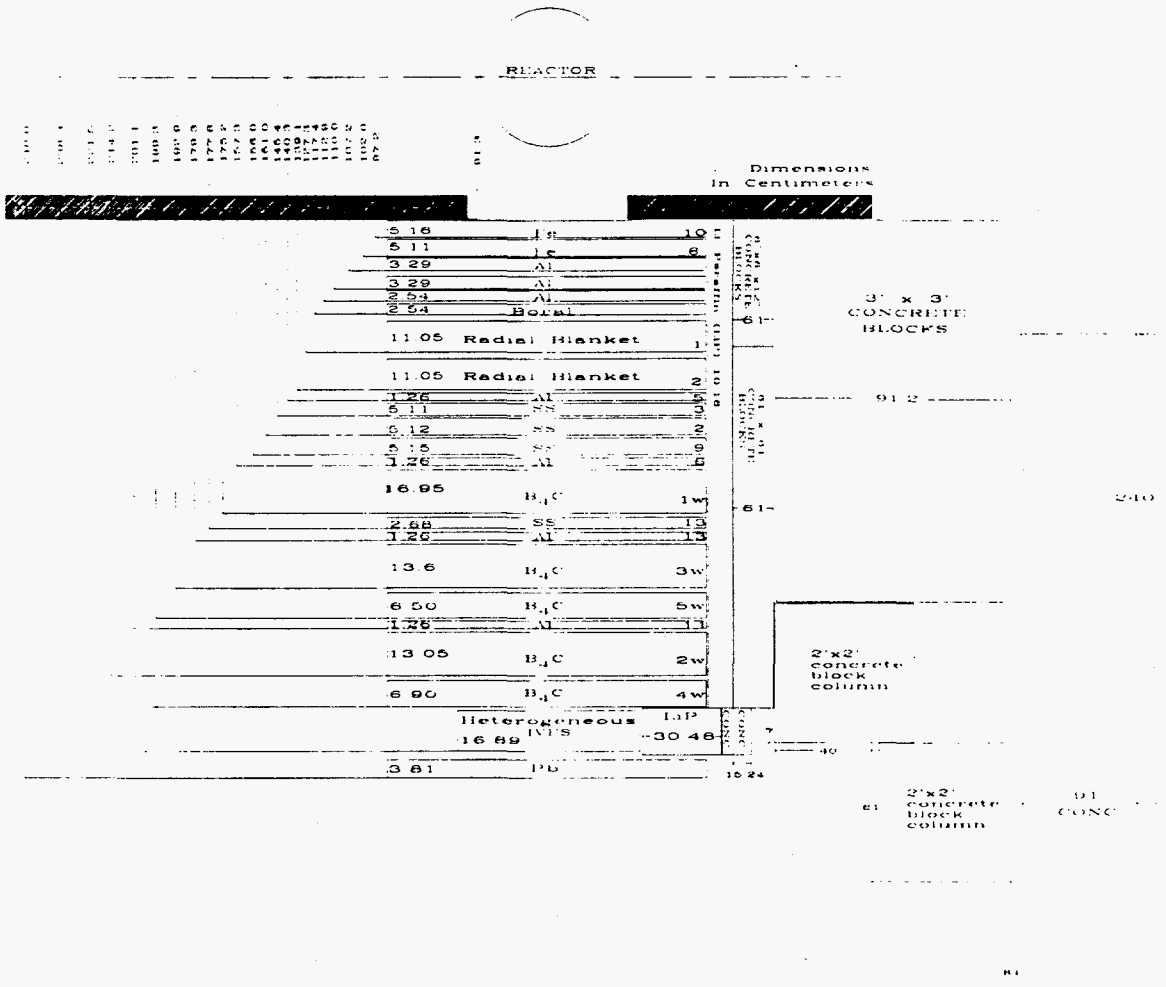

Figure 41. Schematic of SM-1 plus shield configuration for Item IIO plus lead.

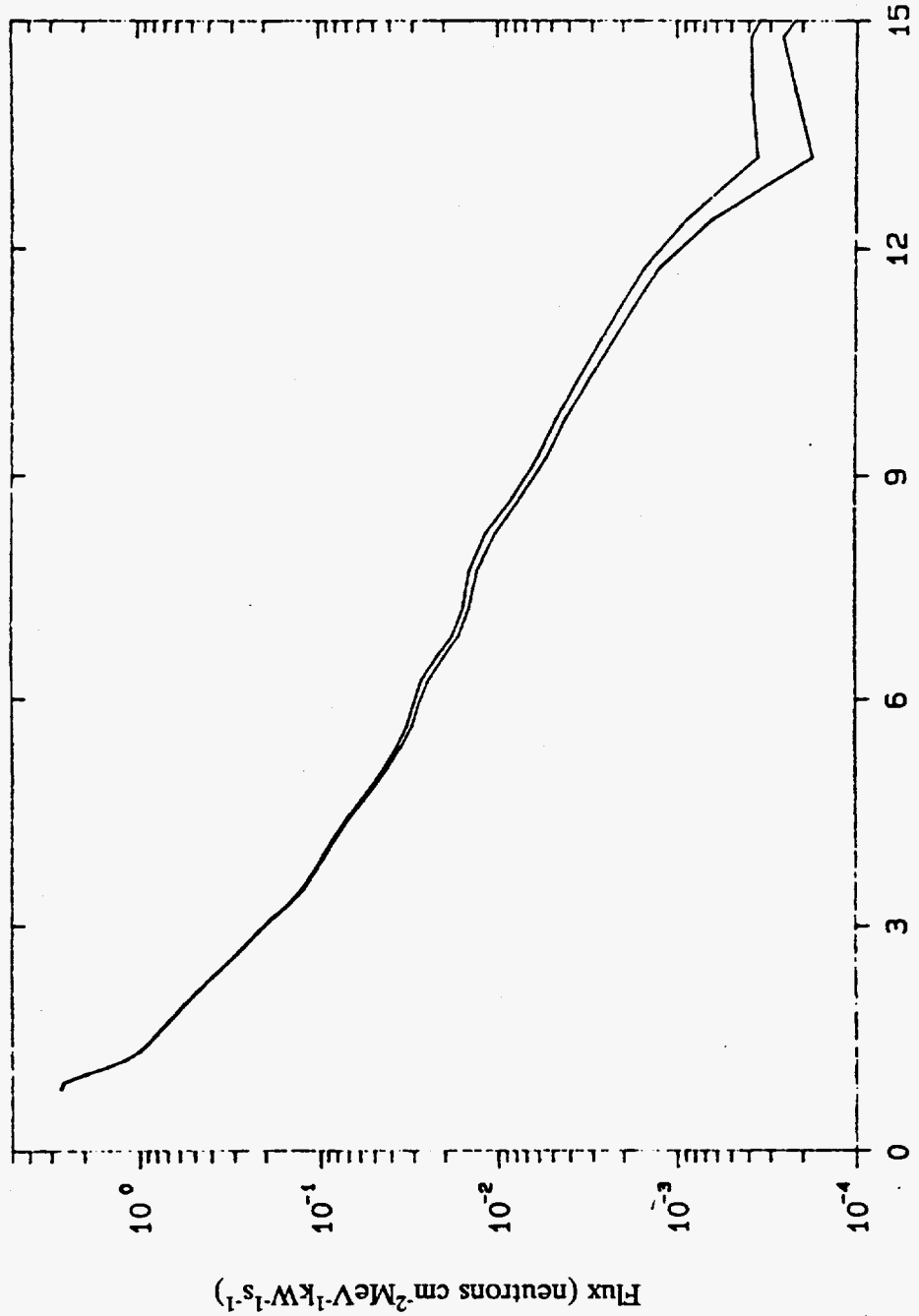

Figure 42. Spectrum of high-energy neutrons (>0.8 MeV) on centerline at 25 cm behind the lead slab (Item IIO) Run 7920.

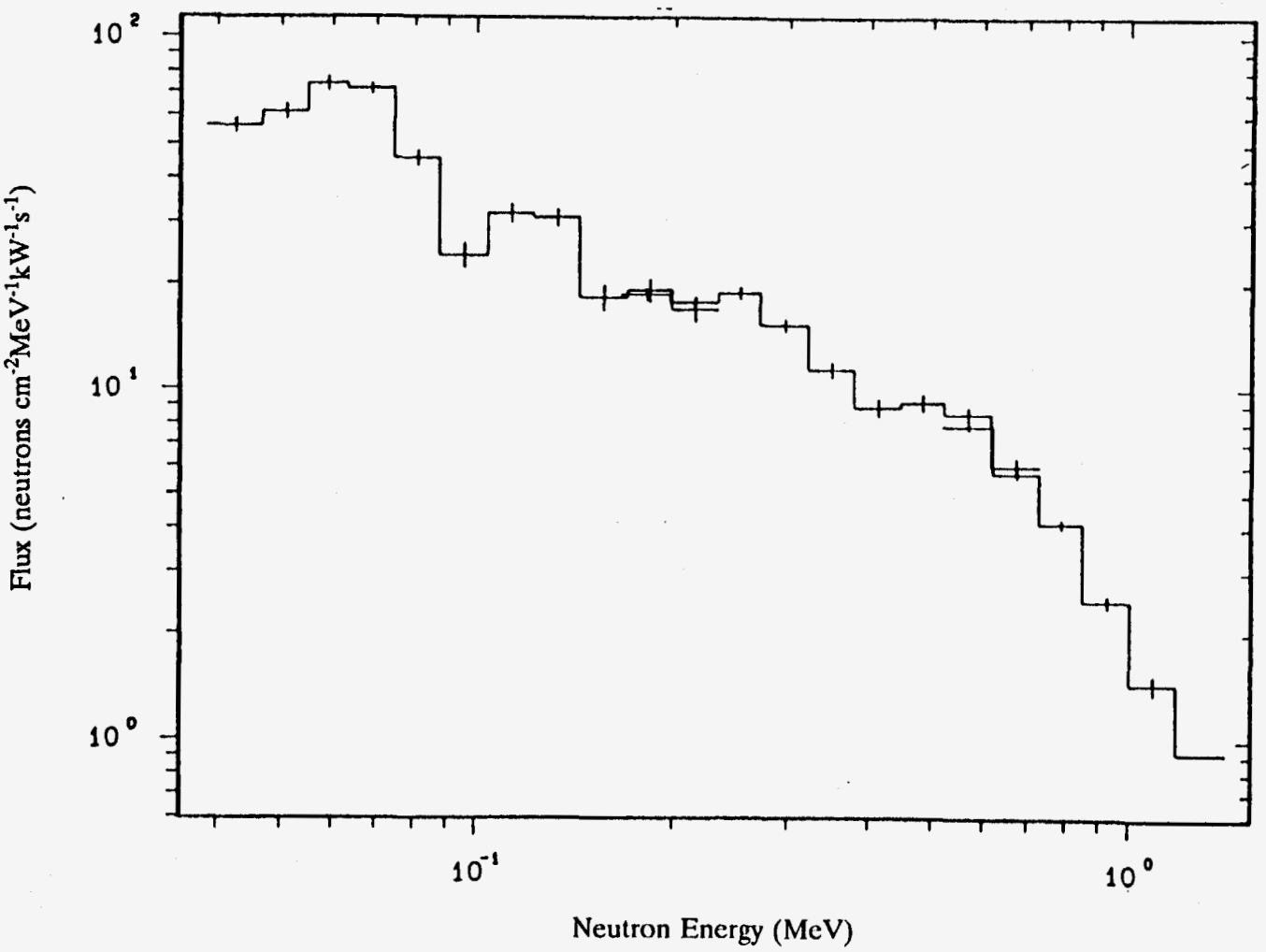

Figure 43. Neutron spectrum (50 keV to 1.4 MeV) on centerline at 25 cm behind the lead slab (Item IIO) Runs 1588.A, 1587.A, 1586.A.

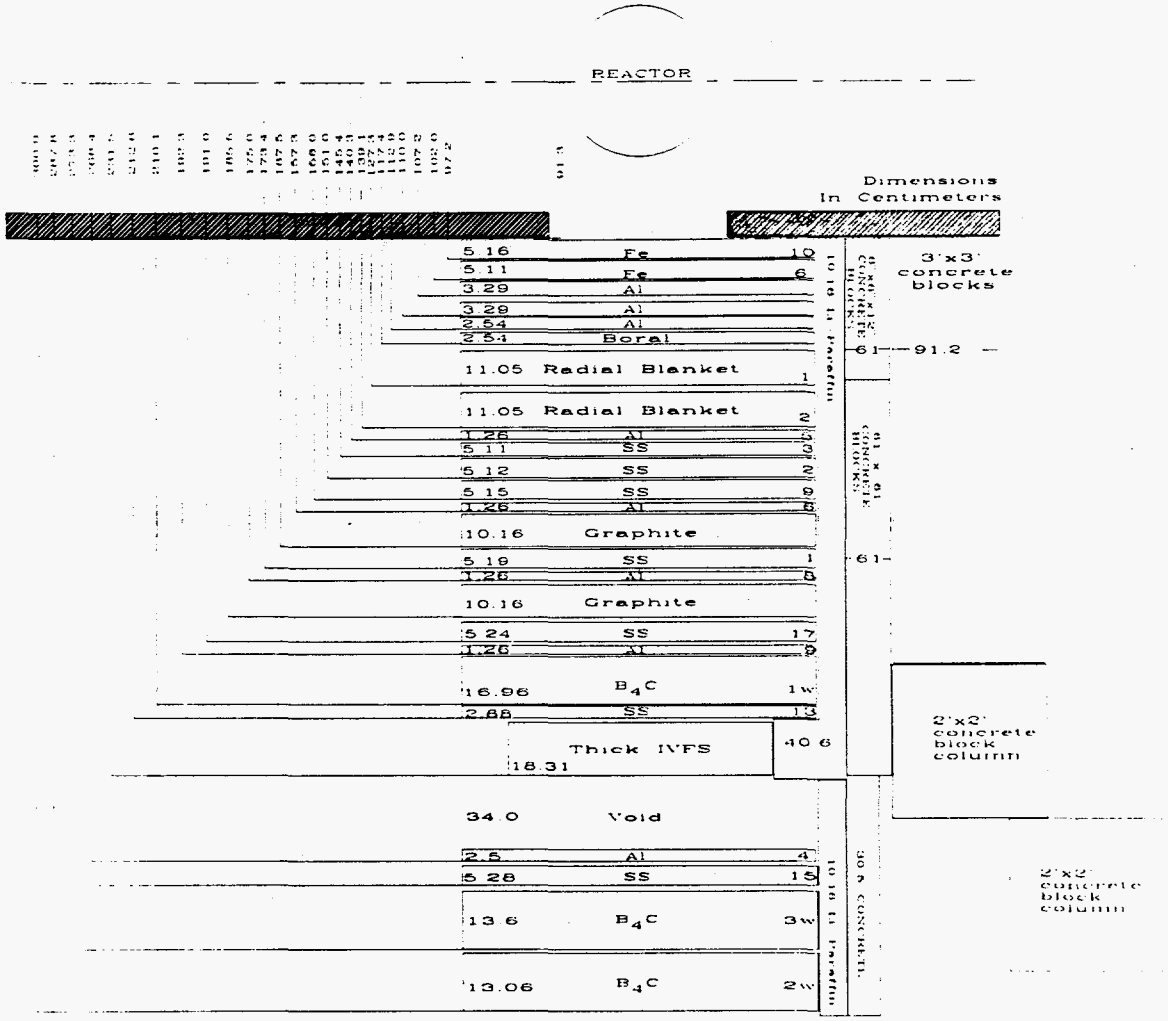

Figure 44A. Schematic of SM-1 plus shield mockup for Item IIP (Note: This mockup was used for measurements with the fission chamber in the void and at 0.7 and 30 cm behind mockup).

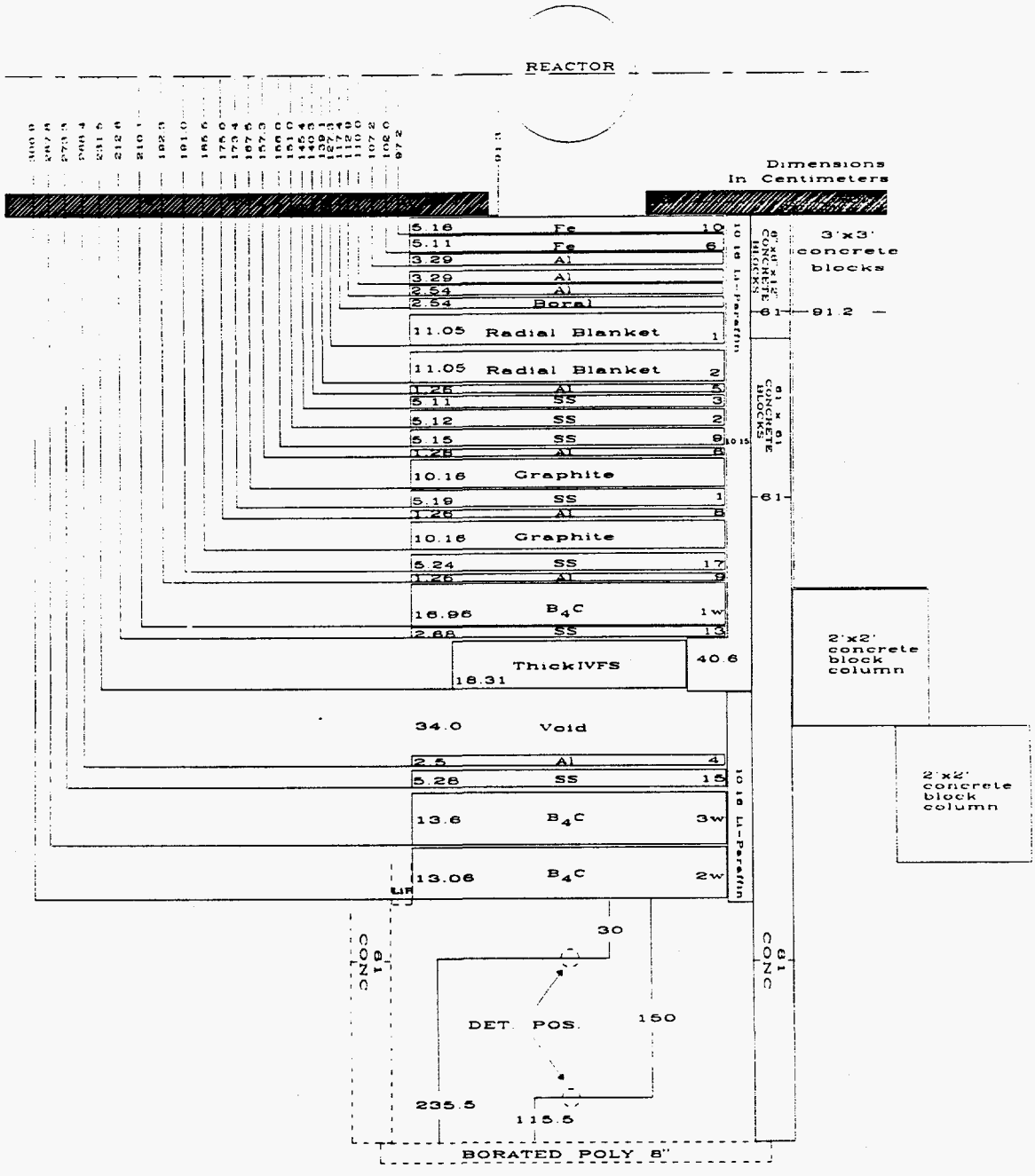

Figure 44B. Schematic of SM-1 plus shield configuration for Item IIP (Note: This mockup was used for measurements behind B_4C slab 2W only).

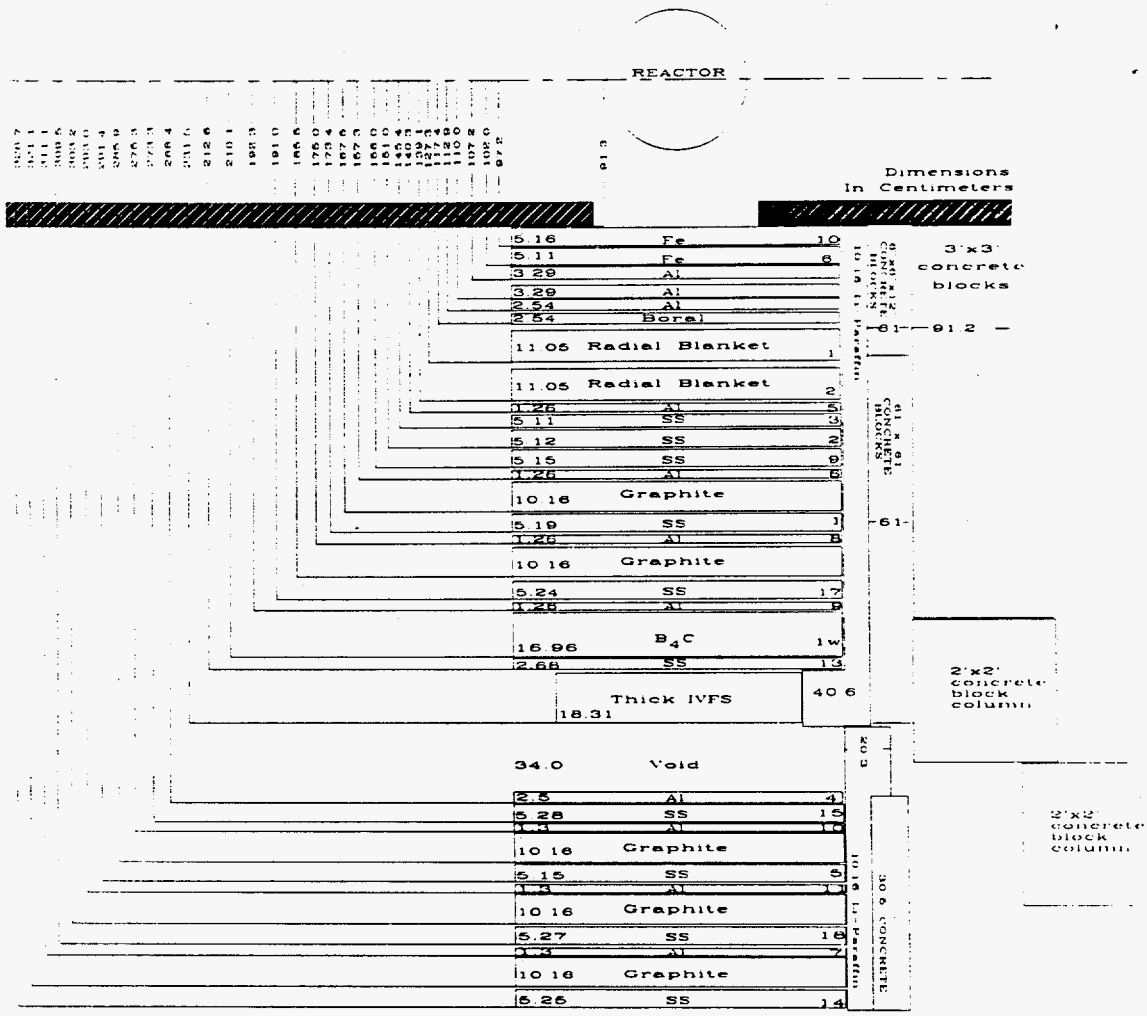

Figure 45A. Schematic of SM-1 plus shield configuration for Item IIQ (Note: Measurements in the void only).

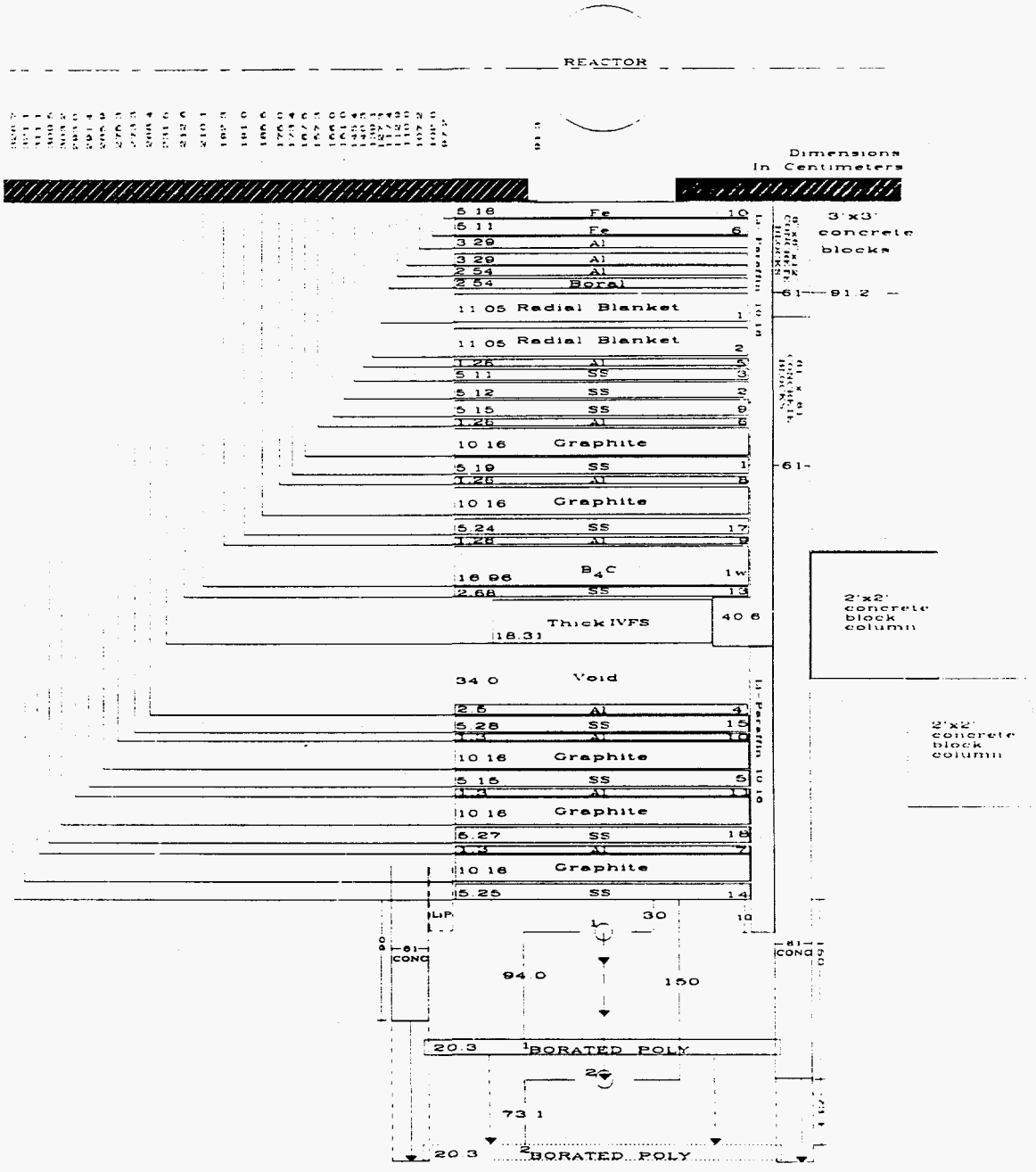

Figure 45B. Schematic of SM-1 plus shield configuration for Item IIQ (Note: Measurements behind mockup only).

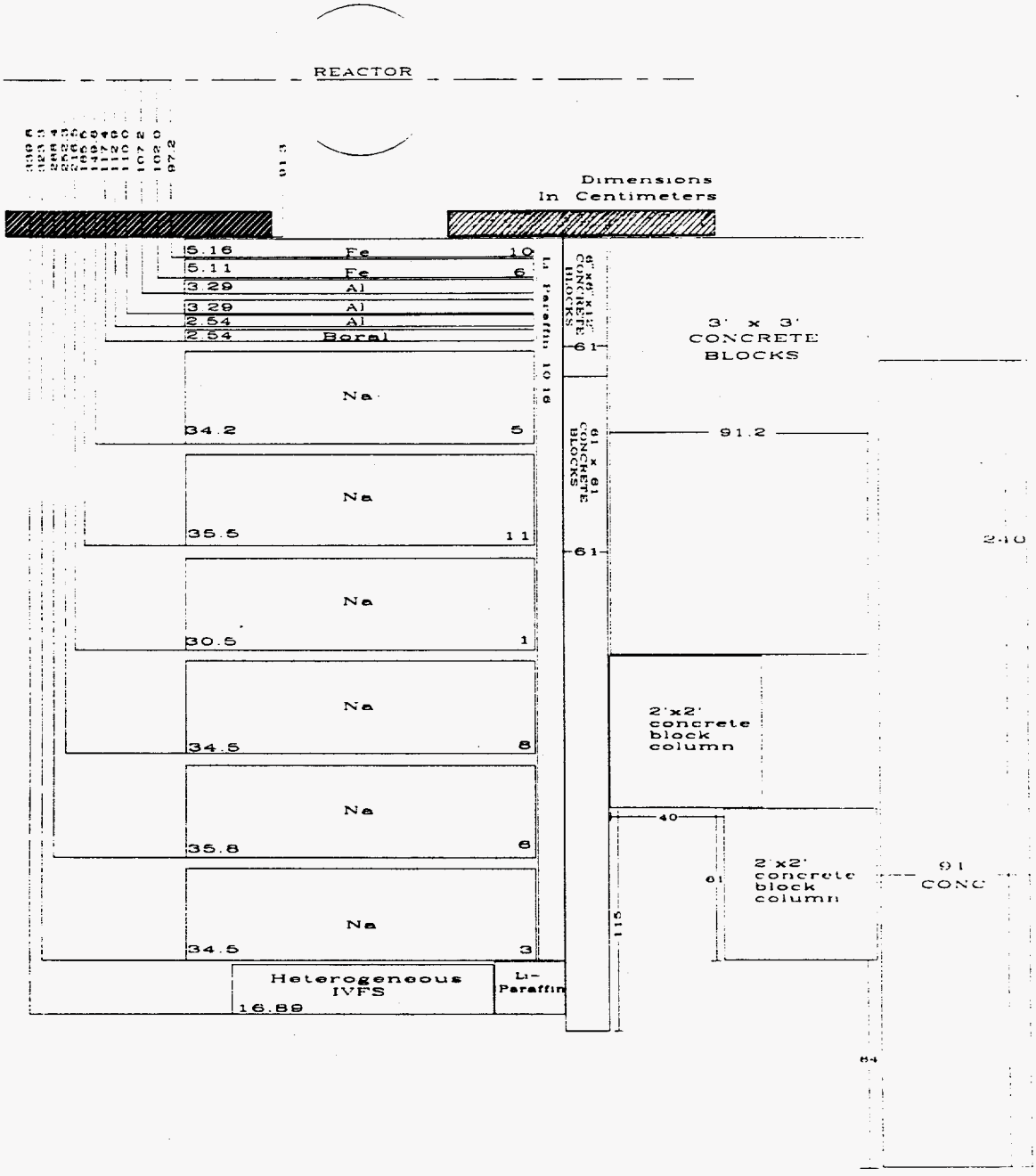

Figure 46. Schematic of SM-2 plus shield configuration for Item IIIA.

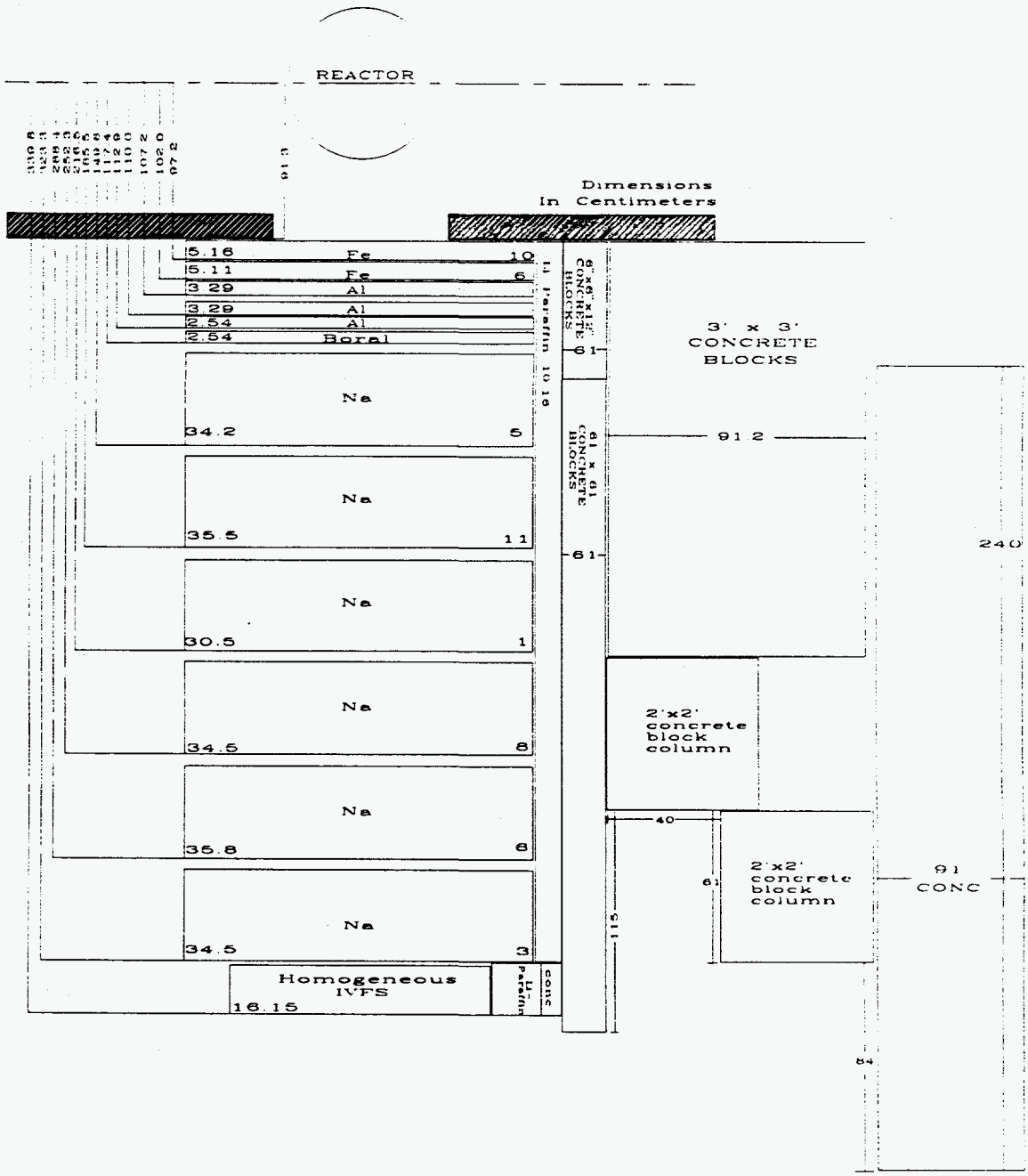

Figure 47. Schematic of SM-2 plus shield configuration for Item IIIB.

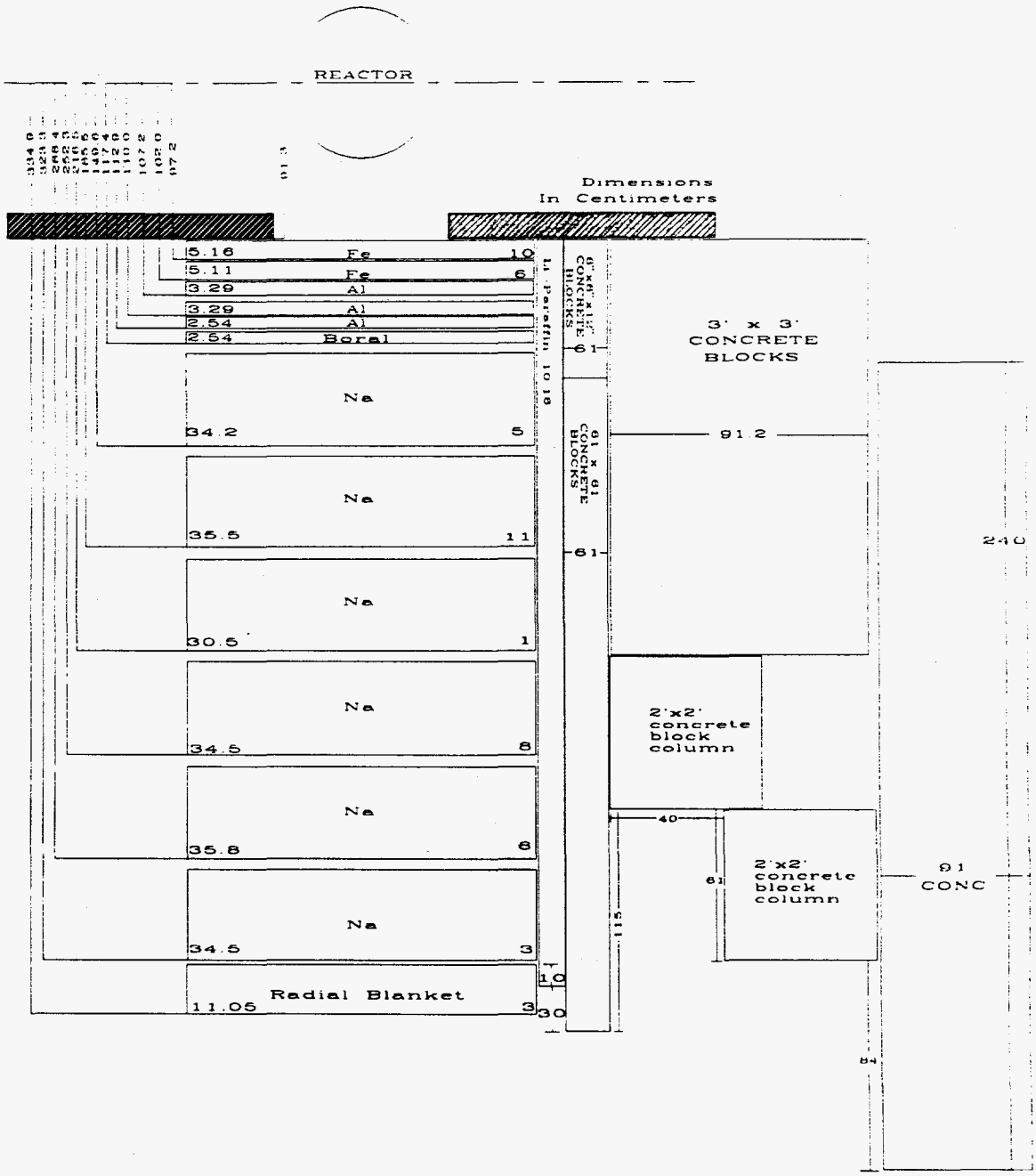

Figure 48. Schematic of SM-2 plus shield configuration for Item IIIC.

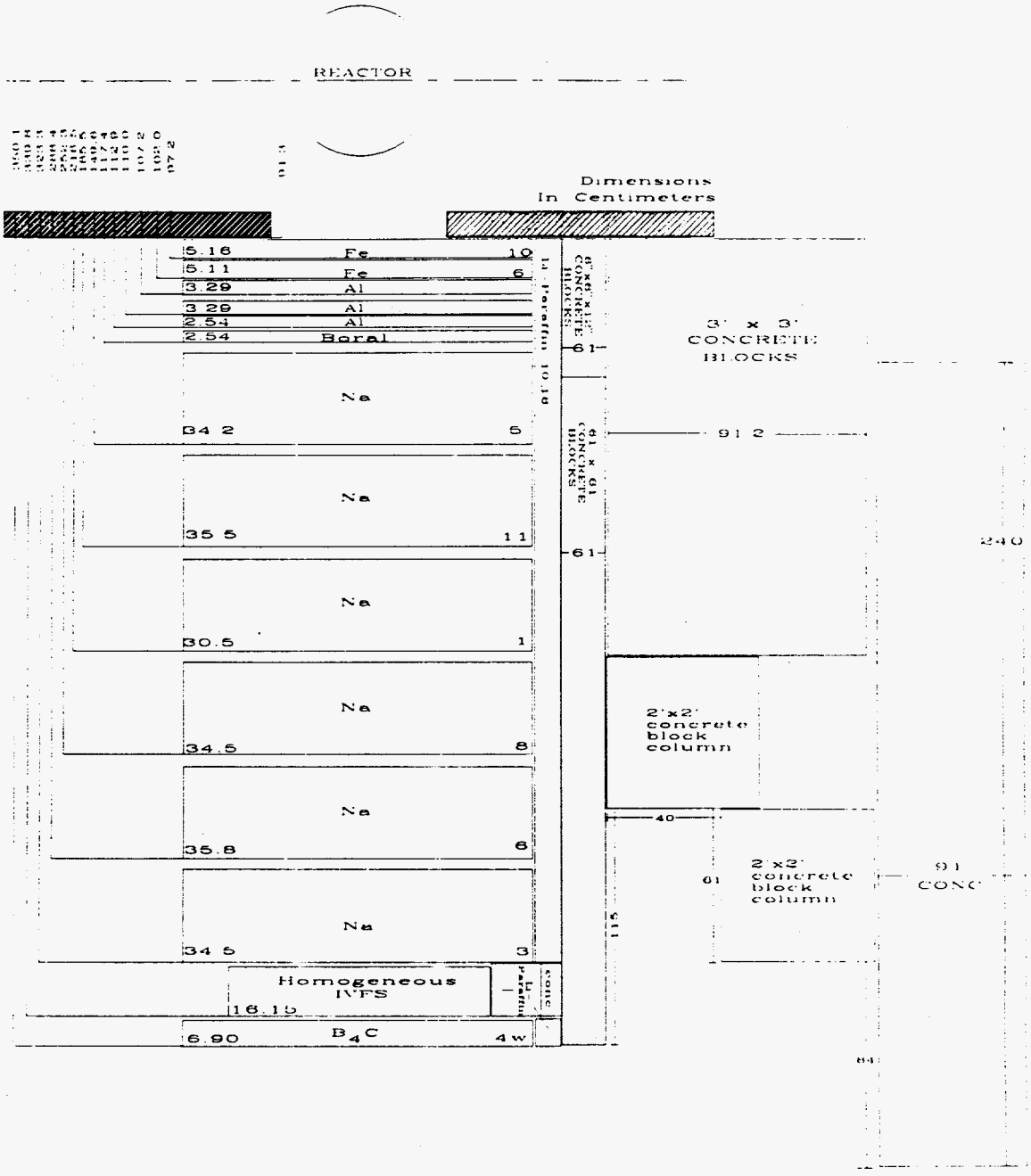

Figure 49. Schematic of SM-2 plus shield configuration for Item IIID.

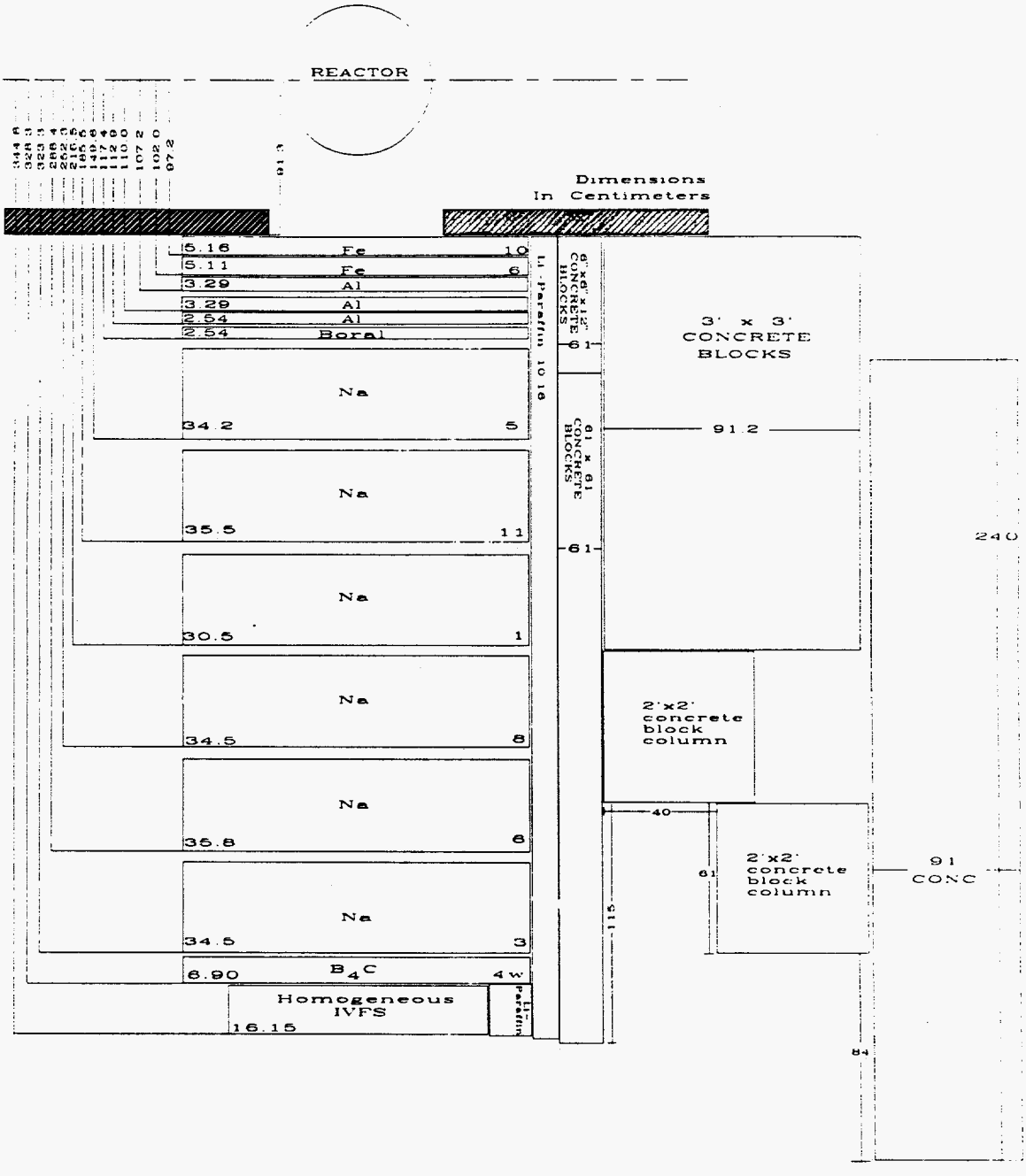

Figure 50. Schematic of SM-2 plus shield configuration for Item IIIE.

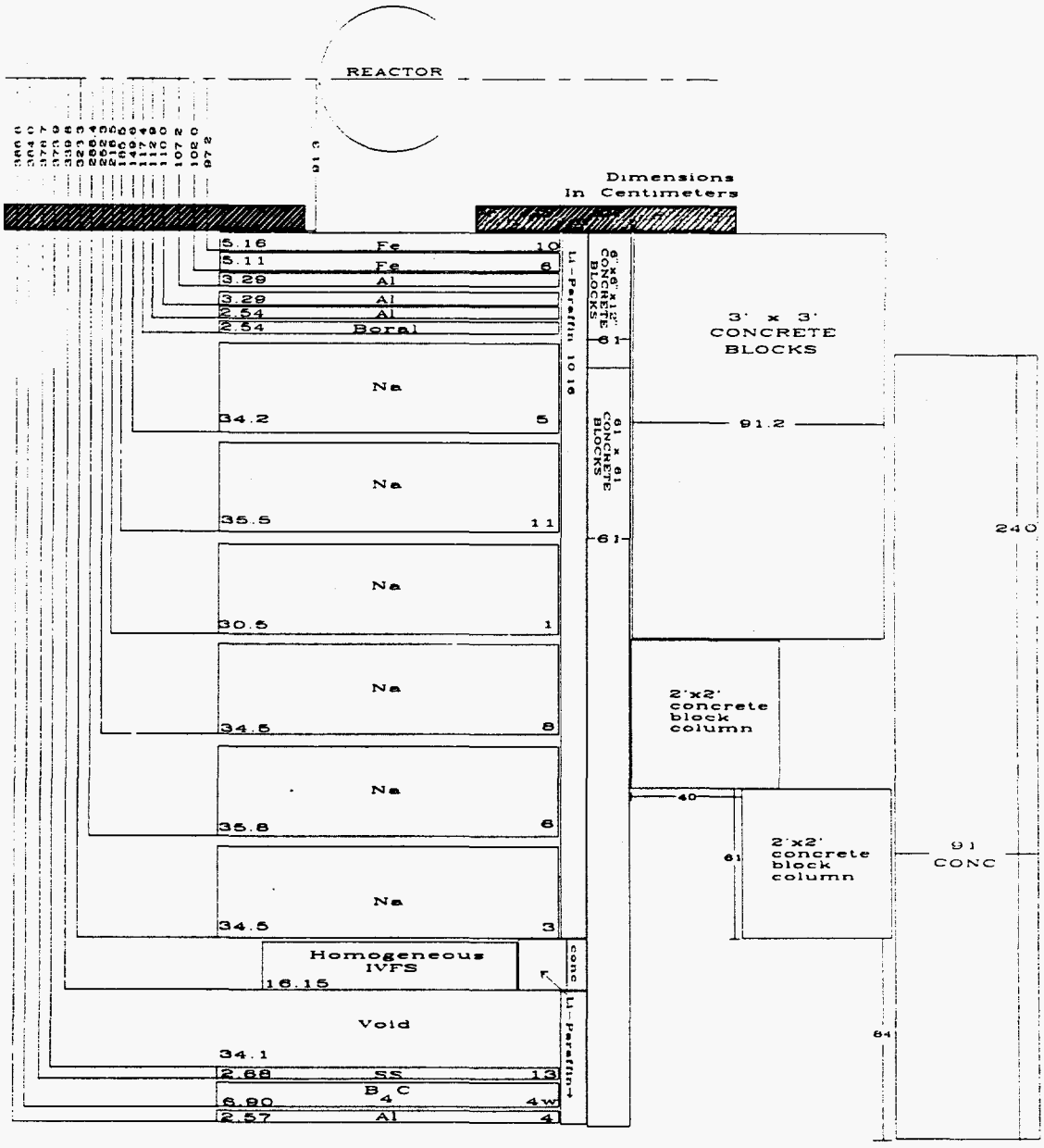

Figure 51. Schematic of SM-2 plus shield configuration for Item IIIF.

ORNL/TM-11989
Distribution Category
UC 534

DISTRIBUTION

1. B. R. Appleton
2. R. S. Booth
3. J. A. Harvey
4. L. B. Holland
5. F. J. Homan
6. J. L. Hull
7. H. T. Hunter
8-17. D. T. Ingersoll
18-19. F. J. Muckenthaler
20. J. V. Pace, III
21. A. Shono
22. C. O. Slater
23. R. R. Spencer
24. R. C. Ward
25. J. D. White
26. L. R. Williams
27. A. Zucker
28. Central Research Library
29-33. EPMD Reports Office
34. ORNL Y-12 Technical Library
Document Reference Section
35-37. Laboratory Records
38. ORNL Patent Office

EXTERNAL DISTRIBUTION

39. Office of Assistant Manager for Energy Research and Development, DOE-OR, P.O. Box 2008, Oak Ridge, TN 37831-6269.

40. L. F. Blankner, Energy Research and Development, DOE-OR, P.O. Box 2008, Oak Ridge, TN 37831-6269.

41. Prof. Roger W. Brockett, Harvard University, Pierce Hall, 29 Oxford Street, Cambridge, Massachusetts 02138.

42. L. L. Carter, Westinghouse-Hanford Company, 400 Area Trailer 1, P.O. Box 1970, Richland WA 99352.

43. R. K. Disney, Westinghouse Electric Company, P.O. Box 158, Madison, PA 15663.

44. Prof. John J. Dorning, Department of Nuclear Engineering and Engineering Physics Reactor Facility, University of Virginia, Charlottesville, VA 22903.

45. P. B. Hemmig, Safety and Physics Branch, Office of Technology Support Programs, DOE-Washington, Washington, DC 20585.

46. Dr. James E. Leiss, Route 2, Box 142C, Broadway, VA 22815.

47. Prof. Neville Moray, Department of Mechanical and Industrial Engineering, 1206 West Green Street, Urbana, IL 61801.

48. Prof. Mary F. Wheeler, Department of Mathematical Sciences, Rice University, P.O. Box 1892, Houston, TX 77251.

49. K. Takahashi, Power Reactor and Nuclear Fuel Development Corporation, Sankaido Building, 9-13, 1-Chome, Akasaka Minato-Ku, Tokyo 107, Japan.

50. M. Tsutsumi, Power Reactor and Nuclear Fuel Development Corporation-Washington, Suite 715, 2600 Virginia Avenue NW, Washington, DC 20037.

51. K. Chatani, Power Reactor and Nuclear Fuel Development Corporation, 4002 Narita-Cho, O-Arai-Machi, Ibaraki-Ken, 311-13, Japan.

52-124. Given distribution as shown in DOE/OSTI-4500-R75, LMFBR-Physics: